Bangor University

DOCTOR OF PHILOSOPHY

Electrical properties of self-assembled films

Gigon, Joanna

Award date:
2009

Awarding institution:
Bangor University

Link to publication

ELECTRICAL PROPERTIES OF SELF-ASSEMBLED FILMS

A thesis submitted to the
University of Wales
in candidature for the

Degree of
Philosophiæ Doctor

by

JOANNA GIGON

Supervisor: Professor Geoffrey J. Ashwell

PRIFYSGOL
BANGOR
UNIVERSITY

School of Chemistry

Prifysgol Bangor – Bangor University

2009

Abstract

One of the ultimate aims of nanotechnology is the development of nanomaterials for dealing with molecular electronics, which require at least one of their dimensions falling in the nanometre scale.[1] Hence, one of the most important steps in the progress of molecular electronics is that of the molecular rectifier systems composed of organic molecules for use in the future electronic circuits.

The work presented, reports on the electrical properties of materials acting as diodes[2] and wires.[3,4] For this purpose, different types of molecular systems were investigated, including chevron-shaped molecules, π-conjugated (**WIREs**) and banana-shaped molecular wires (**BWIREs**) and molecular wires formed by step-by-step deposition. All of these specified systems were fabricated on a gold-coated substrate using self-assembly. Self-assembled monolayer (SAM) films were characterised by the quartz crystal microbalance (QCM) technique and scanning tunnelling spectroscopy (STS).

WIRE1, **WIRE3** and **BWIREs** exhibited symmetrical *I-V* characteristics, typical for conventional molecular wires. Contrary, studies of a molecular wire formed from the sequential synthesis of donor-acceptor-donor (D_w-A-D_s) components demonstrated diode-like behaviour. The bias for rectification was controlled by altering the donor-acceptor sequence. However logically, *I-V* characteristics observed for the film of the initially formed SAM and the resultant wire were different despite the electron-donating characters of both surface-active moieties. This was due to a stronger character of the terminal donor group.

The unusual phenomenon of assembly *via* competing S-Au/NO_2-Au interactions was observed for **WIRE2**. This was ascribed to the very electron deficient difluoronenone core that weakened the conventional S-Au chemisorption.

The single molecule conductivity of the molecular wire systems were determined by the method of Haiss *et al.*[5] which relies on the spontaneous bridging of those molecules between a tip and a substrate.

Acknowledgments

1 Introduction

1.1 Moore's law

Empirical predictions about the continued innovations in silicon technology were described by Moore's law, proposed by Intel's co-founder, Gordon Moore in 1965.[6] The exponential growth of the number of transistors per unit area on a silicon integrated circuit, see Figure 1.1, has so far followed Moore's observation, owing to the continued miniaturisation resulting from lithographic methodologies.[1] The trend by which chip densities double every eighteen months will not last long, as the current semiconductor industry based on silicon oxide (silica) components does not consider physical limitations of transistors. Additionally, the current transistor technology is located towards the end of the predictions made by Moore's law where the feature size of the circuit components reaches the value of *ca.* 50 nm.[7,8] This means that further device miniaturisation, to reach the nanometer scale, with present fabrication technologies inevitably faces growing restrictions dictated by the physical limitations. In order to overcome the technological and economical obstacles associated with the enhancement of the computational industry, the development of new materials, scientific tools and new methodology for fabrication are required.[9] Currently, it seems that the limits of silicon based materials could be overcome by the use of atoms to build nanometer-sized molecular components[10] which could then be assembled into a desired computational circuitry. This fundamentally new approach, that evolves from the level of molecular components, would offer high reproducibility and small size of molecular building blocks.[11,12]
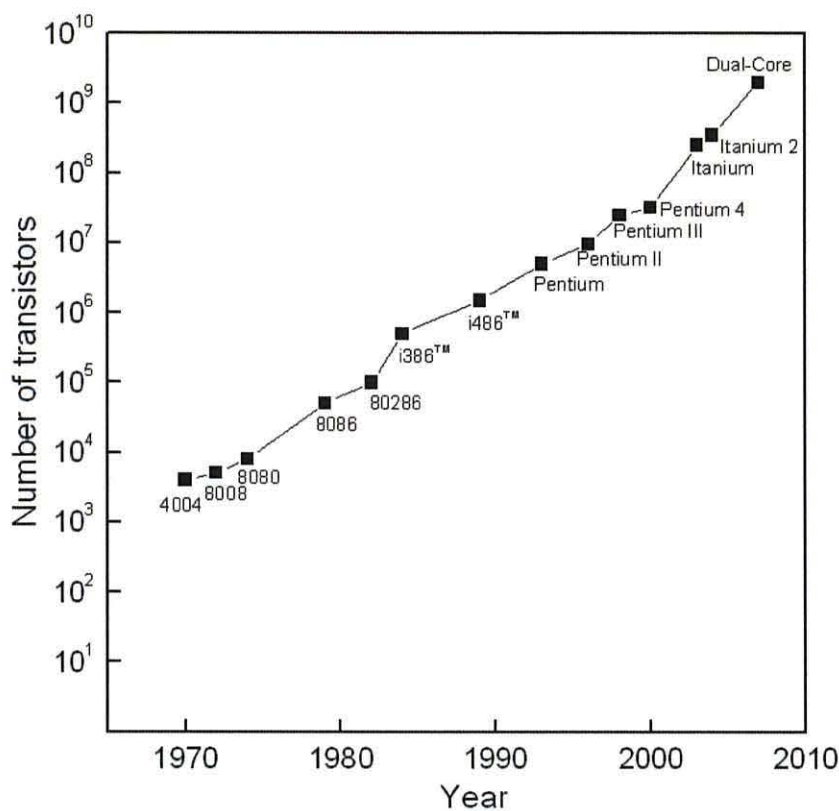
Figure 1.1 Graphic representation of Moore's law.[13] The data used to create the above plot adapted from 13.

1.2   Molecular electronics

Over the last few decades, the process of miniaturisation of electronics has gained the ability to realise real-world applications;[14] it has been the topic of important scientific discoveries resulting in the creation of a number of molecular diodes,[2] devices and circuits designs.[17]

The concept of nanotechnology originated from the talk given by Richard Feynman to the American Physical Society in 1959: "There is Plenty of Room at the Bottom".[15] Feynman outlined two different approaches to nanotechnology, the so-called "top-down" and "bottom-up". The "top-down" approach based on inorganic microchips has progressed by creating "smaller" sized conventional bulk methodologies whereas the opposing, "bottom-up", involves a single molecule methodology of fabrication.

Traditional solid state semiconductor electronics, characterised by the use of sophisticated lithographic and etching technologies for the construction of rectifiers is

due to exceed the critical dimension. The "bottom-up" approach becomes a remarkable alternative for building novel nanostructure system devices. The major reason of replacement of the lithography-based large scale integration technology, by molecular materials, is the capability of reaching the ultimate miniaturisation by decreasing the size of the building blocks by around five orders of magnitude.[16] The cost of chip fabrication can also be reduced. Such a small size is provided along with the components' thermodynamically driven self-assembly and self-recognition,[17] and this opens up the possibility for an era for the fabrication of engineered highly ordered molecular systems. The other major advantage in using single molecule electronics is the ability to scale, in terms of the number of components assembled together as well as in the sizes of the individual components.[18] Furthermore, molecules have electron orbitals delocalised along their length (π-conjugation) simplifying the control of the electronic properties of conductive structures. All of these advantages render single molecules ideal for electronic applications despite the fact they are instable at high temperatures; this was also stated by Feynman in 1959.

However, despite the fact that molecular electronics consisting of single molecule based devices is emerging[19,20] as an alternative for the already limited lithographic approaches, there still remain a great challenge for investigations into the manufacture of reliable materials for commercial use.[21]

1.3 Aims

Ordered films of organic molecules that can be assembled onto metal surfaces are at the forefront of research due to their potential for inclusion in many technological applications. The most important purpose for the self-assembly technique in the field of molecular electronics is to overcome the miniaturisation threshold of silicon based devices.

The primary focus of this research was to investigate the electrical conductivity of surface adsorbed organic molecules. For this purpose, scanning tunnelling microscopy (STM) was employed, to register current-voltage (*I-V*) characteristics of self-assembled material. During the course of these investigations, the behaviour of molecular wires

and chevron-shaped molecules were also analysed. Obtained characteristics, structural and electrical, led to better understanding of electron transport through the tunnelling junction. Additionally, the employment and significance of a multi-step modular chemistry approach in building complex molecular wire systems on gold electrodes was reported.

2   Assembly of molecular films

2.1   Self-assembled monolayers (SAMs)

The essence of miniaturisation is the ability to work at the molecular level to replicate macroscopic material's properties through utilisation of molecular organisation at solid surfaces. One of the approaches, whose importance has grown over the years, is self-assembly. Pioneering work on was reported by Zisman *et al.,*[22] who was the first to mention the monomolecular layer adsorption process. However, real progress on the development of SAMs increased only after the discovery, by Nuzzo and Allara,[23] of the formation of oriented monolayers on gold *via* the adsorption of dialkyl disulfides from dilute solutions. Since then, studies on a number of self-assembled systems have been reported, including organosilicon on hydroxylated surfaces,[24] n-alkanoic acids on aluminium oxide[25,26] and silver,[27] and organosulfur compounds on gold,[23] silver[28] and copper.[29]

The term self-assembly involves the spontaneous arrangement of organic molecules towards an energetically stable, highly ordered monolayer of controlled thickness.[30,31] Additionally, no intervention from outside is required.[32] The alignment of molecular assemblies is determined by its structure rather than the surface lattice.[33] Self-assembly is the most common technique for forming ultra-thin systems either by immersion of the substrate into a surfactant solution[34] or by vapour deposition.[35,36] Noteworthy, is the fact that the formation of SAMs by vapour deposition can sometimes enable much easier control of the surface coverage of adsorbed molecules than solution deposition.[36] Organic components are adsorbed onto a metal surface *via* chemisorption resulting in the formation of a strong chemical bond and therefore, the produced monolayers are

stronger and more stable compared to physisorbed films formed by use of the Langmuir-Blodgett technique.

The fundamental attractiveness of SAMs arises due to their ease of preparation, as there is no need for ultra-high vacuum or specialised equipment in the formation of monolayers. SAMs can be generated on objects of all shapes and can be used as building blocks in the formation of more complex structures.[37] Moreover, they are dense and chemically stable structures and find use in a diverse field of technical applications, such as: nanopatterning,[38,39] wetting,[40] corrosion inhibition,[41] wear protection, molecular sensors[42] and molecular recognition[43] and can be used as barriers in electron and ion transport studies.[44]

The main concept behind molecular organisation of assemblies on metal surfaces formed *via* self-assembly, is the exploitation of chemical reactions between the functional headgroup of the molecule and the exposed surface, see Figure 2.1.
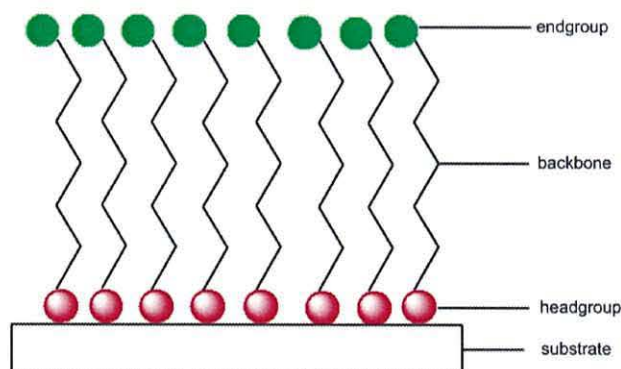
Figure 2.1 Schematic diagram of SAM molecule.[37]

Strong affinity of the headgroup to the substrate enables the molecule to form either polar covalent or ionic bonds with the surface for electrical contact. Depending on the type of molecule, different self-assembly systems can be formed. These include: organosilane derivatives that assemble onto hydroxylated surfaces (for example Al_2O_3[24], SiO_2[45,46]) or quartz, glass, mica[56] *via* Si-O-Si bonds, carboxylic acids on metal oxides (AgO) *via* $-CO^{2-}Ag^+$ and most studied, organosulfur compounds on gold *via* Au-S bond.

The headgroup is also able to displace, from the surface, any random atmospheric materials that adsorb onto the bare surfaces of the metals and metal oxides. This capability is essential, due to the fact that these adsorbates are responsible for the lowering of the free energy of the interface between the metal and the surroundings as well as modification of the surface properties. They can also affect the stability of the nanostructures of the metal and metal oxides.

There are a number of substrates upon which SAMs can be formed, and they are divided into planar surfaces (glass or silicon wafers covered with thin metal layers) and highly curved nanostructures (colloids, nanocrystals, nanorods).[52,56] The selection of a specific type of substrate is dependent on the application of SAMs. The suitable materials that a substrate wafer can be coated with are: gold,[28,44,56] silver,[47] platinum,[48] mercury.[49] However gold is the most commonly utilised due to its inertness and resistance to oxidation that enables samples to be manipulated under atmospheric conditions. Its high conductivity allows use in various techniques, such as physical vapour deposition, sputtering or electrode position.[50]

Whilst the headgroup is responsible for the molecule's chemisorption and pins it to the surface, making the formation of SAMs possible, the two other constituents, the backbone and endgroup, see Figure 2.1, compose the bulk of the molecule and determine its unique features. The backbone (which usually is comprised of an alkyl chain and/or aromatic ring) provides information about the thickness of the molecule and constitutes the physical barrier.[51] The terminal functional group (endgroup) of a SAM is significant for its interfacial properties including a surface's hydrophobic or hydrophilic character, and thus interaction between a substrate and a molecule. It is also responsible for reactivity with the emphasis put on the ability to perform chemical reactions utilising pendent functional groups (carboxylic acids, quinones, amines, anhydrides).[52] There is a wide variety of terminal groups that can be anchored; these are: $-OH$, $-CH_3$, $-(C=O)OCH_3$, $-(C=O)CH_3$, $-(C=O)CF_3$, $-(C=O)C_6H_5$, $-COOH$, $-OSO_3H$.[31,50,53] Although, these moieties which contribute to the architecture of the SAM, can vary, the parallel alignment and ultimate packing within the SAM is always controlled by the lateral van der Waals interaction between neighbouring chains that composes the backbone of each molecule.

Among the number of self-assembly systems, SAMs formed from organosulfur compounds on gold have been intensively investigated, and in particular those derived from alkanethiols, disulfides and sulfides. Sulfur containing compounds, shown in Figure 2.2, have a high affinity to the gold[54] binding the molecule to gold enabling the formation of SAMs in the presence of other functional groups.[27]
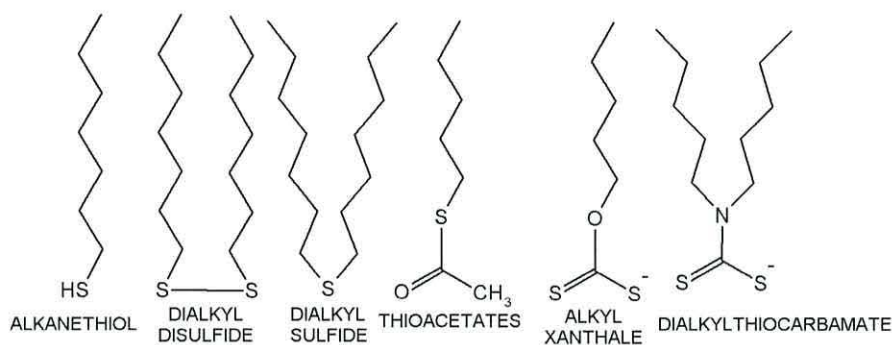
Figure 2.2 Surface active organosulfur that form monolayers on gold.

For this reaction to occur, the chemical activation of the sulfur bond (S-H and S-S bonds of thiol and disulfide respectively) is required. According to the research presented by Nuzzo *et al.*, dimethyl disulfide can be adsorbed onto gold dissociatively.[55] It is reasonable, therefore, to believe that the chemisorption is achieved, due to the dissociation of the thiol anchoring head group to the thiolate. Hence, the formed thiolate link which has a high affinity for gold is linked to the surface by a very strong S-Au bond (estimated of approximately 40 kcal mol^{-1}).[24,56] The hydrophobic character of the thiolate moiety allows for the water (the presence of oxygen causes oxidative conversion of thiol hydrogen) to be excluded from the metal interface. However, there is evidence that the thiol-gold transitional state can exist as an intact thiol.[57] Consequently, the mechanism of the adsorption of disulfides could be considered as follows:

$$RS - SR + Au_n^0 \rightarrow RS^- Au^+ \cdot Au_n^0$$
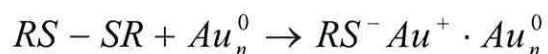
In the formation of SAMs from alkanethiols, the reaction of the oxidative addition of the S-H bond is followed by the reductive elimination of hydrogen. This mechanism would suggest that the adsorption process can occur in a vacuum, in the absence of oxygen[32] as shown below:

$$R-S-H+Au_n^0 \rightarrow R-S^-Au^+ \cdot Au_n^0 + \tfrac{1}{2}H_2$$
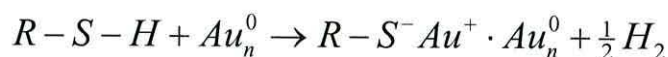
Although these mechanisms presented above are not completely understood,[58] many studies have focused on the self-assembly process of thiolate and analogous molecules on gold substrates which revealed the similarities in structures of monolayers generated from thiols and disulfides.[59] This has been deducted from investigations utilising different surface characterisation techniques. It is believed that due to chemisorption of both, alkanethiolate and dialkyl disulfide, the bonds are cleaved, S-H and S-S respectively, and this leads to the formation of the identical SAMs consisting of Au-thiolates (Au-RS).[31,60,61]

Conjugated thiols create a new platform that constitutes the base of the nanoscale molecular devices. Therefore it is of great importance to investigate the growth mechanism of SAMs and its dependence on different factors. Bain *et al.* reported kinetic studies by use of contact angle measurement and ellipsometry.[51] The formation process occurs in two distinct phases for moderate concentration of solution (10^{-3} M). During the initial deposition, first phase, the alkanethiol assembles with 80% to 90% coverage of the metal surface. The thickness of the monolayer reaches its final value in a second phase lasting several hours. This behaviour suggests that the first step corresponded to an imperfect layer adsorption whilst the completion of crystallisation process occurs in the second phase. At this stage, adventitious materials including solvent are displaced from the monolayer to minimise defects in the SAM and enhance packing.[51] It was assumed that during this process the alkyl chains rearrange undergoing inter-chain and attractive lateral interaction to produce a fully extended all *trans* conformation. The experimental data indicated that a tilt angle (α), see Figure 2.3, of linear backbone of the molecule can vary between 20 to 40° with respect to the surface normal[62,63] and a value of this angle is determined by a packing density of a monolayer and the optimising of the van der Waals interaction between chains.
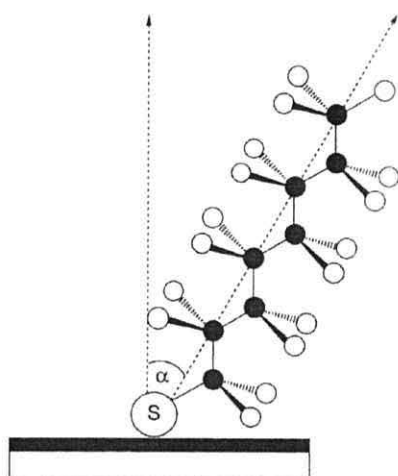
Figure 2.3 Schematic representation of an all *trans* conformation of self-assembled molecule with the alkyl chain away from the gold surface.[37]

Ellipsometric studies reveal that distinct differences occur in the structure of SAMs formed from long or short alkanethiolates.[51] With decreasing chain length the total van der Waals interaction for those SAMs lessens, the coverage decreases and monolayers become less dense. This means that short-chain n-alkyl thiol assemblies which cover surface at a low rate, in practice would lie flat with their hydrocarbon backbones parallel to the gold surface. Whereas at higher surface coverage, the molecule begins to stand-up with a tendency to be tilted at approximately 30° with respect to the surface normal[50] with the overall kinetics for longer alkyl chains being faster. It is assumed to be caused by the increase of total attractive energy of chain-chain interaction.[51]

The two-step SAM growth mechanism has been confirmed by many workers. XPS and optical second harmonic generation (SHG) study was performed by Buck *et al.*[64] whilst quartz crystal microbalance (QCM) results were published by Karpovich and Blanchard.[65] Both groups investigated the adsorption kinetics of alkanethiolate monolayers on gold substrates. Those studies concluded the SAM formation mechanism of investigated systems to follow Langmuir adsorption kinetics. The SPM studies revealed that the adsorption rate is concentration dependant. Yamada and Uosaki found that at low concentration (0.001 mM) of investigated material, the assembly process is characterised by at least three steps,[66] see Figure 2.4.
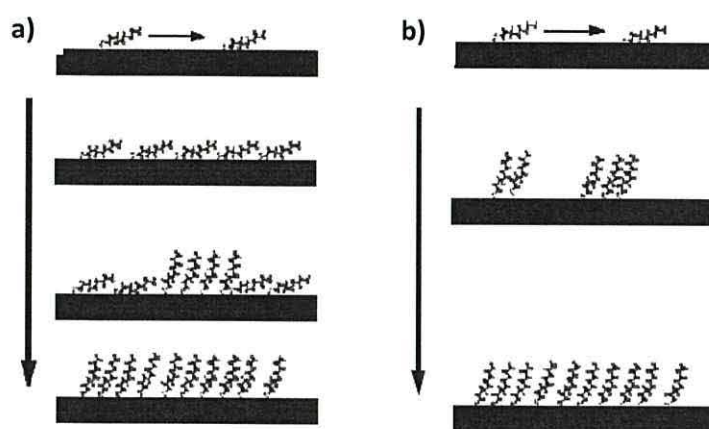
Figure 2.4 Schematic view of the initial phase of an alkanethiol SAM growth: a) in a low concentration solution, b) in a high concentration solution.[66]

However, the increase of a concentration to about 0.01 mM prevented the formation of the intermediate, lying-down phases. This means that the adsorption process described above was confirmed again.[67,68]

Another group of organosulfur compounds forming SAMs on gold are the dialkylsulfides.[69,70] Although SAMs formed from dialkylsulfides seem to be similar to those derived from thiols and disulfides, they are less robust.[44] They exhibit different adsorption, structural arrangement and thickness.[50] In addition, differences can be observed in a lattice structure including the presence of configurational defects in the ordered domains.[71] Zhong and Porter[70] had previously indicated however the similar mechanism of forming SAMs suggesting the assembly of n-dibutyl sulfide onto gold with S-C bond cleavage yielding adsorbed sulfide (S^{2-}) and thiolate (SH^-). This type of formation, identical to SAMs prepared from alkanethiols as seen in Figure 2.5, would make sulfides an interesting subject of research. Unfortunately, Schlenoff *et al.*, based on the coverage measurement, stated that any presence of C-S bond cleavage must be minimal.[72]
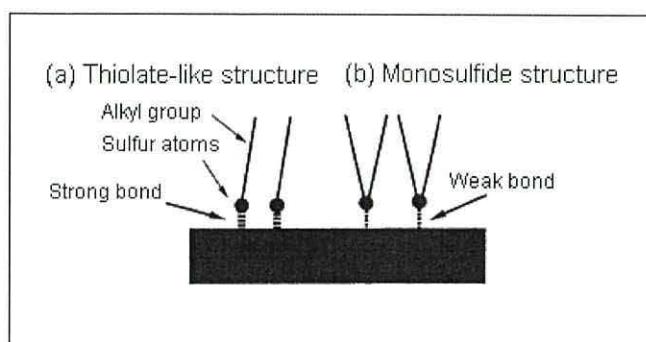
Figure 2.5 Schematic presentation of monosulfide SAMs: (a) thiolate structure, (b) monosulfide structure.[73]

Moreover, recent studies revealed that there was no cleavage of C-S bonds in the formation of SAMs derived from dialkylsulfides,[74] which has been verified.[75,76] In addition, STM results disclosed less dense packing and poor arrangement of monolayers derived from sulfides.[77]

There are many factors that have impact on, for example the rate of adsorption process,[78] the stability, and the arrangement of the resulting monolayer.[72] Thus, for the future applications of SAMs in molecular electronic devices the issue of great importance is to understand how to reduce defects and maximise order in monolayers. For this to be achieved, the influence of those factors on the character of the monolayers and their control must be explored. Some of them can be easily monitored. These are: temperature, type of solvent, concentration and the chain length of the adsorbate and also purity of the substrate and chemicals.

The preferred solvent for self-assembly is ethanol owing to its low toxity. It is able to solvate various alkanethiols irrespective of degrees of their polar character and chain length. Moreover, it has a low tendency to be incorporated into the monolayer formed during the deposition process.[51]

The following two parameters, a concentration and an immersion period, are inversely related in the SAMs formation process. Bain *et al.* implied that the best concentration for experiments would be at about 1 mM,[51] as at lower concentrations, the adsorption process may be acute (conversion of the alkanethiol to disulfide). The purity of adsorbate and the cleanliness of the substrate are also essential for well-defined

monolayers with minimum defects to be formed.[50,53] The crucial factor for determining the range of application in which SAMs could be used is thermal stability. The temperature effect plays an important role within the few first minutes of deposition, as most of the reorganisation of the SAM occurs at this stage.[79] The SAMs appear to be more ordered at elevated temperatures. It was found that the kinetic of the reaction improves above 25°C and the rate of desorption of random adsorbates and physisorbed solvents on the surface increases.[56] Monolayers however begin to desorb when heated to temperatures over 70 °C,[44] with the rate being dependant on ambient conditions. Noteworthy is the fact that, thiol monolayers are more stable compared to dialkyl sulfides on gold (desorb in Ar at 80 °C),[69] but simultaneously less stable than monolayers derived from silane on silicon substrate. The annealing effect of alkanethiol SAMs was observed at around 100 °C,[80] which lasted until the maximum desorption was reached, in a range from 200-220 °C.[31,60,81] To increase thermal stability of SAMs on gold surface, various method have been employed, such as: lateral polymerisation,[82] formation of a hydrogen bonded network derived from amine groups[83] or the extention of the length of the hydrocarbon chain on a terminally fluorinated alkanethiol $(CF_3(CF_2)_{10}(CH_2)_mSH)$[84] and many others. Another interesting strategy was utilised to increase the thermal stability and to avoid decomposition. This method employs rigid conjugated molecules such as oligophenylenes, due to the fact that SAMs derived from oligophenylene are more rigid due to the presence of phenyl rings.[85]

Self-assembled monolayers are unique components for molecular scale electronics as they can organise individual molecules into large assemblies onto surfaces of different size and shape. SAMs are well defined and accessible, and these make them good model systems for studies using analytical techniques such as: surface plasmon resonance,[86] scanning tunnelling microscopy, atomic force microscopy,[87] etc. or more specifically, electrochemical techniques such as cyclic voltametry.[88]

2.2   Langmuir-Blodgett films

Pioneering experiments on ultra-thin films were performed after Franklin's[89] observations of oil on water. Those studies concluded that hydrophobic materials were able to form layers on an air-water interface and they were one single molecule thick (Pockels[90] and Rayleigh[91]). However, the modern understanding of the behaviour of floating monolayers on water and their transfer from liquid onto solid substrates was introduced by Langmuir[92] and Blodgett.[93] These molecular assemblies are referred to as Langmuir-Blodgett (LB) films. Monolayers are formed by amphiphilic molecules, which consist of two dissimilar parts, a hydrophilic head and a hydrophobic tail. The appropriate amphiphilic balance between these two parts is of utmost importance as it dictates the alignment of the molecules adsorbed at the air-water interface; In such a way that the polar region is anchored to the water, whilst the hydrophobic end protrudes towards the air, see Figure 2.6, so that the molecules can form an isolated two dimensional system.
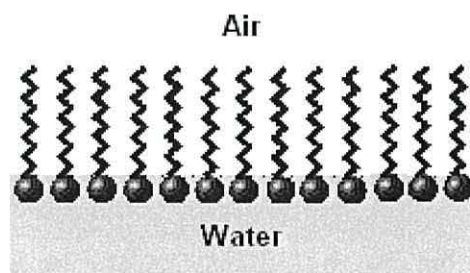
Figure 2.6 The arrangement of an amphiphile-hydrophilic heads and hydrophobic tails at the air-water interface.

However, it should be noted that the association behaviour of molecules and their affinity for interfaces is dependent on the physical and chemical properties of the hydrophobic and hydrophilic moieties of the amphiphile. The molecule comprises a sufficiently long hydrocarbon chain (dodecyl or longer) to increase the hydrophobicity and render the molecule insoluble as a whole. Amphiphiles with shorter 'tail groups', though still insoluble in water, tend to form micelles which dissolve and formation of a monolayer at the air-water interface is suppressed. The head group should be polar to interact with water either *via* its dipole moment or by hydrogen bonding. Commonly, these are: -OH, -COOH, -NH$_2$, etc. To fulfil the requirement of LB film forming ability,

the molecule needs to be soluble in an appropriate solvent, which should be highly volatile (chloroform, toluene or hexane), water-insoluble and chemically[94] inert in relation to the material under study.

Langmuir films[92] formed on the subphase are characterised by their pressure-area isotherm. The surface pressure is given by the relationship between the surface tension in absence of a monolayer and that in the presence of a monolayer. The altering value of surface pressure is monitored with a Wilhelmy plate and these changes can determine the state of the monolayer. The monolayer behaviour can be revealed by measuring surface-pressure *vs.* the area of the water surface available to each molecule, where the resultant plot is called an isotherm.[92] As shown in Figure 2.7, below, the isotherm is divided into three distinct regions, such as: gas, liquid and solid phase.
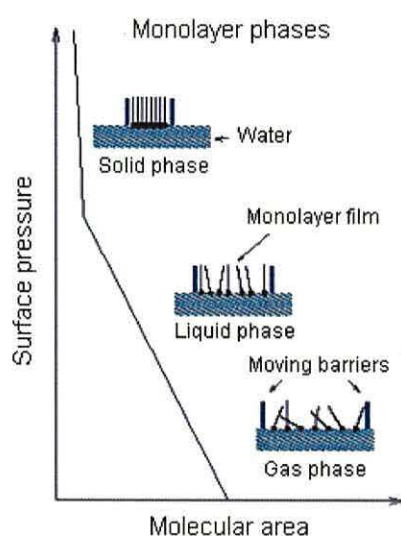
Figure 2.7 Schematic diagram of a generalised isotherm of a Langmuir monolayer.[95]

In the gas phase, the monolayer is very dilute and thus highly disordered, as the distance between molecules is large and so the interactions are weak. Hence, at this stage the monolayer has negligible effect on a surface tension of water. When the barriers start to move along the surface, the intermolecular distance is lowered,[92] approaching the molecules towards each other and thus interactions between them. The surface pressure starts to rise. At this point the two dimensional liquid condensed phase of the isotherm is reached. As the barrier is moved even further, the onset of the solid phase, the molecules arranged in their closest possible packing can be noted by an even steeper

rise in the surface pressure. If the barriers are kept compressed after reaching the solid state, the monolayer film will ultimately collapse (into three dimensional structures). The collapse is usually represented by a sudden drop of surface pressure.[90]

The Langmuir film from the aqueous subphase is transferred onto a solid substrate either as a monolayer or by sequencing the process to form multilayer LB film.[91] Multilayer formation process relies on moving the substrate downwards and upwards through the monolayer interface at constant surface pressure. As the surface pressure is dependent upon the nature of the monolayer, its value is established empirically and usually differs for various monolayers. The monolayer deposition is repeated until a highly organised film of desired thickness is generated. Depending on the type of substrate used in deposition, there are two methods of LB film formation, see Figure 2.8. When the solid substrate is hydrophilic (glass), deposition normally occurs on the up-stroke, whereas the substrate is hydrophobic (HOPG), the monolayer is normally deposited on the down-stroke.
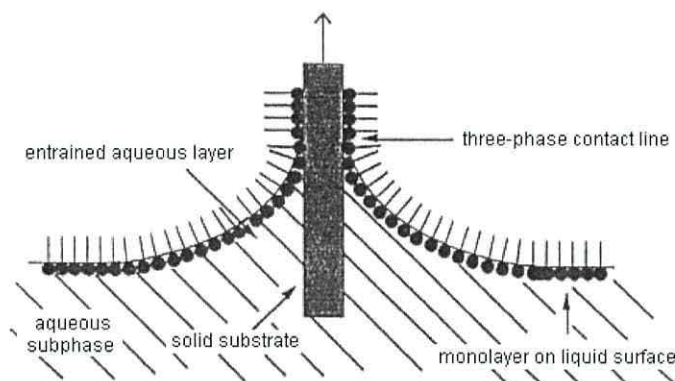

Figure 2.8 Deposition of a floating monolayer on a solid substrate.[96]

The multilayer film formation is dependent on the orientation of the monolayer with respect to the substrate and to other monolayers. There are three types of deposition that can be distinguished, see Figure 2.9.[31,92]
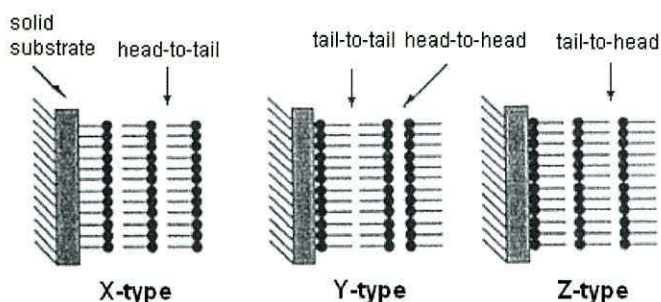
Figure 2.9 Three different types of multilayer deposition.[96]

In the X-type alignment, the first layer as well as subsequent ones are deposited only in the down direction. This type of LB film was originally reported by Langmuir and Blodgett.[97] The opposite sort of behaviour represented by the Z-type in which each layer is transferred only on the downstroke, has been observed in a number of aromatic materials.[98, 99] In the case of Y-type, the multilayer is formed by transfer of monolayers in both up and down directions, so that the deposition of the first layer occurs on the upstroke, whilst the next one on the downstroke. This process is subsequently repeated.

The LB technique provides molecular layers of fairly high quality but due to limitations it does not fulfil the technologist's every desire. The main disadvantage is related to the nature of deposition process (physisorption) as well as the need for clean room conditions.

3   Monolayer characterisation methods

3.1   Quartz crystal microbalance (QCM)

The QCM is an invaluable tool when it comes to determination of the film properties. It is a well known technique for monitoring small amounts of adsorbed or desorbed materials on a surface. The sensitivity enables the measurement of mass with nanogram accuracy and the technique can be used to monitor the adsorption process of both self-assembled monolayers and LB films.[100]

The QCM technique is based on the piezoelectric behaviour of quartz,[101] see Figure 3.1. The piezoelectric effect was first observed in 1880 as a potential difference generated

across two surfaces of a quartz crystal under strain. There was not much interest in piezoelectricity however until 1917 when it was discovered that quartz crystals could transduce and detect ultrasound in water.[102] Additionally, introduction of AT-cut crystal contributed to the prevalence of the quartz crystal among all frequency controlled applications. The advantage of selecting the AT-cut angle is that, the temperature dependence of the resonant frequency at 25°C is essentially zero. On each side of an AT-cut, quartz crystal, are deposited electrodes, which typically comprise a 100 nm thick gold evaporated onto 10 nm thick chromium.
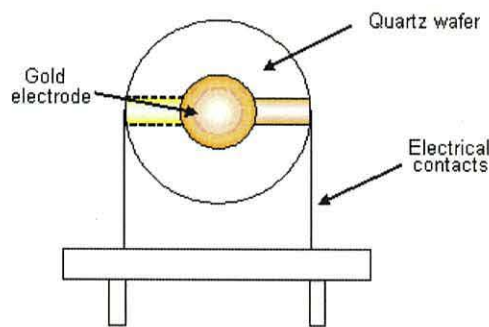
Figure 3.1 Schematic diagram of a piezoelectric crystal,[103] where the broken line represents the electrode on the reverse side.

The sensitivity of quartz crystal to thin adhered films has been utilised since the late 1950's following the work of Sauerbrey,[105] who pioneered the quantitative description of QCM behaviour. When the electrodes are connected to an oscillator and a voltage is applied, the alternating electric field across the connected electrodes causes the quartz crystal to oscillate at its resonant frequency. The frequency alters with every additional mass deposited onto the surface.[104] The magnitude of this change is proportional to the added mass of the adsorbed layer. Thus, the deposited mass can be monitored and mean area occupied by each molecular in a monolayer calculated. The Sauerbrey equation, below, presumes that the crystal with the adsorbed layer behaves as a rigid assembly: [105]

$$\Delta f = \frac{-2\Delta m n f_o^2}{A\sqrt{\mu_q \rho_q}}$$

(1)

where: Δf – measured frequency shift (Hz),

Δm – mass change per unit area (g/cm^2),
f_0 – resonant frequency of quartz crystal,
ρ_q – the density of quartz, 2.648 g/cm^3,
A – the area of electrode,
μ_q – shear modulus of quartz.

Changes in the oscillation frequency can be converted into changes of the disc mass:

$$\Delta m = -(9.09 \pm 0.01) \times 10^{-10} \Delta f \tag{2}$$

The high sensitivity of QCM and the associated ability to monitor mass changes on the crystal sensor in real-time[106] make the QCM a very attractive technique for a wide range of applications, such as gas phase detection, immunosensors, DNA biosensors, drug analysis, thin film formation, etc.[103,109]

3.2   Surface plasmon resonance (SPR)

Surface plasmon resonance[107] is a technique that enables the thickness and dielectric permittivities of ultrathin organic films adsorbed onto metal surfaces (such as gold, silver, copper and aluminium, sodium and inidium[108,109, 110]) to be determined. Owing to the high sensitivity of such a method, small changes in a refractive index and thickness can be detected. SPR is suitable for the study and characterisation of molecular layer growth.[110] Moreover, in association with measurements obtained from the QCM, details of the packing arrangement and properties of adsorbates can be gained.[111]

Since the beginning of the twentieth century, when the theory of this phenomenon was first described, much research on the subject of optical excitation of surface plasmons has been performed.[107,112]

The principle of SPR is based on total internal reflection occurring at the interface between a metal and a dielectric (two transparent media of different refractive indexes). The incoming light passing from the medium of a higher refractive index to a lower one is partly reflected and partly refracted below a certain angle of incidence. Above a critical angle the light is no longer refracted, but totally reflected, where the metal surface acts as a mirror, and the total internal reflection is observed. At the same time,

the electromagnetic field associated with the light beam penetrates the lower refractive index medium generating an evanescent wave whose amplitude decays exponentially with increasing distance from the interface.[113] Under certain conditions, when the interface between two refractive media is coated with a suitable conducting material, the energy carried by the photons may tunnel through this field and excite surface plasmons. This manifests itself as a reduction in the reflected light intensity for a p-polarised and monochromic incident beam.[114] The SPR angle is mainly determined by factors such as: properties of the metal film, the wavelength of the incident light, the thickness of any thin metal film as well as molecular layer deposited onto that metal film and dielectric permittivities of all media including the prism.

In order for the conversion of photons into surface plasmons to occur, the momentum and energy of each must be conserved. A plasmon is the electron density oscillation that is able to propagate along a thin metal film and dielectric interface. Among the various metallic elements, which could be useful for SPR, gold is this most practical one, due to its resistance to oxidation and well-developed surface chemistry. It is of great importance that the thickness of deposited gold is around 47 nm, thereby the excitation of plasmons results in an optimum dip in reflective light at a specific angle of incidence with a sharp angular dependence on the resonance.

The most common setup for SPR studies of adsorbed molecules and films was developed by Kretschmann,[115] see Figure 3.2.
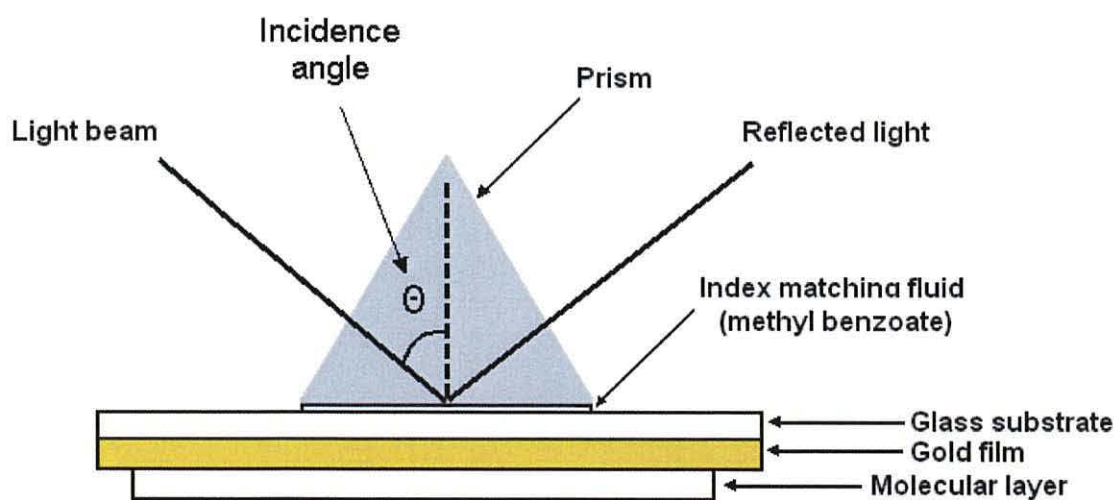
Figure 3.2 The Kretschmann configuration for SPR studies.

It utilises a prism in contact with a coated glass by using an index matching fluid. In this configuration, the angle of incidence of p-polarised laser beam (e.g. HeNe $\lambda= 632.8$ nm) is altered and the reflected intensity is monitored. The intensity of reflected p-polarised laser radiation recorded for the range of different incident angles is compared to the intensity measured before deposition. The data analysis results in a plot of reflectivity *vs.* angle (a curve of reflectance[116]), see Figure 3.3. Thus the thickness of the adsorbed material can be provided.
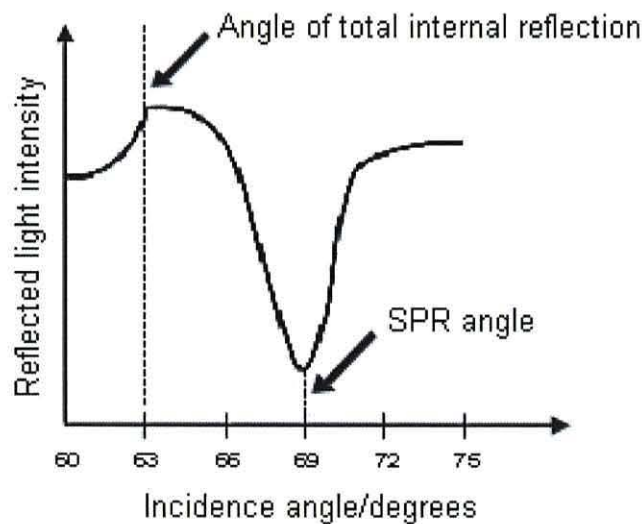
Figure 3.3 The curve of reflectance.

3.3   Scanning Tunnelling Microscopy (STM)

Pioneering studies of the nature of metal surfaces were researched by Young[117] with use of his invented precursor instrument, a type of field-emission microscope, called a Topografiner, see Figure 3.4.

Figure 3.4 Diagram of a topografiner. Both, the left(y) and the right(x), piezo drivers scan over the 'specimen' surface. The center (z) piezo driver is keeping the distance between tip and surface, because the voltage is constant due to the control by a servo system. The results obtained with the Topografiner are shown at the bottom right.[117]
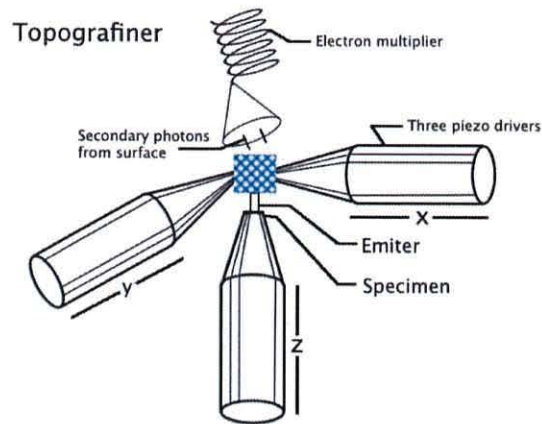
The main breakthrough with this instrument was adequate vibration isolation to stabilise the positioning of the tip above the surface. This was achieved for the scanning tunnelling microscope designed by Binning and Rohrer,[118] who were awarded the Nobel Prize in Physics in 1986. The invention of STM ushered in the development of a modern family of instruments - scanning probe microscopes (SPMs) - that allow characterisation of surface properties as well as surface modification on an atomic scale. SPM techniques, contrary to other surface science methods, are not restricted to vacuum conditions, and can also operate in gaseous and liquid environments.[119] They have therefore become indispensable tool for the study of the dynamic phenomena of interface processes, such as chemical reactions[120] as well as individual molecules and large aggregates,[121] bonded or adsorbed. The main concept of all SPMs techniques is based upon interaction between a sharp tip and a surface of the sample while scanning. STM technique involves transmission of electrons between these two electrodes with tunneling effect due to quantum mechanical phenomenon. As the tip approaches the sample surface at a distance of the order of 1 nm, and a voltage bias is applied, the overlap of tip and sample electron wavefunctions is large enough, thus electron tunnelling occurs.[122] The probability of an electron transmission through the barrier decays exponentially with the barrier width:

$$I_t \propto e^{-2\kappa d}$$

(3)

where: I_t -tunnelling current, d-distance between tip and sample, κ-the constant value depended on the height of the potential barrier.[123]

This means that the tip-surface distance must be maintained with accuracy of better than 0.01 Å,[123] as an increase of the tunneling distance of 1 Å decreases the tunnelling current by an order of magnitude.

The most crucial element of the STM that influences sample topography and its I-V characteristics is the quality of the tip (geometry and chemical identity). For the atomic resolution to be achieved, the tip should terminate with a single metallic atom. Most commonly materials used for STM tips are: Pt/Ir and gold[124] due to their resistance to oxidation whereas tungsten is used for UHV applications. The use of nonmetallic atom at the end of the tip or cluster of atoms would contribute to untrue representation of electronic characteristic of a sample surface. Moreover, lack of tunnelling current stability can be observed.

The position of the tip is accurately controlled during the approach mechanism. It is attached to a piezoelectric tube and so tiny deflections above the surface are feasible while scanning by maintaining either a constant height or a constant current. As the tip is brought to the close proximity of the sample, the surface is scanned point by point in three dimensions. The scanning mechanism enables the tip to be rastered in the X and Y directions whilst at the same time vertical (Z) direction is being adjusted to maintain a constant tunneling current. The lateral and vertical resolutions can reach 0.1 and 0.01 nm respectively. Generating 3D profile of the surface gives information on roughness together with the size and conformation of individual molecules. Moreover, high resolution images of individual molecules show sufficient detail to resolve the aromatic and aliphatic parts of molecules.[125] In addition to its ability to image the sample topography, such an instrument is used to record current-voltage (I-V) characteristics revealing information about the electrical properties of the studied material.

Considering the resolution and sensitivity of the STM, structural rigidity of the microscope is essential for its successful operation. This stems from the exponential dependence of the tunneling current on the tip-sample separation. The control over

distance between these two electrodes is monitored by the feedback loop in such a way, that tunneling junction remains constant. Feedback loop allows the tip to follow the roughness of the surface by adjusting the height of the tip for the constant tunneling current to be maintained. Scanning at constant current provides information on the topography of the probed surface,[126] see Figure 3.5b. In case of very flat surfaces, the feedback loop can be disabled as only current is displayed. The tunnelling current will alter depending on the nature of the sample surface. Constant-height mode is mainly used to study the electronic properties of the sample,[127] see Figure 3.5a.
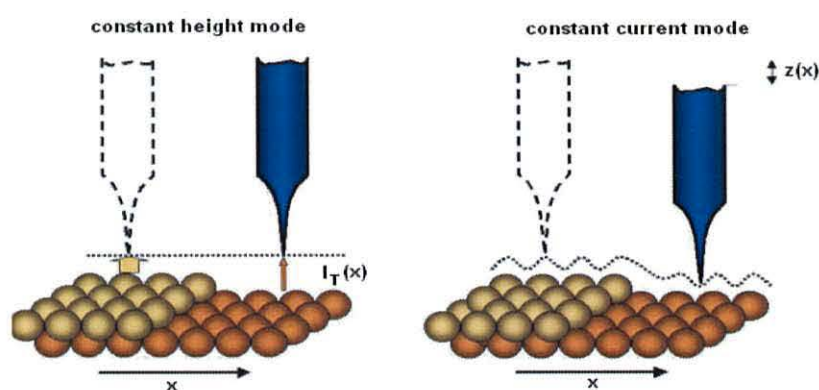

Figure 3.5 STM tip with respect to the sample surface is kept constant (a) – **constant height**-mode. The controller keeps the measured tunneling current constant **(b)** – **constant current**-mode.[128]

The STM is a powerful tool for investigating molecular and atomic structure. Since Binning and Rohrer's discovery, scanning tunnelling microscopy has been successfully utilised in different fields of science.

In recent years, the modification of a surface, manipulation of atoms[129,130] and molecules through tip-sample interactions has become a major advance in the application of STM. This stems from growing possibilities of constructing atomic or molecular scale devices directly from single atoms.[131] Single atom manipulation is dependent on polarity, magnitude and duration of a voltage bias applied between tip and sample as well as tip-sample separation. When the tip approaches very close to the surface and a voltage is applied, spontaneous formation of molecular bridges between both electrodes can be observed. Thus, an atom can be lifted from the surface and moved across to be deposited elsewhere due to the occurrence of a repulsive force between both electrodes. It has been demonstrated by Haiss *et al.*[5, 133] that this

mechanism can be employed to measure single molecule conductivity. They investigated the electrical properties of non-rigid alkanethiol molecules bonded between two gold contacts. To ensure spontaneous attachment and detachment of molecules between tip and surface, the feedback loop was disabled. The difference in the tunnelling current monitored in the absence and presence of molecules in the tip-substrate separation can be observed as a current jump, see Figure 3.6. The occurrence of several molecules trapped within the gap was recorded as multiples of a basic current jump. [132] The tunneling current can be monitored either as a function of distance (s), as the molecule is stretched in a junction or time (t) in which current jumps are attributed to molecules forming and breaking contact. The methods are referred to as $I(s)$ [133] and $I(t)$,[5] respectively.
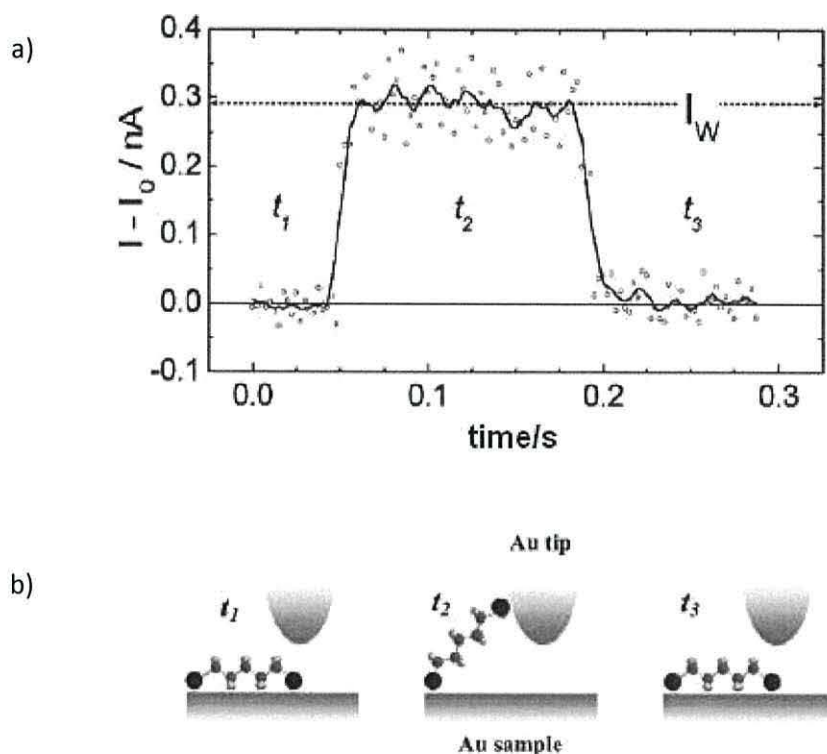

Figure 3.6: a) the representation of current jumps recorded on the gold substrate; b) the schematic diagram of spontaneous adsorption and desorption of molecules within the tip-sample gap. At t_1, t_3 molecules are detached from the tip, whereas at t_2 molecules are attached to the tip as well as the substrate. Taken from a reference 5.

4 Molecular rectification

Although Feynman explored the benefits that might occur from being able to control the arrangement of molecules on a small scale, the development of molecular electronics, a new area of physics, defined as a "study of molecular properties that may lead to signal processing"[134] was initiated in 1974 by Aviram and Ratner.[135] They proposed a rectifying system, composed of a donor-bridge-acceptor structure, that under applied voltage would conduct electricity better in one direction that in the other. The concept was analogous to that of semiconductor p-n junctions, in which silicon with electron-poor, p-type (doped with positive metallic ions) and electron-rich, n-type (doped with negative ions) regions is placed between two electrodes. The barrier which arises at the interface results in the easier flow of electrons from the electron-rich side. The effectivness of this system as an electronic device stems from its ability to convert an alternating current (AC) into direct current (DC) resulting in electronic rectification. The occurring rectification process can be monitored by observation of current-voltage characteristics, which is displayed as the suppression of current in one direction. Such rectifying junctions can also be used in the fabrication of solar cells.[136]

4.1 The Aviram and Ratner model

The precursory model of molecular rectification was predicted by Aviram and Ratner, who suggested that organic molecules can act as molecular rectifying diodes.[135] In order to realise such an efficient rectifier, the molecule should mimic the properties of a solid-state p-n junction diode. Aviram and Ratner proposed that suitable molecules conforming to this specification need to be composed of an electron-poor moiety connected by an insulating σ-bonded alkane bridge to an electron-rich moiety. Electron-withdrawing functional groups decrease the electron density in the aromatic π system and thus raise the electron affinity in such a system. Hence, the subunit becomes an electron acceptor (p-type analogue). Conversely, the electron-donating substituent enhances the π-electron density resulting in lowering the ionisation potential, so that the subunit becomes an electron donor (n-type analogue). According to calculations, such D-σ-A molecule, when placed between two electrodes, would exhibit the rectification of

current with the preferred electron flow in the cathode-acceptor-donor-anode direction.[135] However, for this system's rectifying behaviour to be achieved, donor (D) and acceptor (A) π subunits must be effectively separated from each other to provide the potential barrier for electrons moving from one end to the other. Otherwise, the resonance of the entire molecule would be reached very quickly, and consequently the rectification ability would be lost.

The first organic molecule that was expected to demonstrate rectifying properties, was hemiquinone, see Figure 4.1, with methoxy (-OCH$_3$) groups being the donor subunit whith the benzoquinone group being the acceptor.[137] The donor and acceptor moieties of this molecule are separated by a saturated σ-bridge.
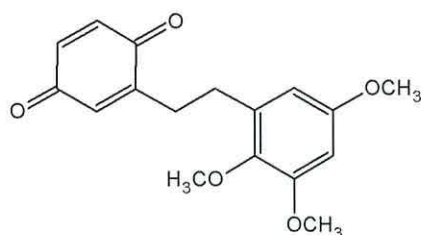

Figure 4.1 Structure of D-σ-A molecule composed of the quinone acceptor and catechol donor.

According to Aviram and Ratner's theoretical establishment, the molecule shown in Figure 4.2, was believed to be the classic example of the molecular rectifier, because is comprised of a strong electron donor (TTF-tetrathiafulvalene) and a strong electron acceptor (TCNQ-tetracyanoquinodimethane). These two moieties are linked by a triple methylene σ-bridge instead of a single, as in a molecule presented above, to ensure molecular rigidity. However such a molecule has never been synthesised.
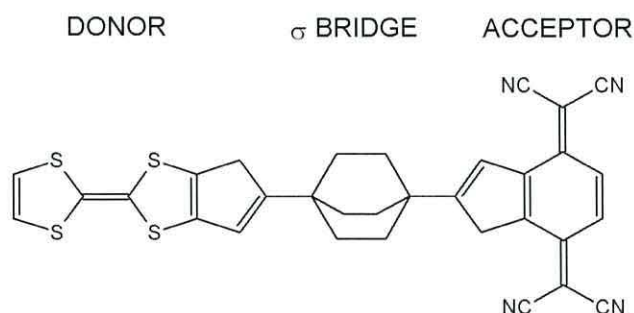

Figure 4.2 Gedankenmolekül (D-σ-A molecule) proposed by Aviram and Ratner as a molecular rectifier.[135]

The mechanism of rectification is associated with the fact that the excited state D^+-σ-A^- is relatively accessible from the ground state D-σ-A in comparison to the opposite state D^--σ-A^+, which is inaccessible.[138] When such a system is assembled between two electrodes, it is more likely for rectification to occur and as a result of the application of a suitable bias voltage; highly asymmetric *I-V* characteristics should be observed. The concept of rectifying behaviour can be explained by examining the energy-level diagram for this system, which is illustrated in Figure 4.3.
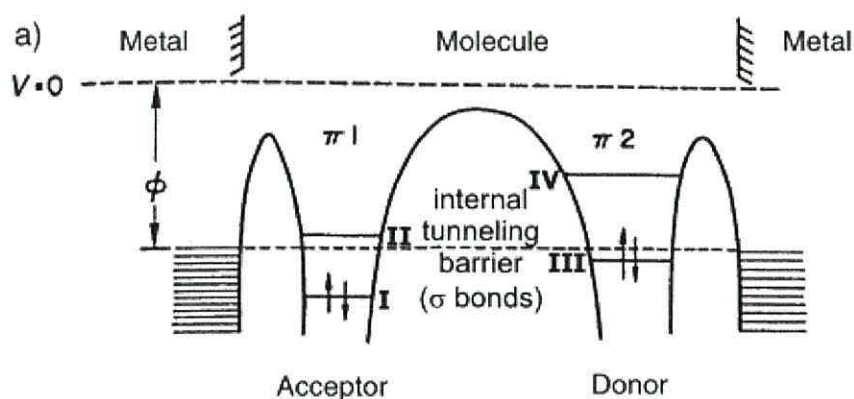

Figure 4.3 Energy diagram of the proposed Aviram-Ratner rectifier placed between electrodes.[135]

Upon the application of a forward bias, the electrons pass through the molecule in a two stage process. The first step involves the transfer of electrons from the cathode to the acceptor and from the donor to the anode. However, it should be noted, that the electron transfer from the cathode is possible when the Fermi level of metal aligns with the lowest unoccupied molecular orbital (LUMO) of the acceptor, see Figure 4.4, represented by "A". When the energy level of the anode, is lowered sufficiently, then electrons can flow from the highest occupied molecular orbital (HOMO) of the donor to the anode, see Figure 4.4, represented by "C". Thus, when the energy of the acceptor LUMO is close enough to the energy of the donor HOMO, the intramolecular tunneling of electrons from the LUMO of the acceptor, towards the HOMO of the donor, can be observed in the second step, see Figure 4.4, represented by "B". As a result of moving the electron from left to right under forward bias, the D-σ-A molecule's ground state is restored.
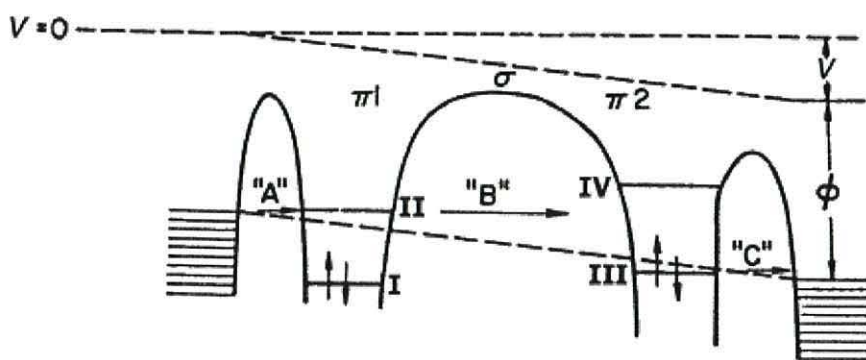
Figure 4.4 Energy diagram of the proposed Aviram-Ratner molecule under forward voltage.[135]

Under reverse bias (see Figure 4.5), for a similar process to occur, the Fermi level of the electrode adjacent to the acceptor would need to be brought below the HOMO (I) of the acceptor allowing electron transfer from I to the metal. Thus, the electrons can flow from III to I. However this process is not energetically efficient, as a much higher initiate threshold voltage is required to fit the larger gap between the HOMO of the acceptor and LUMO of the donor.

Figure 4.5 Energy diagram of proposed Aviram-Ratner rectifier under reverse voltage.[135]

Since the Aviram and Ratner proposal, numerous different systems have been studied, including alternative D-π-A molecules with twisted π bridge instead of σ-bonded.[139,140,141,142] Other theories related to this subject have also risen (section 4.2, 4.3.6).

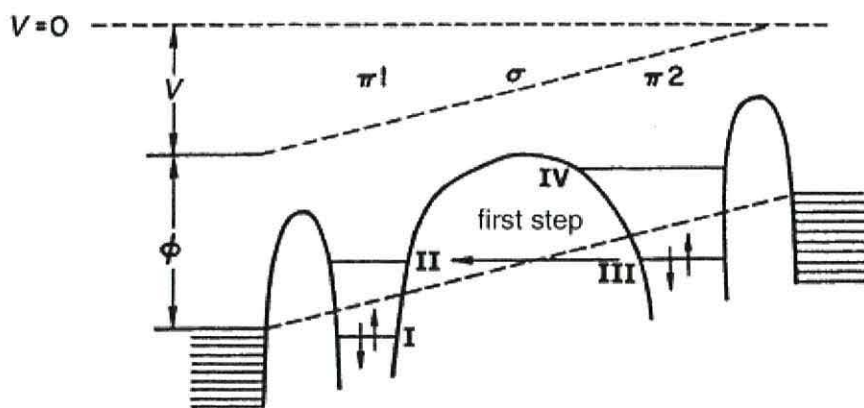## 4.2   Ellenbogen and Love rectifier

A minor variation of the Aviram and Ratner model[135] was proposed by Ellenbogen and Love.[143] Their theoretical rectifying system utilises chemically doped polyphenylene-based molecular wires as the conductive backbone. This planar structure was applied to enhance the conductive properties of the diode. Altough such a system differs slightly from that demonstrated by Aviram and Ratner, the operational principle of both designs is based on the same concept of a molecular rectifying diode. This means that the molecule proposed by Ellenbogen and Love, see Figure 4.6, is composed of both, electron releasing (X, commonly groups such as: $-NH_2$, $-OH$, CH_3, CH_2CH_3) and electron withdrawing (Y, commonly groups such as: $-NO_2$, $-CN$, $-CHO$, COR', R'-an aliphatic chain) substituent groups connected by a semi-insulating bridge (R, most likely aliphatic dimethylene chain). This potential energy barrier prevents the equilibrium of electron densities in the substituted complexes on either side of the molecule, however, still enables for electrons to pass through under a voltage bias.
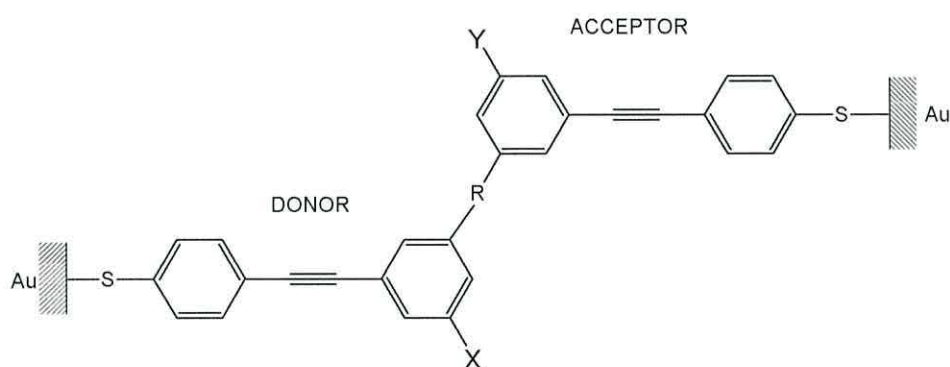
Figure 4.6 Molecular structure of polyphenylene-based molecular rectifying diode proposed by Ellenbogen and Love.[143] X-donor substituent (NH_3, $-OH$, $-CH_3$), Y-acceptor substituent ($-NO_2$, $-CN$, $-CHO$), R-σ bridged barrier (CH_2 or CH_2CH_2).

As can be seen in Figure 4.6, on the left side of the insulating barrier, R, an electron-releasing group (X) is bonded to an aromatic ring. This results in an increased electron density of the ring. The additional repulsive interactions among the electrons within the donor "half" of the molecule occur and consequently raise the energy level of the HOMO and LUMO. On the other side of the central barrier, an electron-withdrawing substituent group (Y) is linked to an aromatic ring, and thus the electron density is lowered causing reduction of electron repulsion in the acceptor "half". This affects the

HOMO and LUMO, so that the energy levels of these molecular orbitals are lowered. These electron releasing and withdrawing substituents bound to a single molecule were named as "intramolecular dopants".

As a result of the above description, the energy levels of the π-orbitals in both (sub complexes) halves of the molecule are correlated to the presence of intramolecular dopants even when no external bias is applied, see Figure 4.7.
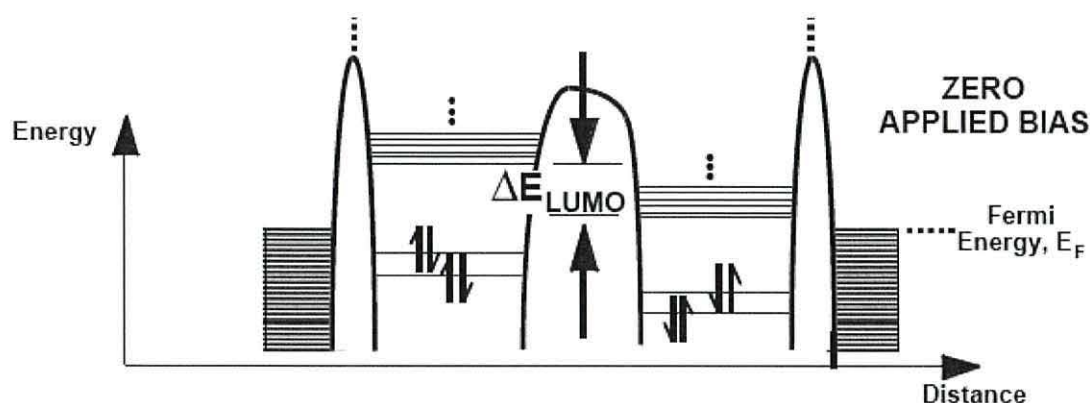
Figure 4.7 Energy diagram of Ellenbogen and Love model.[143]

Upon the application of a forward bias, the voltage was balanced to be higher on the left-hand electrode than on the right one. Consequently, the electrons in the occupied levels of the high-energy electrode on the right were induced to flow through the insulating barrier of the molecule until the lower energy left-hand contact was reached. However, electrons were able to tunnel from right to left only, if the applied voltage bias was enough to raise the Fermi energy of the right-hand electrode to at least as high as the LUMO energy of the acceptor subunit. Once the right to left tunnelling of electrons occurred, electrons could flow again from the LUMO of the acceptor subunit to the donor LUMO subunit, see Figure 4.8.

Figure 4.8 Energy diagram of Ellenbogen and Love model under forward voltage.[143]

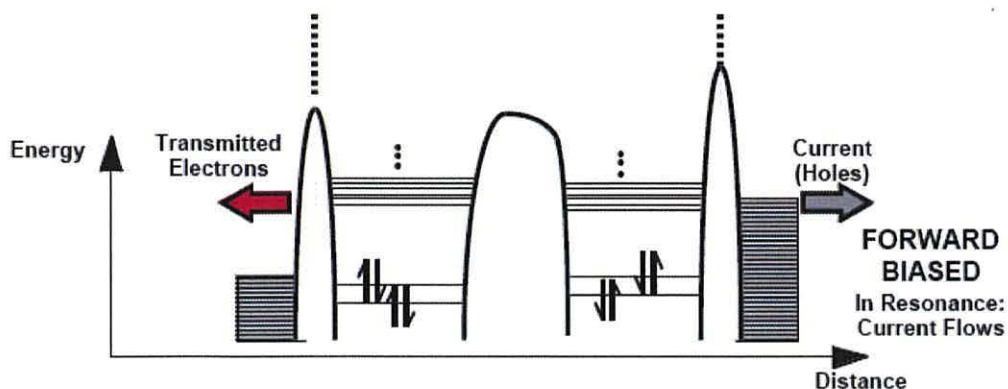At reverse bias, the positive bias was applied on the right-hand electrode causing an increase of Fermi energy on the left, and a decrease on the right, so that electrons can tunnel from left electrode through the central insulating barrier of the molecule to the right one. However, for this left to right electron transfer to occur, the applied voltage bias must be sufficient to raise the left electrode Fermi level, so that the donor and acceptor LUMO's would be at least brought in line with each other, see Figure 4.9.
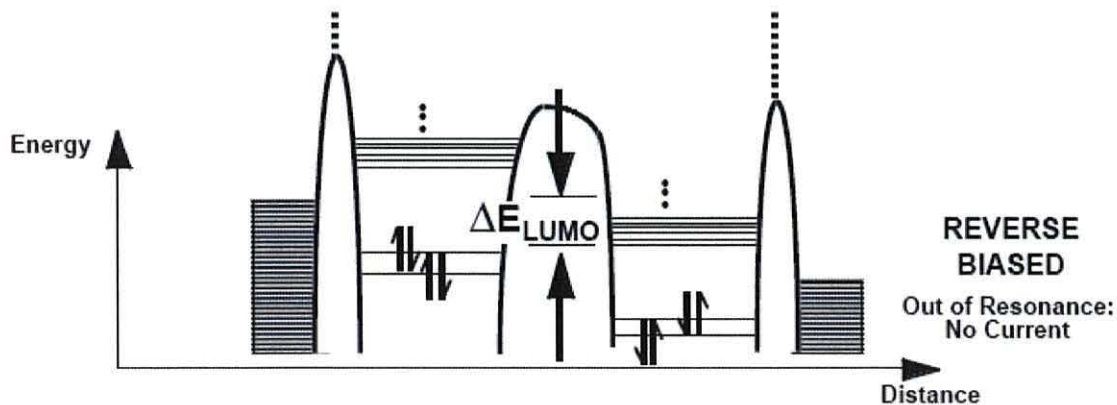
Figure 4.9 Energy diagram of Ellenbogen and Love model under reverse voltage.[143]

For conduction to occur, the applied voltage in the case of reverse bias needed to raise the Fermi energy of the left electrode must be much greater than in forward bias mechanism. This is due to the presence of intramolecular dopants which affected the energy level of donor and acceptor halves of the molecule beforehand. Therefore, the molecule can exhibit rectification behaviour. However, the system described above has not been verified so far by any experimental studies.

4.3   Molecular rectifiers

4.3.1 The Aviram-Ratner's TTF-TCNQ rectifier system

The challenge of synthesising a TTF-TCNQ hybrid molecule has become the subject of numerous attempts since Aviram and Ratner's theoretical paper.[135] The first who claimed the achievement of covalently linking TTF and TCNQ was Hertzler.[144] However the product of the reaction TTF-diisocyanate with TCNQ-dialcohol was characterised only by elemental analysis and electrical conductivity. In 1984 Panetta *et al.*[145] reported the synthesis of a TTF-TCNQ donor-acceptor molecule, see Figure 4.10. Unfortunately, the obtained product tended to coexist in zwitterionic and neutral states which were found to be inseparable.
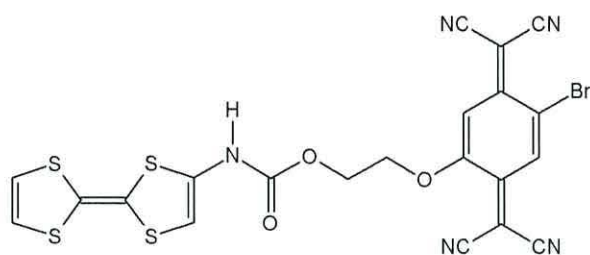

Figure 4.10 Molecular structure of possible rectifier molecule.[145]

Although the TTF-TCNQ hybrid structure has been a topic revisited in further research,[146,147] the successful synthesis of a well-characterised TTF-TCNQ donor-acceptor was reported by Perepichka *et al.*[148]
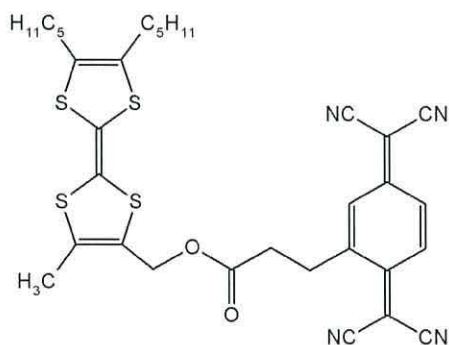

Figure 4.11 The structure of TTF-σ-TCNQ donor-acceptor.[148]

Detailed studies of the obtained product, which is shown in Figure 4.11, exhibited its ability to form high quality Y-type LB films on different substrates, however poorly conductive. This was explained by the molecular arrangement of the TCNQ moiety, which deposits flat on the surface whilst the TTF part makes an angle of around 45° with the surface, according to the calculation of molecular area and monolayer thickness.[148] The specific film arrangement was found to prevent donor-acceptor interaction between moieties. Analysis also predicted an unprecedentedly low HOMO-LUMO gap that should cause the facile transfer of electron. However, the rectifying behaviour of such a donor-acceptor molecule has remained unrealised due to the difficulties in establishing of reliable top electrode.

4.3.2 D-σ-A molecular rectifiers

Although the framework for the molecular rectification mechanism was introduced in the mid-1970's, numerous experiments have been performed with the invention of the scanning tunnelling microscope that enabled the obtainment of information about a studied material. [125,149] Since then, the fabrication of a rectifying molecule has become a challenge for many researchers. In 1988 Aviram et al.[150] attempted to synthesise and characterise an Aviram and Ratner type rectifier contacted by STM, see Figure 4.12. Although the resultant LB film exhibited asymmetrical I-V plots, the results were later withdrawn as further investigations suggested that such behaviour could have arisen from contact between the tip and the monolayer. Another conclusion stated that as a result of the sample exposure to the electric field, the realignment within the film could have occurred.
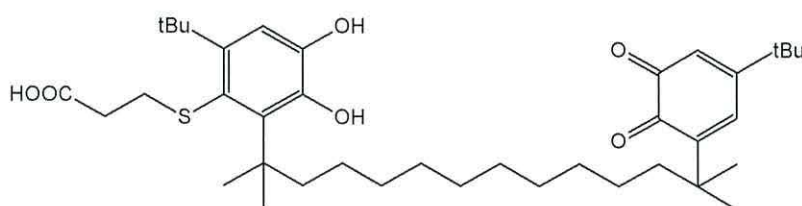
Figure 4.12 Molecular structure of the first attempted rectifier.[150]

Among the few D-σ-A molecules produced[151,152,153,154,155] Geddes and co-workers[156] reported rectification of a system composed of dodecyloxyphenyl (a weak electron donor) linked with a strong electron acceptor (bromo(hydroxyethoxy) tetracyanoquinodimethane) by a carbamate covalent bridge, see Figure 4.13. The D-σ-A molecule was deposited using the LB technique onto a platinum pad, whereas the counter electrode was made with magnesium overlaid by silver to suppress oxidation.
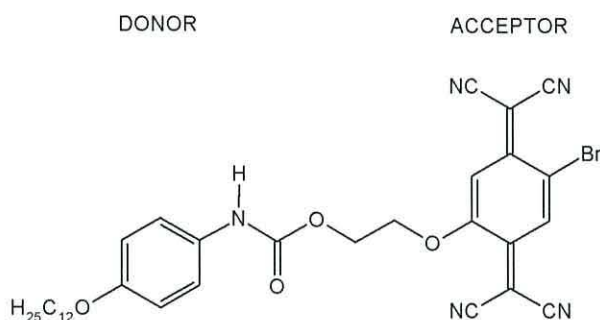
Figure 4.13 Chemical structure of DOP-C-BHTCNQ investigated by Geddes and co-workers.

When a voltage was applied across a system, the asymmetric current-voltage characteristics with the higher current in a positive quadrant were observed, see Figure 4.14. The enhancement of the asymmetry in such a way was believed to be indicated by the hydrophobic nature of the platinum electrode and thus the alignment of the molecule with the acceptor moiety being closer to the top contact.
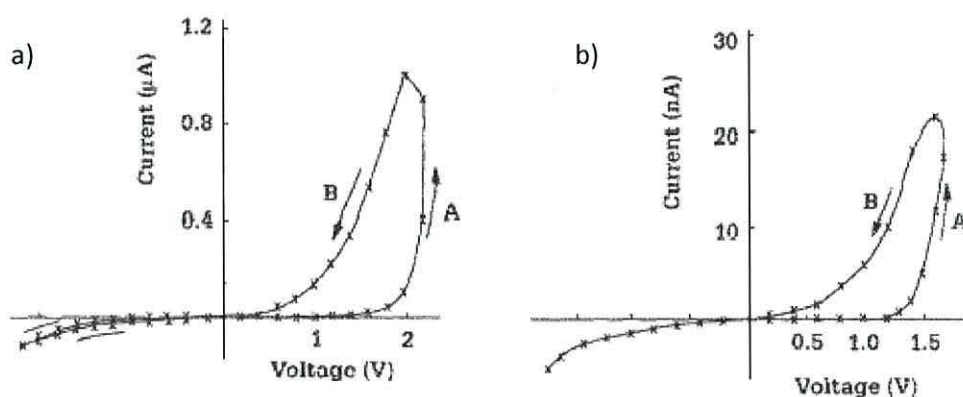
Figure 4.14 *I-V* characteristics for Pt | DOP-C-BHTCNQ | Mg, Ag system: a) initial behaviour; b) after annealing at 70 °C.[156]

Although, high values of the rectification were achieved, the origin of the asymmetry thought to be due to Schottky diode effects, as a Schottky barrier forms easily between Mg and TCNQ.[157] Additionally, the use of two different metallic electrodes could have caused the rectifying behaviour of the system. The long aliphatic chain could be also the factor contributing to the observed results. Moreover, the appearance of hysteresis might suggest a change in the molecule's alignment during STM measurements due to the presence of a flexible bridge.[159]

Most recent examples of molecular rectifiers discussed in numerous research publications have been focused on a π-bridge system which does not follow entirely the Aviram and Ratner specification. Moreover, those σ-bridged systems studied so far were surrounded by controversy over the origin of rectification. However, the recent report opposes that trend. Ho *et al.* developed the first molecular tunnelling devices based on D-σ-A system.[158] The proposed molecules, see Figure 4.15 were believed to be the reliable candidates for molecular electronic devices due to the composition of strong electron-donor and electron-acceptor moieties and the presence of aliphatic chains which enabled their deposition by the LB technique.
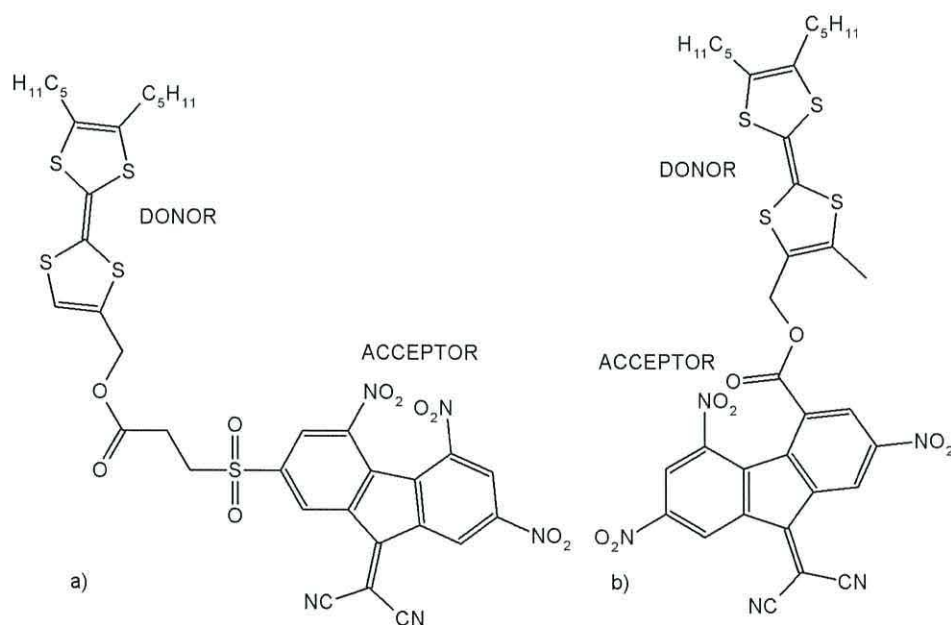

Figure 4.15 TTF donor-σ-acceptor molecules, as proposed by Ho *et. al.*[158]

Studies of the molecule **a** revealed that a long and flexible σ-bridge provided an unwanted head-to-tail conformation[158] with additional tunnelling resistance.[166] Therefore, the electrical investigations were performed on the **b** D-σ-A molecule with shorter σ linker. The molecule, when sandwiched between two conductive electrodes exhibited electrical asymmetry with a value of rectification ratio related to the area per molecule. It was also confirmed, that the system was stable with repeated cycling of the applied bias. The direction of rectification was demonstrated to be dependent on the electrode, and varied for n-Si/TTF-σ-A/Ti and Au/ TTF-σ-A/$C_{16}H_{33}S$-Hg. The rectifying behaviour was attributed to the studied junctions despite the use of the oxidisable titanium contact in previous device. Ho *et al.* claimed to control the rate of rectification by using a vacuum during the deposition of Ti.[158] Moreover, the high reactivity of titanium would cause the cleavage of terminal C-H bonds, and prevent the further penetration of Ti atoms within the film as a result of the layer of titanium carbide formed on the studied surface.[158] To investigate the impact of the electrodes on the rectification, the electronic studies were carried out on the same molecule placed between gold and mercury contacts. The *I-V* characteristics of the latter system were also asymmetrical, albeit in the opposite direction to those stated above. Such behaviour has not been entirely explained, however it was believed that the low HOMO-LUMO gap might change the ground neutral state into zwitterionic in the mercury junction.

4.3.3 Rectification from zwitterionic molecules.

Continuing the work of Geddes and co-workers[156,157] and Ashwell *et al.*[159] reported a strong rectification ratio for the zwitterionic molecule $C_{16}H_{33}Q3CNQ$, see Figure 4.16, which represented a novel π bridged donor-acceptor system.

Electron flow at forward bias
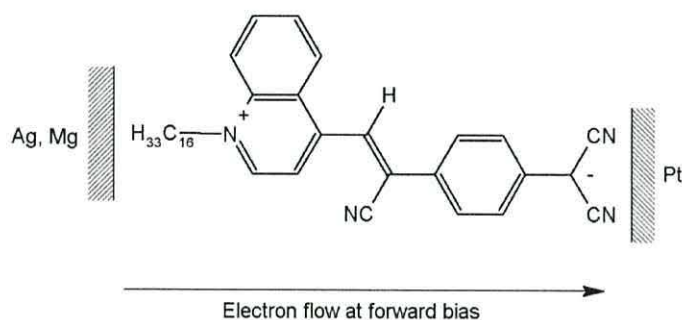
Figure 4.16 The chemical structure of (Z)-β-N-hexadecyl-4-quinolinium-α-cyano-4-styryldicyanomethanide ($C_{16}H_{33}Q3CNQ$).

The junction was generated by sandwiching of an LB film of a dye between two electrodes, where evaporated magnesium electrode was protected by non-oxidising silver. The STM measurements revealed *I-V* characteristics, see Figure 4.17, with the current flow preferred in one direction.
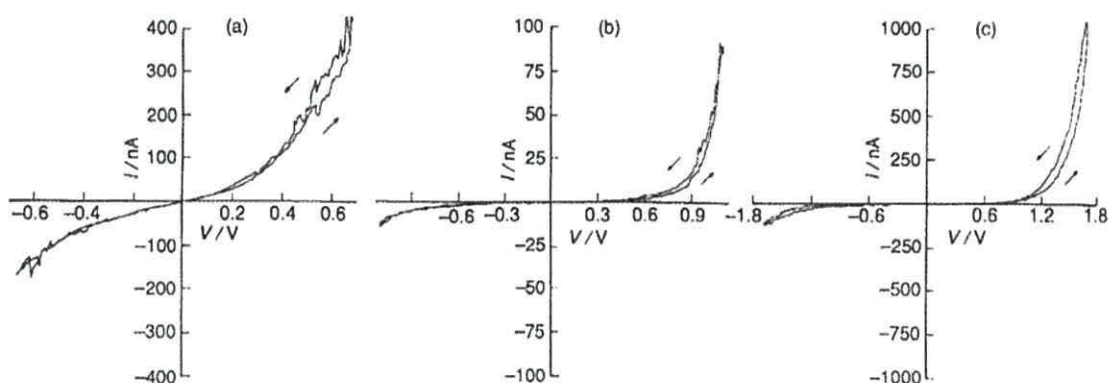
Figure 4.17 *I-V* characteristics from Ashwell's zwitterions.[159]

Such a system was attributed to the Aviram and Ratner model, even though, the active part of the molecule consists of a donor (the tricyanoquinodimethanide ($3CNQ^-$) moiety) and an acceptor (quinolinium moiety) separated by sterically hindered π bridge. Electron tunnelling was observed in the same direction as was presented for a D-σ-A system. The mechanism of the electron motion through the junction can be summarised as follow. In the first step, an electron is transferred from the Mg anode to quinolinum cation (D^+) and simultaneously from the acceptor (A^-) to the platinum cathode. The second step indicated the transfer from the donor moiety (D^0) to the acceptor one (A^0).

$$Mg \mid D^+\text{-}\pi\text{-}A^- \mid Pt \rightarrow Mg \mid D^0\text{-} \pi\text{-}A^0 \mid Pt \rightarrow Mg \mid D^+\text{-}\pi\text{-}A^- \mid Pt$$
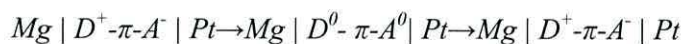
However, it was noted that this mechanism may not be the only interpretation of the obtained rectification, as oxidation of the magnesium electrode could result in a Schottky barrier.

Evidence suggesting the rectifying behaviour being molecular in origin despite using magnesium electrode in the junction's fabrication was provided by Martin *et al.*[160] The magnesium was chosen again, to minimise the thermal damage of the organic film during electrode evaporation.[157] In the reported experiment, the molecule was separated from metal electrodes (Mg, Ag) by ω-tricosenoic acid multilayer to prevent the molecule's chemical interaction with the electrodes, and thus the Schottky barrier effect.[181] The system Ag | 22TA | $C_{16}H_{33}Q$-3CNQ | 22TA | Mg | Ag exhibited asymmetry with an enhanced current in the positive bias, 4.18, similar to behaviour of the film comprising only zwitterionic molecules. However, the current of the latter structure was around 10 times larger than the composite junction.[161] To support the hypothesis of rectification being attributable to the molecule, the active zwitterionic layers were bleached. As expected, the behaviour of the film was modified[162] in such a way that no electrical asymmetry was observed when the LB film was bleached by acidification, see Figure 4.18.[163]
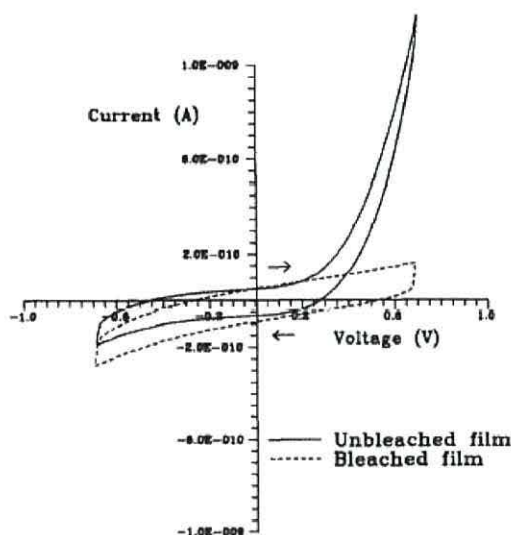

Figure 4.18 *I-V* curves for bleached and unbleached film junctions, copied from reference 163.

The presented sets of results would suggest that the donor-π-acceptor system plays a dominant role in providing the asymmetrical *I-V* plots. However, the authors concluded that work on a better understanding of the rectification mechanism must be continued.

In 2001, Xu *et al.*[164] obtained unambiguous molecular asymmetry from a $C_{16}H_{33}Q3CNQ$ dye sandwiched between Au electrodes, see Figure 4.19. In order to reduce damage to the LB film, a special "cold gold" deposition technique[165] was applied. In this technique gold undergoes multiple scattering by argon (at 4×10^{-3} Torr); the substrate is separated by a barrier, a copper plate cooled to liquid nitrogen temperature for thermal protection. [164,182]
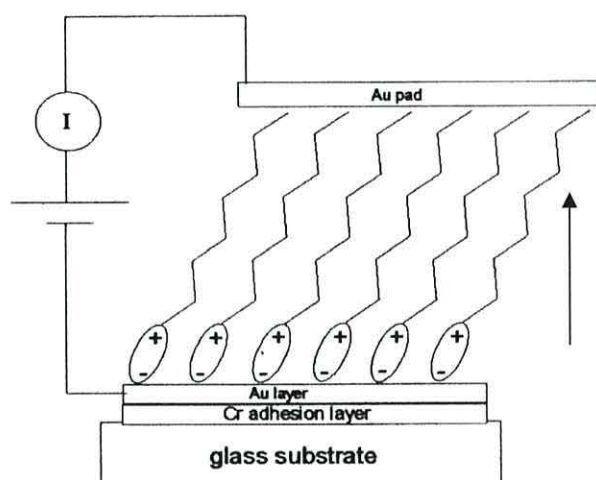
Figure 4.19 The system composed of LB monolayer of $C_{16}H_{33}Q3CNQ$ sandwiched between Au electrodes with indicated direction of electron flow under forward bias.

The electrical measurements of the Au | $C_{16}H_{33}$-Q3CNQ | Au structure revealed rectifying behaviour for both, monolayer and multilayer systems, with rectification ratios of up to 27.5 at ± 2.2 V confirming the molecular origin of the rectification. However, the asymmetry tended to decrease with the number of cycles. The occurrence of such behaviour could be explained by reorientation of the molecule under application of the electric field or eventually the chemical degradation stemming from the irreversible electrochemical oxidation of the molecule.

Studies on a multilayer film of $C_{16}H_{33}$-Q3CNQ deposited in the same manner as that presented by Xu *et al.*[164] were reported by Okazaki *et al.*[166] This experiment was

performed at various temperatures ranging from 8 to 295 K in order to eliminate rectification dominated by thermal effects and to determine the conduction mechanism. Initial measurements of the Au | ~ 20 layers of $C_{16}H_{33}$-Q3CNQ LB film | Au system exhibited rectification with the higher current in the positive quadrant. The same behaviour was recorded by Metzger.[182] After continuous application of a voltage for 20 minutes, the enhancement of current appeared in the opposite quadrant with rectification ratio of *ca.* 4 at the highest voltage ± 15V. Results suggested that the initial rectification stemmed from ionic contamination trapped within the film. Further investigations were performed, in order to explain the dependence of the current upon applied voltages. Theoretical calculations led to the conclusion that aliphatic tails in studied LB films provided a conduction barrier within the structure hence rectification behaviour originating from a hopping process.

Xu *et al.* designed and synthesised an analogue of TCNQ[167] believing that such a molecule would provide the rectification with the desired rectification ratio. The system was fabricated by sandwitching an LB monolayer between gold electrodes, see Figure 4.20.
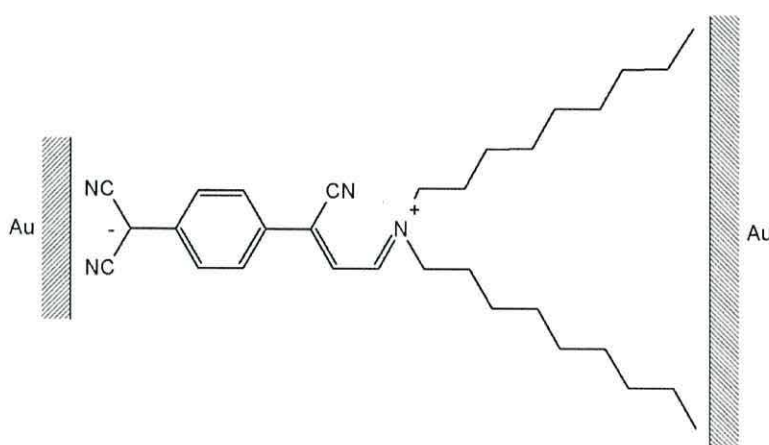

Figure 4.20 The structure of non-rectifying zwitterion, didecylammonium tricyanoquinodimethanide $(C_{10}H_{21})_2N^+$-3CNQ⁻.

Unfortunately, measurements revealed only a small rectification ratio of 1.4 at ± 1 V that was probably caused by the disorganisation of the molecules within the LB monolayer. It was also believed, that the character of the alkyl chains was not

sufficiently hydrophobic to maintain the parallel orientation of the molecules at the air-water interface.

In 2003 Ashwell et al.[168] designed and investigated the self-assembling analogue of $C_{16}H_{33}$-Q3CNQ, whose molecular structure is presented in Figure 4.21. The STM studies were performed on four different configurations. In the first two, the molecule was assembled onto gold-coated HOPG and a gold tip or decanethiol ($C_{10}H_{21}$-S) coated tip were used as the second electrode. The latter two configurations were fabricated by assembly of a dye on the tip that contacted with an uncoated or decanethiol-coated gold substrate, see Figure 4.21
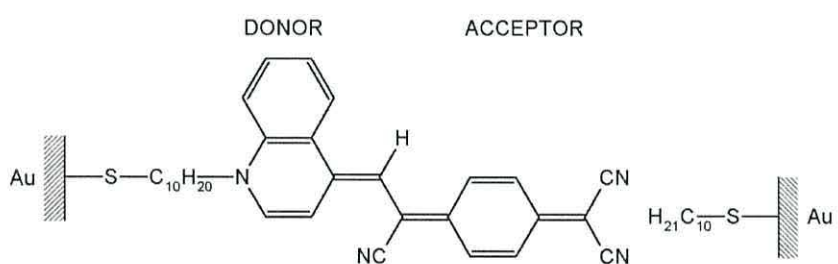
Figure 4.21 Self-assembled monolayer of 2-(4-{1-Cyano-2-[1-(10-methanesulfanyl-decyl)-1H-quinolin-4-ylidene]-ethylidene}-cyclohexa-2,5-dienylidene)-malononitrile chemisorbed on gold.

The detailed analysis revealed the asymmetric current-voltage characteristics for all four configurations. However, the slight reduction of a current was observed when the counter contact was coated with decanethiol. The obtained data also indicated that the central localisation of the chromophore with respect to both electrodes did not contribute to the rectification behaviour. Moreover, the reversed polarity of the rectification was recorded for the geometrically opposite configuration, i.e. the dye self-assembled on the tip. The occurrence of the higher current as illustrated in Figure 4.22 signifies the electrons flowing from the tip to the substrate, and thus suggests the electron-acceptor being the $C(CN)_2$ group. Consequently, the alignment of the molecules within monolayer film was consistent with the adoption of the quinonoid form, as shown in Figure 4.21 rather than the zwitterionic one, depicted for the LB deposited analogue. Although these results are in conflict with the previously reported,[164,166,169] further investigation suggested that zwitterionic form was polarisation induced.
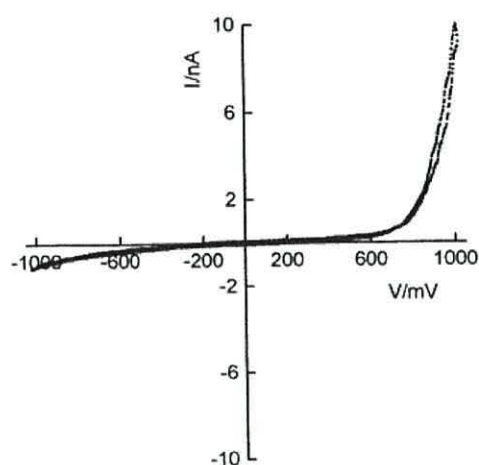
Figure 4.22 *I-V* curve of self-assembled monolayer for a dye-coated gold substrate and decanethiol coated tip. The bias voltage is applied to the sample electrode. Taken from reference 168.

4.3.4 Systems with oxidisable contacts

An experiment conducted in 1999 found rectification ratios in excess of 100 at ± 1 V in a D-σ-A Z-type multilayer system. Brady *et al.*[170] fabricated junctions based on the same principle as Geddes *et al.*,[156] in which the resultant LB film, of 3, 5 dinitrobenzyl 7-(1-oxohexylamino)-pyren-2-ylcarbamate, OHAPy-C-DNB, was transferred onto a silver substrate with magnesium contacts evaporated on the top, see Figure 4.23.
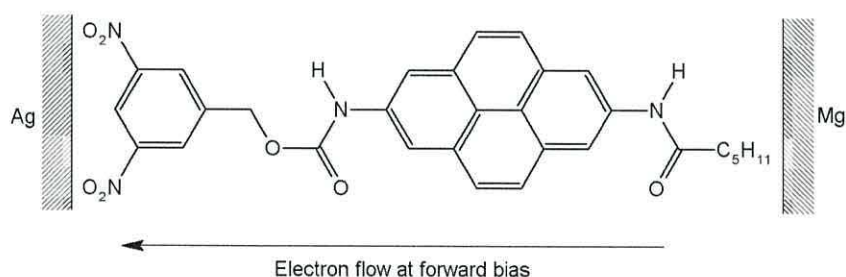
Figure 4.23 Possible rectifier (OHAPy-C-DNB) placed between metallic electrodes. Indicated direction of electron flow at forward bias.

Electrical studies of the junction exhibited asymmetrical characteristics with the current flow under forward bias in the opposite direction to that predicted by Aviram and Ratner,[135] illustrated in Figure 4.23. Such behaviour was supported by molecular modelling which indicated that the enhancement of a current was caused by electronic

alignment of molecular orbitals (HOMO and LUMO). Hence, according to the theory, under application of forward bias, the accessibility of the biopolar excited state increased resulting in the decreased size of the energy separation between HOMO and LUMO. This conduction mechanism, similar to that described by Ellenbogen and Love[143] would involve the electron flow between donor and electrode and acceptor and electrode followed by subsequent intramolecular relaxation. Although the asymmetrical characteristic was claimed to originate purely from the molecule, doubts remained, due to the possibility of a Schottky barrier forming by use of oxidisable magnesium electrodes.

Due to controversy surrounding the use of different electrodes which may contribute to the enhancement of the asymmetry, Metzger et al.[171] fabricated the rectifying junctions using the same, aluminium electrodes on both sides. Chen and Metzger [172] reported the investigation of the system depended on sandwitching an LB film of the zwitterionic dye between two aluminium electrodes, where the second electrode was added by evaporation. They performed the study of the Al | Al_2O_3 | $C_{16}H_{33}$-Q3CNQ | Al_2O_3| Al structure within the range of temperatures from 105 to 370 K. The film exhibited rectifying behaviour between these temperatures, suggesting that rectification could not be thermally activated, but it was not molecular in origin either. The asymmetrical behaviour was induced by Schottky barrier formed between one end of a molecule (presumably 3CNQ end) and Al electrode (Al easily oxidises on air).

Additionally, the authors demonstrated the advantages of applying the same electrodes on both sides, as in previous experiments[156,157,159] the choice of the counter contact was restricted by sublimation temperatures of many noble metals. Consequently, the electrode most used to protect the organic film from damage was a magnesium one, which unfortunately readily oxidises after exposure to air or reacts with the molecule creating Schottky barriers in the system. Although the rectification ratio improved, the assignment of such behaviour remained ambiguous.

More recently Vuillaume and co-workers[173] attempted to explain more detailed electron transfer mechanisms through the metal | $C_{16}H_{33}$-Q3CNQ | metal system and the role played by Al_2O_3 between the metal electrode (Al) and the LB film. The experimental data revealed three different types of behaviours for the Al | Al_2O_3 | $C_{16}H_{33}$-Q3CNQ |

$Al_2O_3|$ Al junctions, including electrical asymmetry in the positive quadrant with a rectification ratio of *ca.* 20 at $\pm$ 1 V, symmetrical *I-V* plots and asymmetrical *I-V* characteristics with the higher current in a negative quadrant (rectification ratio of *ca.* 5 at $\pm$ 1 V). The observation of positively rectifying junctions corresponded to the modified model[170] of rectification being in agreement with Aviram and Ratner proposal.[135] Junctions exhibiting no rectification were claimed to indicate the bleaching effect, caused by either ionic contamination in the subphase during LB film formation or by light exposure. The fact that rectification occurred in a negative quadrant was thought to be dominated by defects in the LB film. The observations of these three classes of junction suggest the molecular rearrangement within the monolayer that may take place after LB deposition,[174] during storage periods,[173] metal deposition[156] or electrical measurements.[175]

The alternative explanation for the occurrence of a variation in the behaviour of the studied system proposed the geometrical asymmetry within the electrode | LB film | electrode structure. In the case of the experiment described above, the rectification in the positive quadrant might have resulted from the closer alignment of the zwitterion molecules to the top electrode than to the bottom one, whereas the opposite rectification would arise from the reverse array. A symmetric junction would appear at equal distances from both electrodes.

Although this study reported the rectification induced by the molecule, it should be recognised that the aluminium electrodes are not oxide free, so that the oxide may be formed on the surface of the contact, in the same manner as in the previous reports, where the oxide covered the magnesium electrode.[174]

The reports claiming molecular rectification from films contacted by Ti/TiO_2[176, 177] have also remained unconvincing, due to the ease of titanium oxidation after exposure to air, whose oxides are most likely to form Schottky rectifiers.[178] The investigation of the electrical behaviour by use of titanium electrode was published by Chang *et al.*[176] They observed a high rectification ratio of 5×10^5 at $\pm$ 2.3V for a SAM of alkoxynaphthalene thiol assembled onto platinum electrode, whereas the counter titanium contact was deposited on top, see Figure 4.24.
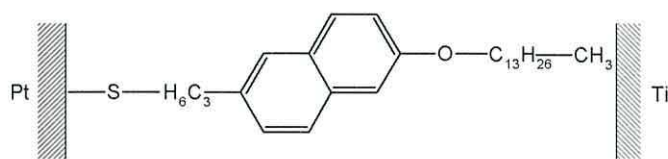
Figure 4.24 Chang's molecule.

The provided explanation for the large rectification ratio was that the asymmetry was partially caused by the different work functions of Pt and Ti and the asymmetric tunnelling barriers of the molecule.[188,191] The rectification was later attributed to a oxide-induced Schottky barrier,[179] rather than any molecular effects.

Molecular rectification was also claimed by McCreery *et al.*,[180] who reported asymmetrical characteristics of nitroazobenzene (NAB) when sandwiched between a pyrolysed photoresist substrate (PPF) and a titanium top electrode. When a positive bias was applied to PPF electrode, the authors observed greater electron transfer compared to that at negative voltage. This behaviour was explained to occur due to the existence of the molecule in two forms; phenyl, under no bias, which 'switches' to quinoid under the application of positive bias, indicated in Figure 4.25 below. The enhanced conductivity under forward bias was believed to result from the closer electronic alignment of the HOMO and LUMO in the quinoid form.
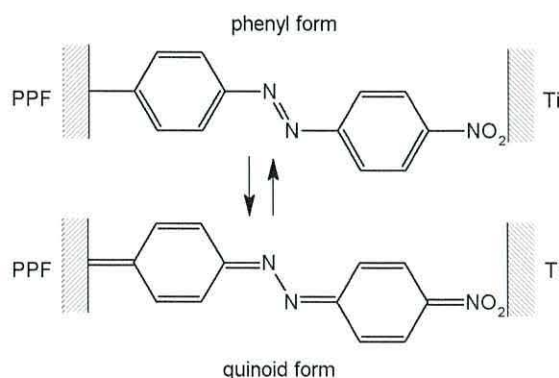

Figure 4.25 Representation of phenyl and quinoid forms of NAB.

Despite the belief that the origin of the strong asymmetry (rectification ratio of up to 600 at ± 2 V) arose from the 'switching' effect, further verifications confirmed the presence of titanium oxide and thus retracted the molecular effect.[180]

Molecular films contacted by oxidisable electrodes usually exhibited high rectification ratios. However, the electrical asymmetry in these systems is more likely to be induced by Schottky barriers at the oxidisable contact. The Schottky barrier will fail to provide the conclusive results about the rectifier properties of the molecular diode. The Schottky-Mott theory[181] described this phenomenon as the difference between the surface dipole of the metal and that of the semiconductor.

The Schottky barrier has troubled scientists in many fields of research. However the problem of oxidation and differences in work function of electrodes was discarded once the oxide-free gold electrodes were introduced as candidates for fabrication of rectifying junctions.[182]

4.3.5 Rectification from other D-π-A systems

The first example of rectification that may be unambiguously assigned to the molecule's structure was reported by Ashwell *et al.* for LB films of cationic donor-(π-bridge)-acceptor dyes.[183] The rectifying junction was fabricated by the co-deposition of 100 layers of the molecule, shown in Figure 4.26 in a ratio 1:1 with octadecanoic acid and placement between gold electrodes. Electrical characterisation of this system demonstrated asymmetry with rectification ratios of 70 at ±1 V.

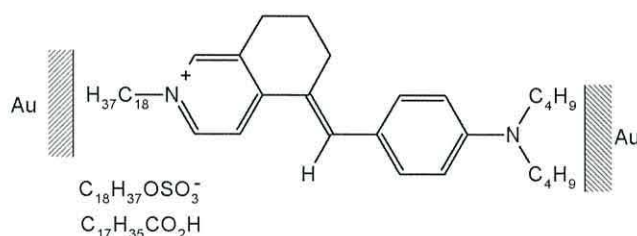**Figure 4.26** Au/(LB film)/Au device showing the isoquinolinium rectifying molecule and octadecanoic acid.

In order to highlight the influence of the alkyl chain length on the through-plane conductivity, the same group performed further experiments on two analogues[184] illustrated in Figure 4.27. Both systems were formed by the LB deposition of the cationic molecule in a 1: 1 ratio with an octadecyl sulfate counterion.
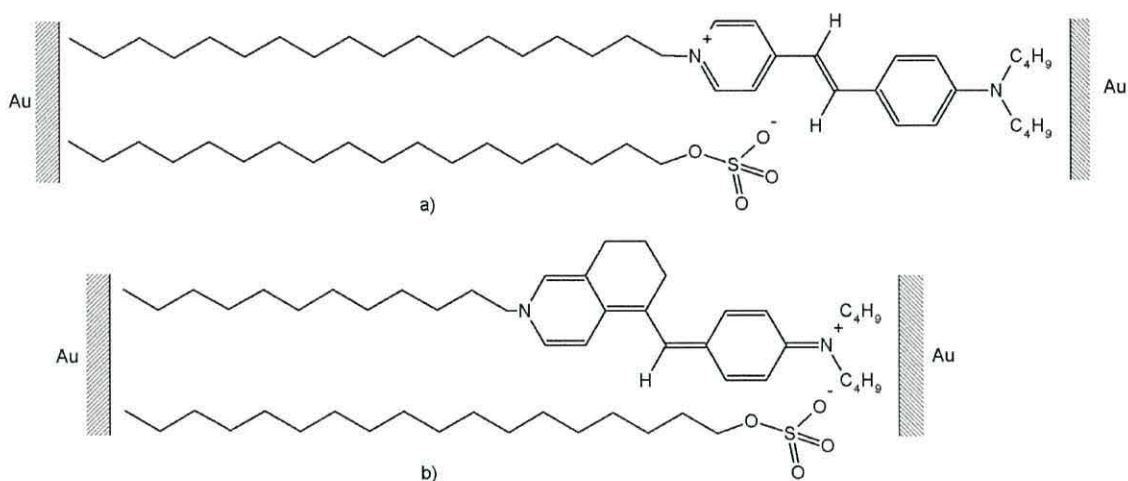
Figure 4.27 Molecular structure of the isoquinolinium hemicyanine showing the lengths of the octadecyl a) and dodecyl b) analogues relative to the length of the octadecyl sulfate counterion.

When placed between gold electrodes, both analogues revealed asymmetrical *I-V* characteristics, however unexpectedly the current enhancement occurred in inversed quadrants, as shown in Figure 4.28.

Figure 4.28 *I-V* characteristics of the dodecyl (x) and octadecyl (•) analogues of isoquinolinium hemicyanine, which rectify in the positive and negative quadrants, respectively. Taken from reference 184.

The difference in behaviour was assumed to stem from the dipole reversal effect that induced the relocation of the negatively charged counterion to the opposite end of the

chromophore. This is manifested in the molecule's structure by transition from benzenoid to quinonoid form. Supporting evidence was provided by theoretical calculations.

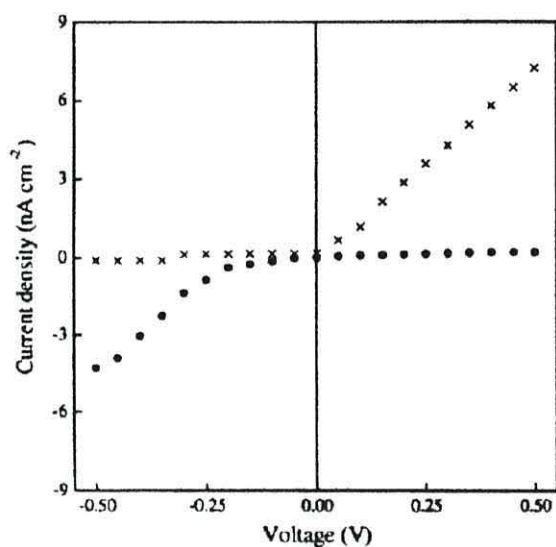Further work was performed on another hemicyanine derivative, see Figure 4.29. The LB film was deposited and subsequently five Z-type layers of such a dye were sandwitched between gold electrodes.[185] The molecule exhibited rectification consistent with the Aviram and Ratner[135] type mechanism. Moreover, the observed disappearance of the electrical asymmetry supported the previous conclusion that the position of the negatively charged sulfate counterion influences the film properties.
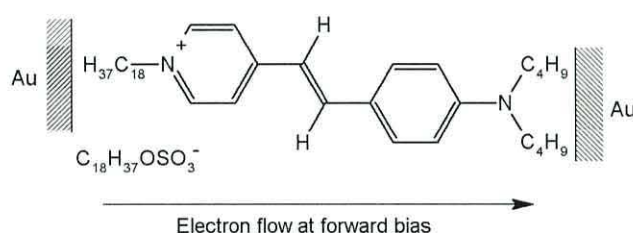
Figure 4.29 Au/(LB film)/Au device showing quinolinium rectifying molecule with indicated electron flow at forward bias.

A novel type of molecular rectifier featuring a chevron-shaped molecule, see Figure 4.30 was developed by Baldwin, Ashwell and Metzger *et al.*[186,187]
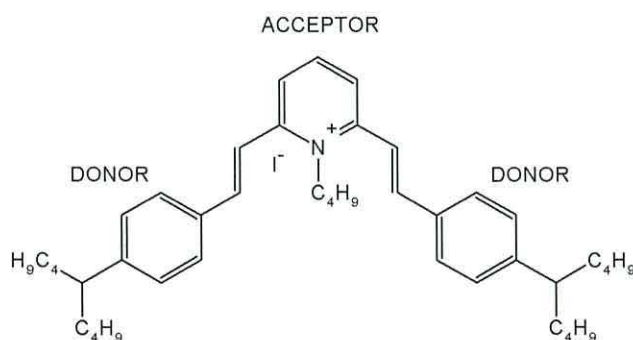
Figure 4.30 Molecular structure of chevron-shaped molecule.

This molecule, although lacking a long aliphatic chain usually required for LB alignment was deposited using such a technique. The successful alignment of the LB

film manifested itself by electrical asymmetry yielding rectification ratios of up to 60 at ± 1 V. However it was more likely, that the rectification arose from the back electron transfer from the iodide to the pyridinium ion rather than being assigned purely to the molecule. The detected chemisorption of the iodide to the gold made it an organic analogue of a Schottky barrier.[179]

Further investigations revealed that, as often happens with LB films, repeated measurements of the asymmetry showed it decreasing until entire disappearance, as a consequence of the realignment of the film caused by successive cycling of the voltage bias to the junction. Therefore, the exact alignment of the molecules on a surface, and more robust method of deposition would be required to affirm the unambiguous mechanism of rectification.

The observed gradual reorientation of molecules in an LB monolayer made research towards combining the advantages of LB assembly with those of self-assembly, the most promising. Due to the self-assembly technique, the disadvantages of LB films including a dependence on the length of the alkyl tail and the position of donor-acceptor moieties between electrodes have been overcome.

4.3.6 Asymmetric molecular geometry

Since the concept of molecular rectification was first proposed, this field of nanoscience has become one of the principal subjects of theoretical and experimental interest. Originally, the proposed model of the rectifying system applied only to donor-acceptor moieties, and the direction of the tunnelling current,[135] whereas a more recent one is concerned with the geometrical location of the molecule between electrodes. Krzeminski et al.[188] performed a theoretical study of an LB film of the previously investigated zwitterionic molecule, $C_{16}H_{33}Q3CNQ$[171,189] sandwiched between aluminium or gold electrodes. According to the calculations of Krzeminski et al.,[188] the π-bridge in this D-π-A molecule does not constitute a sufficient barrier between D and A moieties, and thus molecular orbitals were delocalised over the entire molecule. It was indicated that the rectifying behaviour of the molecule is dependent on the position of the LUMO and HOMO with respect to the Fermi level of the electrode before applied

bias, as well as the location after applied bias. The placement of an electroactive conjugated unit between electrodes was also stated to be an important factor towards the asymmetry of the molecule, for this reason the rectification was predicted to be affected by the length of the alkyl chain, i.e. the shorter the alkyl chain, the more symmetrical an *I-V* curve was observed. Moreover, the asymmetric position of the chromophore could result in the rectification being in contrary to the one proposed by Aviram and Ratner.[135] To supplement the mechanism described by Krzeminski *et al.*,[188] Kornilovitch *et al.*[190] reported that asymmetrical *I-V* characteristics with high rectification ratios (based on theoretical calculations) needed only to consist of one conductive subunit located closer to one of the electrodes. The HOMO and LUMO of this electroactive unit placed asymmetrically with respect to the Fermi level of the electrode do not require a complex molecule, and thus the mechanism of molecular rectification can be realised by utilising more simple molecules, such as the one illustrated in Figure 4.31. Due to the assumption that the rectifying behaviour is more likely to be attributable to asymmetric tunnelling barriers produced by the asymmetrical positioning of the molecule, the molecule below was named as "an asymmetric tunnelling barrier molecular rectifier".
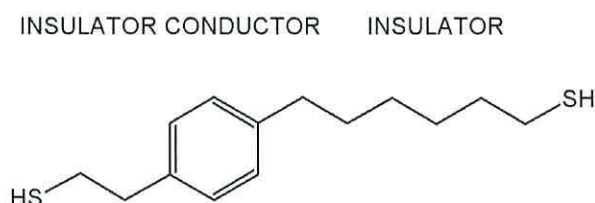
Figure 4.31 Schematic representation of an asymmetric tunnelling barrier on the top, Kornilovitch's proposed molecular rectifier.[190]

This molecule can be placed between two metal electrodes (gold or silver) owing to two "clip" groups, thiols, whose role is to provide better contacts to electrodes and can easily self-assemble onto metal surfaces. Such a rectifier consists of a phenyl ring insulated by two saturated groups with different lengths. The difference in the length of those two latter units is an issue of great importance in the achievement of high rectification ratios.

In this mechanism of molecular rectification, see Figure 4.32 a, when no external voltage bias is applied, the LUMO energy of the conjugated unit (phenyl ring) should be

close to the Fermi level of the two electrodes. Under forward bias, see Figure 4.32 b, the potential applied to the left electrode lowered the Fermi level of that electrode as well as the LUMO. For the system to conduct the LUMO must be brought to the same level as the Fermi energy. Under application of the reverse bias, see Figure 4.32 c, the Fermi level of the left electrode and LUMO increases. In order for current to flow and realise the system to demonstrate rectifying effects at reverse bias, the applied voltage would need to be greater to that at positive bias.
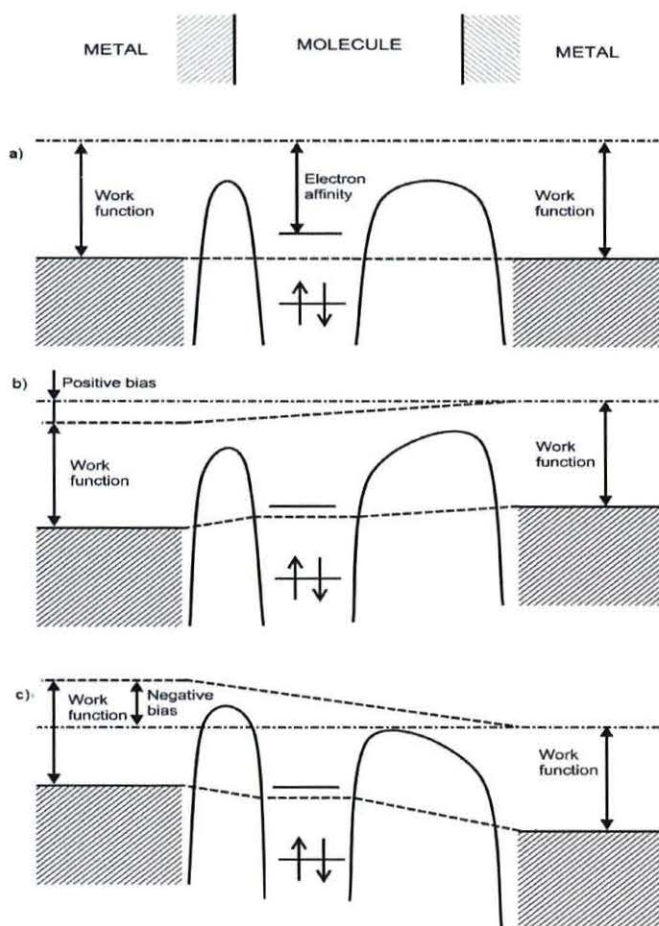
Figure 4.32 Energy diagram of Kornilovitch model: a) asymmetric molecule place between two electrodes b) forward bias causes alignment of the LUMO and Fermi level of anode, c) reverse bias causes matching of the LUMO and cathode. Figure adapted from 190.

According to the theoretical calculation, the mechanism presented above enables the system to show asymmetry with rectification ratios of several hundred. However, no experimental proof was found to confirm the above model. Moreover, Ashwell and

Stokes[191] reported conflicting behaviour against that mechanism. They investigated a squaraine chromophore that was connected to a gold substrate via a C_3H_6-S or $C_{10}H_{20}$-S tail. SAMs of that squaraine dye exhibited the non-rectifying I-V curves even though the use of C_3H_6-S or $C_{10}H_{20}$-S bridges imposed the asymmetrical position of the chromophores with respect to the electrodes. Hence, the experimental data conflicts with the model proposed by Kornilovitch,[190] which predicts high current in the case of asymmetrically positioned chromophores.

Moreover, Ashwell et al.[192] performed further investigations on a series of self-assembled Au-S-C_nH_{2n}-Q3CNQ films with different C_nH_{2n} bridge lengths; the aim was to manipulate the position of the chromophore with respect to the electrodes, and simultaneously verify its contribution to the rectification. The studied $(CH_2)_3$ and $(CH_2)_{12}$ analogues of the self-assembled Au-S-C_nH_{2n}-Q3CNQ monolayers revealed electrical asymmetry when contacted with either PtIr or Au tips with typical rectification ratios of 30 at ± 1V. Moreover, the observed I-V curves are almost identical discrediting the effect of geometric localisation proposed by Krzeminski[188] and Kornilovitch,[190] see Figure 4.33.
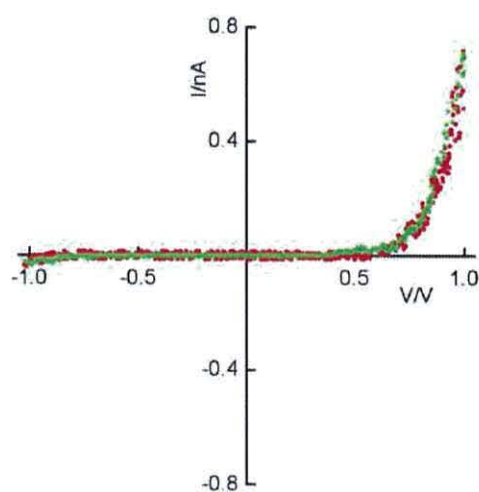

Figure 4.33 I–V characteristic of CH_3CO-S-C_nH_{2n}-Q3CNQ structure (n=3, green), (n=12, red). Copied from reference 192.

The suppression of the rectification upon the exposure to HCl vapour and subsequent restoration induced by NH_3 was observed and provided unambiguous evidence that the

electrical asymmetry was intrinsic to the D-π-A molecule rather than any geometrical effect.

4.3.7 Further work on D-π-A systems

Further investigations of the electrical properties of self-assembled molecules were carried out on a cationic dye with a truncated S-C$_3$H$_6$ link,[193] see Figure 4.34, which was deposited from a disulfide precursor onto gold-coated HOPG. Thus, a break of S-S bond during assembly *via* a chemisorption process is assumed.[56]
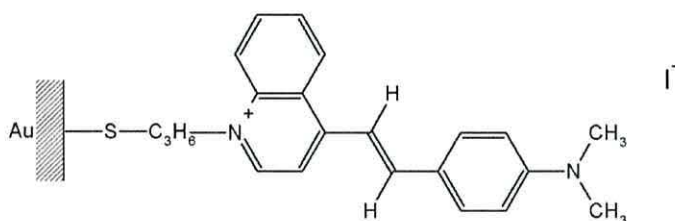

Figure 4.34 Molecular structure of the SAM of the cationic dye with truncated alkyl.

The STM recorded asymmetric *I-V* characteristics with a rectification ratio of 12 at ± 1 V with a higher current occurring at a negative quadrant, see Figure 4.35. Such behaviour indicates electron flow from the HOPG substrate to the tip and is consistent with the electron tunnelling from the electrode to the cationic acceptor (A$^+$→ A^0) at one end and from the donor to the adjacent electrode (D^0→ D$^+$) at the opposite end. The restoration of the ground state of the cationic dye was achieved by intramolecular transfer from A^0 to D$^+$. The observed diode-like behaviour appeared to follow the Aviram and Ratner model[135] albeit modified for a sterically hindered π-bridge. However, in order to verify the stated conclusion, the monolayer was subjected to the protonation and subsequent deprotonation process. Upon initial exposure to acid vapour, the generated *I-V* characteristics were suppressed, see Figure 4.34a due to protonation of the donor moiety [C$_6$H$_4$-N(CH$_3$)$_2$→ C$_6$H$_4$-NH(CH$_3$)$_2$] but fortunately the asymmetry could be restored by exposure to NH$_3$, see Figure 4.35b.
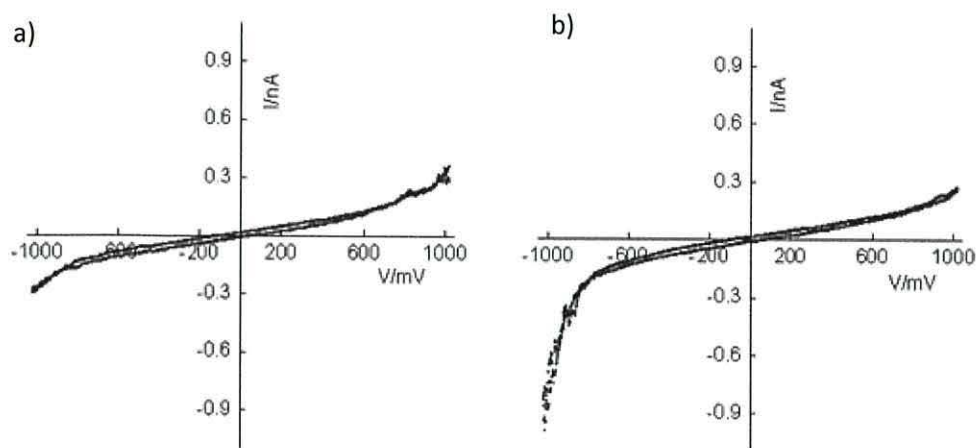
Figure 4.35 *I-V* characteristics of the SAM of the cationic dye: a) upon exposure to HCl vapour, b) upon subsequent exposure to ammonia vapour.[193]

The theoretically calculated data of the studied isoquinolinium and pyridinium hemicyanine dyes demonstrated the importance of the twist angle between the donor and acceptor moieties, as shown in see Figure 4.36. The asymmetric *I-V* curve with a rectification ratio of 5 at ± 1 V was observed for the isoquinolinium dye which exhibited a dihedral angle of 48°, whereas *I-V* characteristic for the almost planar pyridinium analogue was slightly asymmetrical.

Figure 4.36 Molecular structures of SAMs of hemicyanine analogues studied by Aswell *et al.* [194]

It was also found that the protonated forms of quinolinium, isoquinolinium and pyridinium merocyanine dyes revealed *I-V* characteristics with a maximum rectification ratio of *ca.* 2 at ± 1 V. These results were attributed to the unstability of the merocyanine form, which additionally readily protonates $[C_6H_4-O^- \rightarrow C_6H_4-OH]$ when exposed to the atmospheric H_2CO_3.
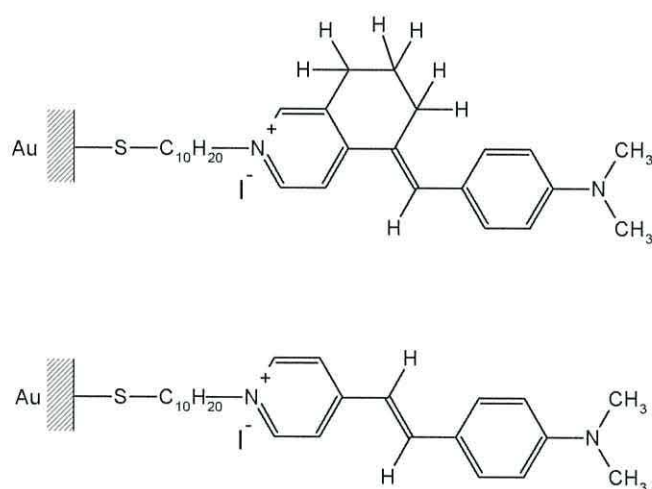
The same group reported the comparison of the electrical properties of Au-S-$C_{10}H_{20}$-Q3CNQ with those of quinolinium hemicyanine. The SAM of both molecules exhibited rectification when contacted with decanethiolate-coated gold tips, albeit in opposite quadrants. The occurrence of the higher current in the way illustrated in Figure 4.37, below, indicates the quinoid form of Q3CNQ and aromatic form of the hemicyanine. Hence, signifying that the terminal $C(CN)_2$ and $N(CH_3)_2$ groups act as donor and acceptor, respectively. Noteworthy is the fact that the asymmetry was maintained even though the chromophores were centralised with respect to the electrodes.
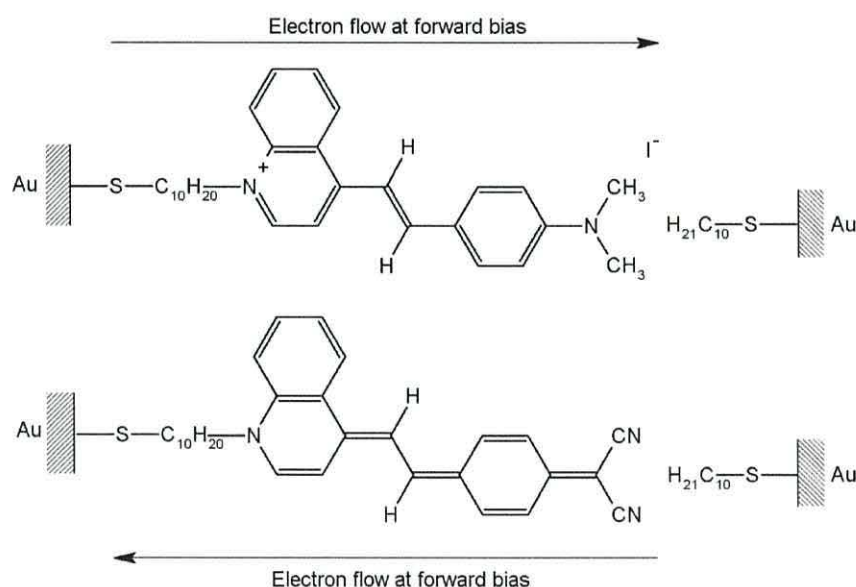
Figure 4.37 Schematic representation of preferred electron flow through Au-S-$C_{10}H_{20}$-QCNQ with that of quinolinium hemicyanine when placed between gold contacts contacted by a docanethiolate-coated gold tip in order to locate the chromophore symmetrically. .

More recently, even further justification was provided by studies on SAMs with sterically hindered D-π-A groups, see Figure 4.37. The manipulation of the position of the chromophore with respect to the electrodes was performed on the hemicyanine

dye.[194] The electrical measurements exhibited rectification of 18 at ± 1 V when the asymmetrically deposited active part was contacted with PtIr or Au tips. In the case when the chromophore was centralised and contacted by pentanethiolate ($Au-S-C_5H_{11}$) or decanethiolate ($Au-S-C_{10}H_{21}$) coated gold tips the ratios corresponded to values of *ca.* 11 and 5 at ± 1 V, respectively, see Figure 4.38.
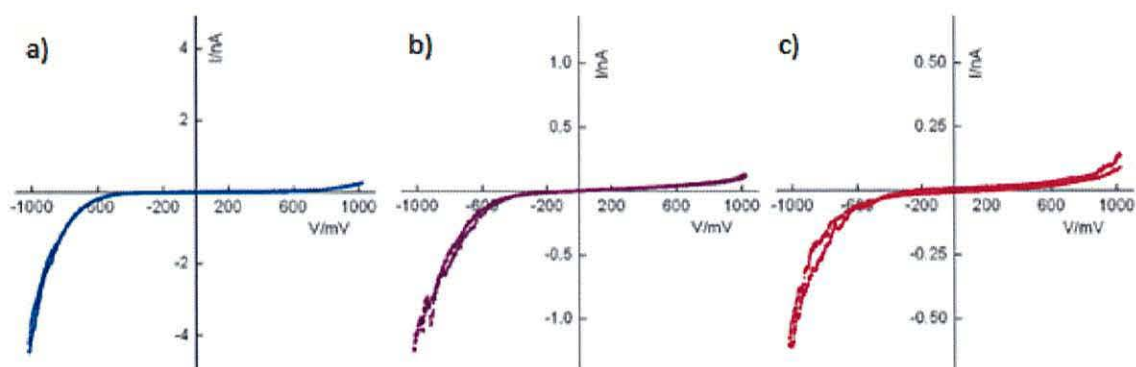
Figure 4.38 *I-V* characteristics of hemicyanine dye when contacted by three different types of tips a) uncoated tip, b) pentanethiolate-coated gold tip, c) decanethiolate-coated gold tip.

Although the presented configurations initially showed different values of rectification ratios the *I-V* characteristics appeared to become identical (rectification ratio of *ca.* 5 at *ca.* 220 MV) when thicknesses were adjusted. It was also reported that the rectification could be reversibly switched off by initial exposure to acid then switched on by exposure to base, thus confirming the D-π-A moiety induced asymmetry.

Ashwell *et al.*[195] reported the importance of steric hindrance in D-π-A dyes for electrical asymmetry. The analogue of the molecule presented in Figure 4.39 with an almost planar chromophore (pyridinium benzene acting as an electron-acceptor and metoxyphenyl electron-donor) did not yield any rectification. The observed behaviour was attributed to the sterically unhindered D-π-A structure. *I-V* characteristics of the D−π−A system depicted in Figure 4.39, were performed using three different types of tip.

ACCEPTOR   DONOR
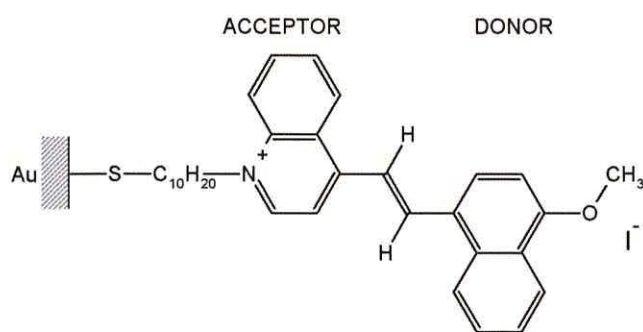
Figure 4.39 Structure of iodide salt of a sterically hindered D-π-A.

The *I-V* characteristics obtained from STM studies and mercury droplet electrodes shown in Figure 4.40 were indistinguishable in the case of the film being in contact with either Au or PtIr probes and resulted in rectification ratio of *ca.* 30 ± at 1 V. However, the location of the chromophore midway between two electrodes by using pentanethiolate coated gold tip (Au-S-C$_5$H$_{11}$) caused a drop in the current ratio to *ca.* 10 ± at 1 V. The behaviour observed for the latter configuration suggested that the potential barrier formed by the aliphatic tail affected the rectification, thus confirming the authenticity of the Aviram and Ratner model[135] rather than the one proposed by Krzeminski[188] and Kornilowitch.[190]
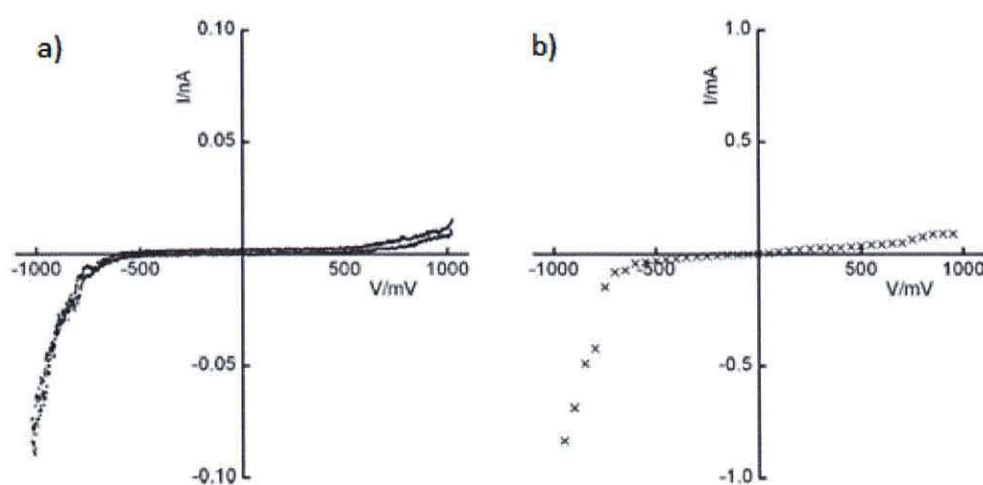
Figure 4.40 *I-V* characteristics of a sterically hindered D-π-A measured by a) STM, and b) mercury droplet electrodes.[195]

Improved intrinsic electrical asymmetry from the more sterically hindered analogue of dimethylaminphenyl[193,194] was achieved more recently by Ashwell and Mohib,[196] see Figure 4.41.
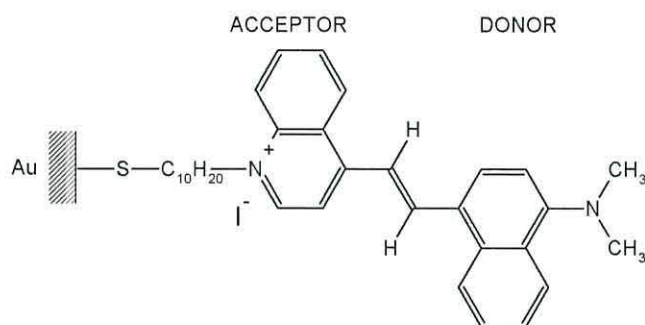
Figure 4.41 Structure of 1-(10-acetylsulfanyldecyl)-4-{2-(4-dimethylamino-napthalen-1-yl)-vinyl}-quinolinium iodide.

The enhanced rectification ratio (50-150 at ± 1 V) of the system depicted in Figure 4.41 was assigned to the controlled alignment of the D-π-A structure, as well as to the steric hindrance of the chromophore, Au-$C_{10}H_{20}$-A^{+}-π-D. The induced nonplanar structure caused the effective separation of the molecular orbitals of donor and acceptor moieties. The molecular origin of the rectification was verified by its ability to reversibly switch. This conclusion was further supported by the observation the suppression of asymmetry upon the exposure to acid and the subsequent restoration of the original form and electrical behaviour upon exposure to NH_3, see Figure 4.42.
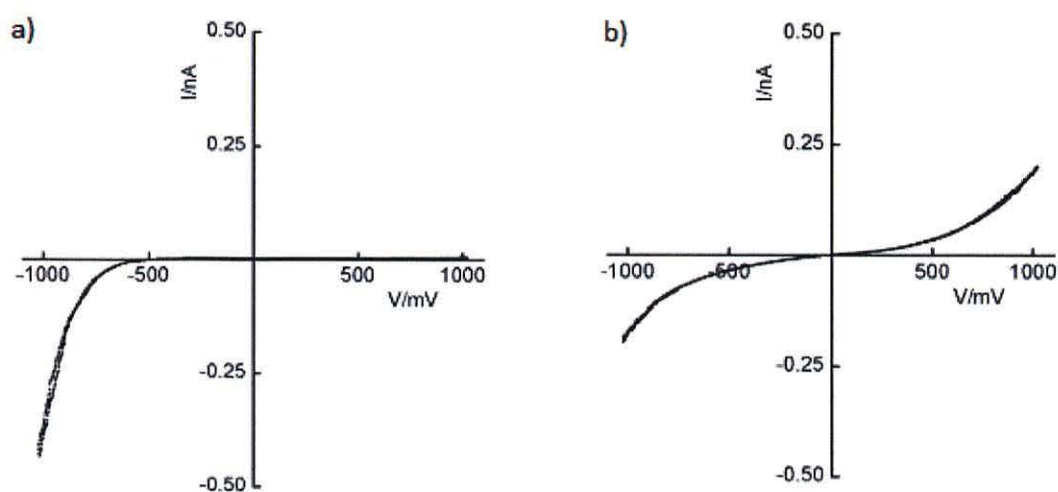
Figure 4.42 *I–V* characteristics of 1-(10-acetylsulfanyldecyl)-4-{2-(4-dimethylaminonapthalen-1-yl)-vinyl}-quinolinium iodide measured before a) and after protonation b).

Further evidence of the dipole reversal was provided by Ashwell *et al.*,[197] who performed an investigation on the LB films of two isomers of N-alkyl-5-(4-dialkylaminobenzylidene)-5,6,7,8-tetrahydroquinolinium iodide, see Figure 4.43.
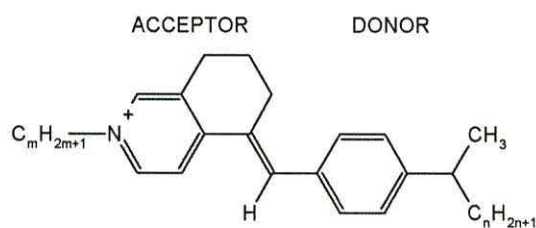
Figure 4.43 Structure of N-alkyl-5-(4-dialkylaminobenzylidene)-5,6,7,8-tetra-hydroquinolinium iodine.

The chemical substitution by two methyl and one hexadecyl groups enabled the alignment of the molecules at the air-water interface in such a way that the configuration with the lowest free energy could be adopted. This meant that depending on the location of the long aliphatic chain in D-π-A structure, the molecules were deposited with either donor or acceptor being closer to the substrate. The different orientation of the chromophore resulted in enhanced current in opposite quadrants, see in Figure 4.44.
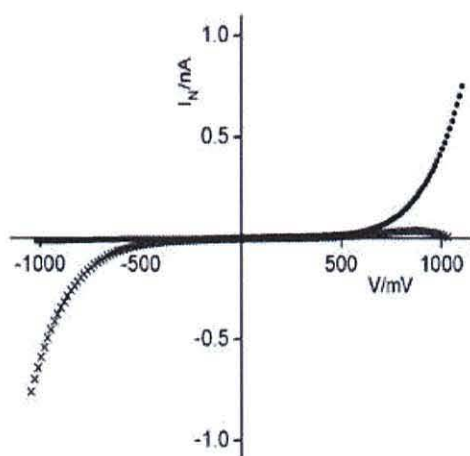
Figure 4.44 *I-V* characteristics for N-alkyl-5- (4-dialkylaminobenzylidene)- 5,6,7,8 -tetrahydrouinolinium iodide. [A-π-D-C_nH_{2n+1}] structure- higher current in a negative quadrant, while [D-π-A-C_mH_{2m+1}] structure-asymmetry in a positive quadrant of the *I-V* plot.[197]

The presented results are consistent with the Aviram and Ratner rectification mechanism,[135] albeit for sterically hindered D-π-A systems instead of D-σ-A ones. Additionally, the above conclusion was supported by an experiment relying on the deposition of both isomers in a 1:1 ratio. The electrical measurements of the film of the mixed analogues exhibited symmetrical *I-V* characteristics due to the random orientation of the molecular dipoles and confirmed the Aviram and Ratner theory according to which the electrons would expect to tunnel in both directions causing the cease of rectification.

4.3.8 SAM/LB hybrid rectifiers

In seeking the ideal molecular rectifier it was concluded that due to the effect of the gradual molecular reorientation observed in an LB monolayer, combining the advantages of LB assembly with those of self-assembly could be most promising for further research.

An outline for a hybrid SAM/LB system was introduced in 1986,[198] and such a concept has been the topic of recent research. Moreover, the study of a SAM/LB squaraine configuration performed by Ashwell and Berry[199] revealed the importance of these hybrid bilayers in designing desired components for molecular scale electronics. They

reported the unexpected recifying behaviour when the squaraine molecules of such a hybrid system were differently aligned in separate layers, whereas the current-voltage characteristics of separated monolayers were symmetrical.[199, 200] It seems that the molecular asymmetry in donor-acceptor-donor (D-A-D) molecule which was chemisorbed to the gold substrate by one of the donor group *via* $Au-S-C_3H_6$ was not sufficient to induce any rectification, see Figure 4.45.
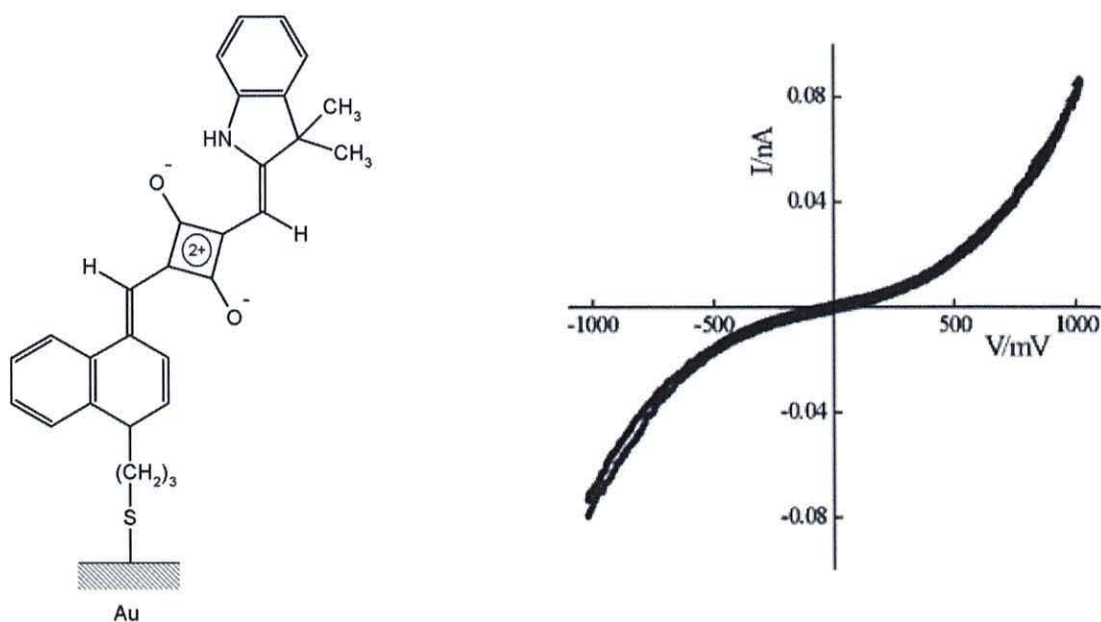
Figure 4.45 Structure of squaraine self-assembled monolayer on the left and its symmetrical *I-V* characteristics obtained when contacted by a PtIr tip.[199]

The non rectifying characteristics were also exhibited by LB films in which the chromophores were centric. However, the molecular rectification of such a hybrid device could be induced by the diverse molecular orientation of deposited layers. Thus, the vertically aligned squaraine, as shown in Figure 4.46, with its donor towards the lower substrate in the SAM, and the horizontally aligned squaraine with the long axis of its chromophore in contact with the upper electrode in the LB film, resulted in rectification with a ratio of *ca.* 12 at ± 1V. The rectification exhibited by the SAM/LB device was consistent with the Aviram and Ratner model[135] with the LB deposited squaraine acting as an electron acceptor and the SAM squaraine an electron donor. The studies led to the conclusion, that observed behaviour stemmed from different orientation of the molecules with respect to both electrodes.
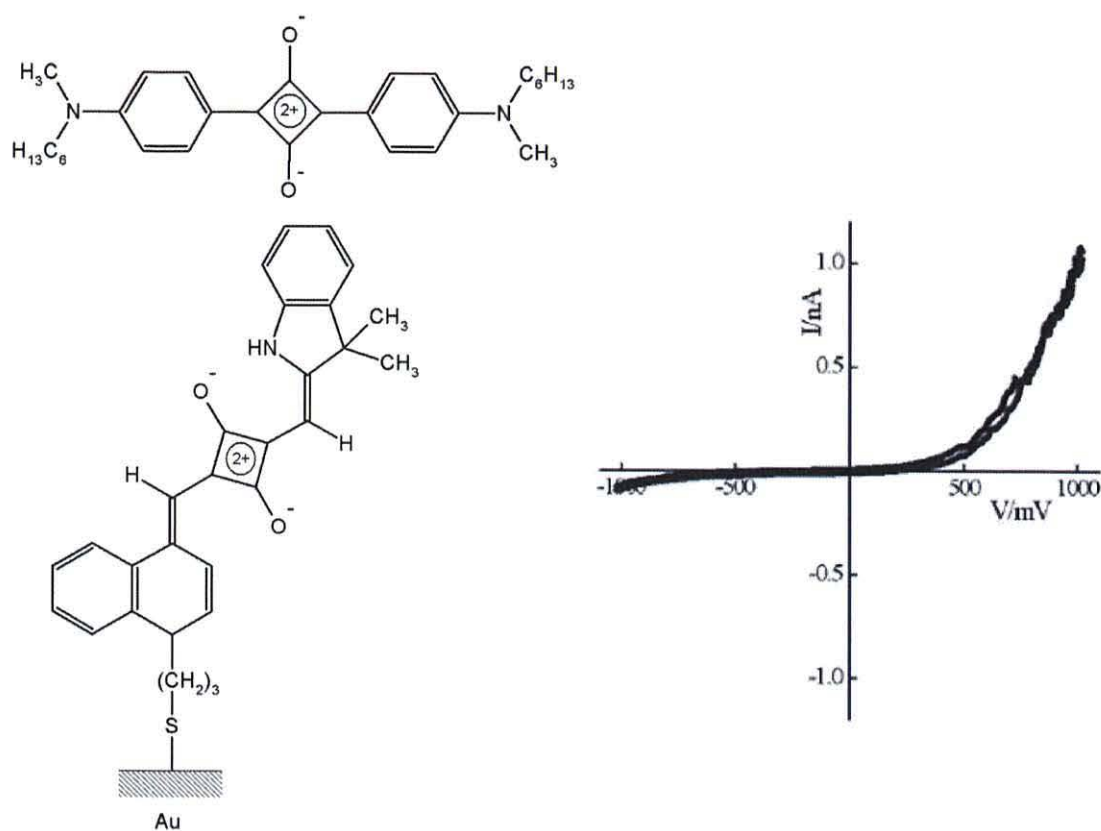
Figure 4.46 The chemical structure of SAM/LB hybrid system on the left and its typical *I-V* characteristics obtained when contacted by a PtIr tip.[199]

Further work reported studies on homomolecular squaraines with the $CH_3CO-S-C_3H_6$ anchoring groups located at both ends of the chromophore.[201] The QCM and SPR measurements indicated two, vertical and horizontal possible orientations with one or two linking groups chemisorbed to the gold electrode, respectively. It was demonstrated that such a random distribution within the monolayer caused the asymmetrical behaviour of the system, as the study on squaraines with only one anchoring group provided contrasting results.[191] However in contrary to the hybrid SAM/LB bilayer behaviour, the higher current occurred in the opposite quadrant of the *I-V* plot. This can be explained by the fact that the long axis of D-A-D chromophore was in contact only with the substrate electrode.

Other studies on hybrid SAM/LB structures revealed a new rectifier that of a chevron-shaped dye. As is well known, for an LB film to be formed at the air-water interface, a molecule requires a long hydrocarbon chain,[94] which unfortunately reduces the

conductivity of the molecule. Therefore, attempts have been made to overcome this requirement.[186,202] However, the limited compromise between the achievement of an ideal LB compound and an ideal molecular rectifier still remains. This statement was also confirmed by recent studies, in which a chevron-shaped D-π-A-π-D cationic dye comprising of truncated alkyl substituents instead of a long aliphatic tail was used. It was reported that, although, the resultant LB film exhibited molecular rectification, the diode like behaviour was inherently unstable. This was due to the molecular reorganisation and thus suppression of the rectification.[203] However, Ashwell et al.[203] have also been able to achieve long term stability of such a cationic chevron-shaped dye, by its LB deposition on an anionic surface, which acted as the counterion. The anionic layer was formed via chemisorption of sodium 3-mercapto-1-propanesulfonate on a gold-coated substrate, see Figure 4.47.
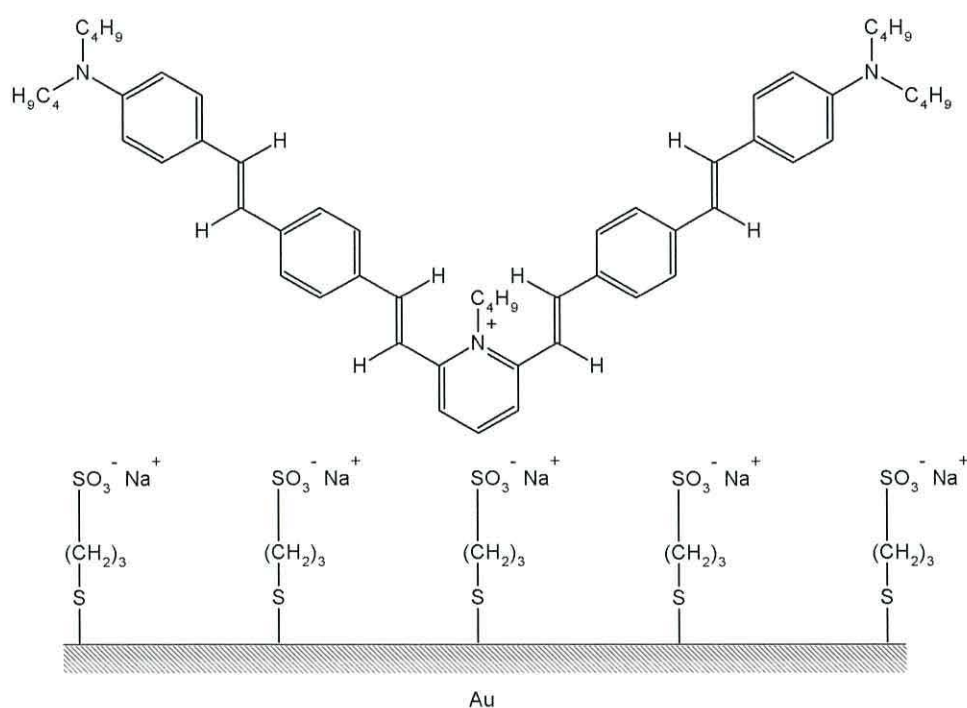

Figure 4.47 The chemical structure of hybrid Au/SAM/LB.

The electrical properties of the resultant structure, shown in Figure 4.47, above, deposited on gold-coated HOPG were investigated by STM using a PtIr tip. Such a hybrid Au/SAM/LB device exhibited asymmetrical *I-V* characteristics with high rectification ratio of 25 at ± 1 V. These results combined with second-harmonic

generation (SHG) confirmed the non-centrosymmetric alignment of the film and its stability. The reported results prove that the alignment of an LB film may occur without resorting to a long hydrocarbon chain.

Further evidence for the validity of the rectification produced by the ionically coupled system has been achieved by investigation of other films prepared by ionic assembly.[204] Moreover, this method of alignment resulted in a significant improvement of the electrical behaviour[204] for the molecular diode with ratios of 100-200 at ± 1 V.[192] In the recent report, similarly to the previous one, the rectifying junction was built up in two stages. N-methyl-5-(4-dibutylaminobenzylidene)-5,6,7,8-tetrahydroisoquinolinium molecules were self-organised *via* metathesis onto an ionic surface provided by sodium 3-mercapto-1-propanesulfonate, see Figure 4.48.
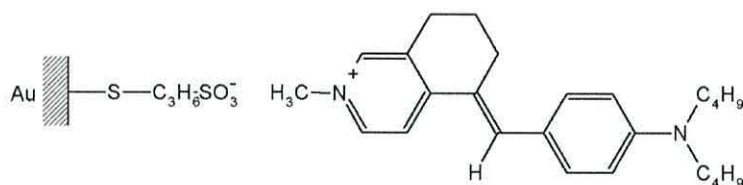
Figure 4.48 Hybrid structure of Au-S-C_3H_6-SO_3-|A+-π-D |Au system.

The resultant system exhibited the asymmetry in the negative quadrant with rectification ratio of 450 at ± 1 V, which is in agreement with the Aviram and Ratner theory. Based on the obtained results, it was concluded that the electrical asymmetry of the system tended to be weaker when the dye possessed less sterically hindrance, whereas the bulkiest analogue resulted in a higher rectification. The described behaviour was demonstrated to be dependent on steric hindrance, which was responsible for the nonplanarity in the bulky molecule. The steric hindrance results in the molecular orbitals being localised on both donor and acceptor moieties of these π-bridged molecules and hence, effectively separated.

4.3.9 Rectifying junction

The successful fabrication of organic rectifying junctions of Au/LB/Au structures was reported by Fischer *et al.*[205] Such a technique was used as it allowed a direct observation of electrons tunnelling through molecular states. The investigated system involved an LB heterostructure built up of 6 monolayers of an octasubstituted metallophthalocyanine (PcPd) and 6 monolayers of a perylene-3,4,9,10-tetracarboxyldiimide derivative, which were sandwiched between two non-oxidisable gold electrodes, see Figure 4.49, in order to prevent the schottky barrier effect.[179]
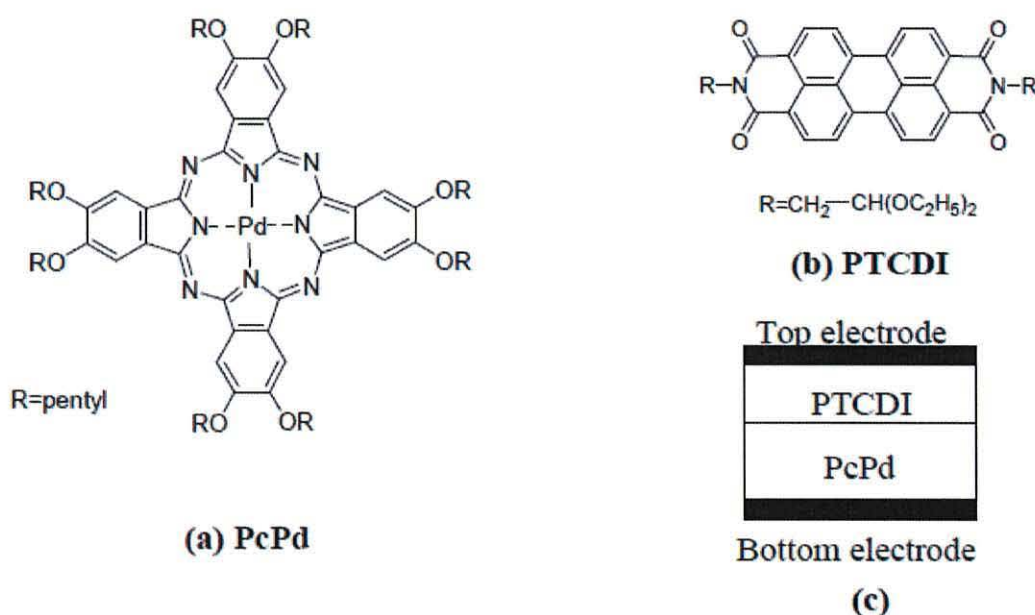
Figure 4.49 Structures of PcPd (**a**), PTCDI (**b**) and (**c**) layer configuration of the hybrid between two electrodes.[205]

The measurements were taken at liquid helium temperatures, as Fisher believed that higher temperature may cause the hopping process. The *I-V* characteristics of the hybrid structure exhibited the rectifying behaviour for negative as well as positive bias. However it was found that the thresholds for negative and positive bias differ from each other and occur at -0.40 V and +0.91 V respectively. It was believed that electrical asymmetry was a consequence of the different positions of the HOMO of PcPd and PTCDI moieties with regard to the Fermi levels, see Figure 4.50.
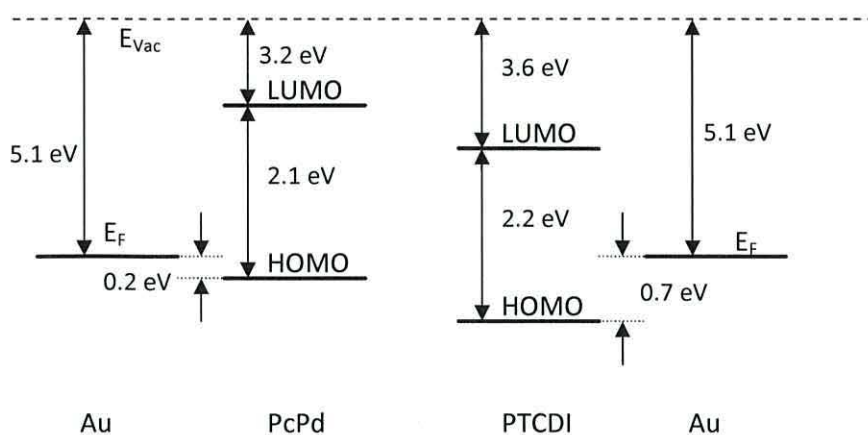
Figure 4.50 Schematic diagram of the estimated energy levels of the PcPd and the PTCDI compared to the gold Fermi level. Taken from reference 205.

This conclusion was verified by STM measurements of devices fabricated from only one type of molecules (PcPd or PTCDI) sandwiched between Au electrodes. Both homolayer systems, Au/10 monolayers of PcPd/Au and Au/20 monolayers of PTCDI/Au, showed symmetrical characteristics, and thus suggests that the asymmetry arose as a result of the molecular states.

The first rectifying junction that used the self-assembly technique in order to generate the molecule-electrode contact was demonstrated by Chabinyc *et al.*[49] The proposed metal | SAM || SAM | mercury system was composed of a SAM derived from the molecule depicted in Figure 4.51.
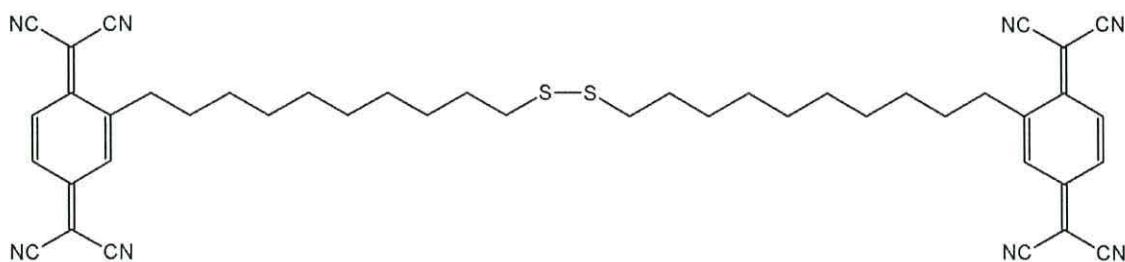
Figure 4.51 The structure of $(TCNQC_{10}S)_2$.

Upon rupture of the central S-S bond the molecule anchored by chemisorption to the bottom silver electrode, whilst the SAM formed from an alkanethiol was linked to the top mercury contact, see Fig 4.52.
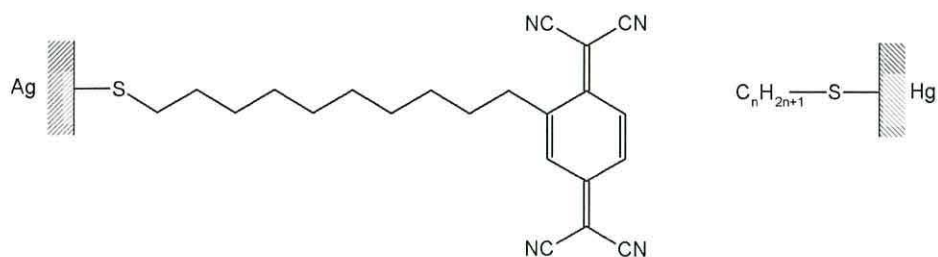
Figure 4.52 Possible packing of Chabinyc rectifier.

The electrical study revealed the enhanced current (rectification ratio of 9.0 ± 2.0 at ± 1 V) when the mercury electrode was positively biased. It was also observed that the rectification ratio decreased at a given voltage with an increase in the chain length of the alkanethiol that assembled to the mercury contact. This results suggested placement of an electron acceptor in the insulating layer could contribute to the electrical properties in a metal | insulator | metal system. Although the authors claimed molecular rectification from the junction, the doubts remained due to the ability of TCNQ to self-assemble onto the silver and yield a polycrystalline $Ag^{\sigma+}TCNQ^{\sigma-}$. [179]

A system utilising the electron-donating properties of phthalocyanine was reported by Mukherjee and Pal.[206] They investigated a bilayer structure that was composed of electrostatically bound monolayers of the donor, copper phthalocyanine, and that of the acceptor, rose of bengal to fabricate donor-acceptor (D/A) assembly, shown in Figure 4.53.
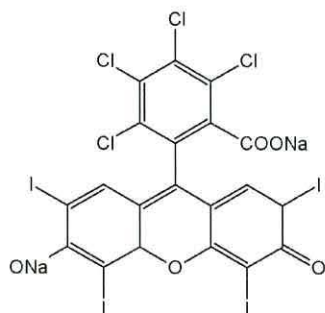
Figure 4.53 Structure of Rose Bengal.

The *I-V* measurements of such a system sandwiched between Si and Hg electrodes exhibited rectifying behaviour with a higher current in the negative quadrant. This would suggest that electrons flow from the donor moiety to the acceptor in conflict with Aviram and Ratner theory.[135] However, it was believed that the electrical asymmetry (RR of 30 at ± 1.9 V) resulted from CuPc/RB assembly, as the *I-V* characteristics of donor and acceptor moieties studied separately showed no rectification.

Ashwell *et al.*[207] demonstrated molecular rectification of the ionically coupled ultra-thin donor-acceptor structure. In such a system, unlike that described as a molecular diode[18] where donor and acceptor moieties are linked by a covalent bridge; organic moieties are connected by physical attraction between their opposite charges. The organic rectifying junction of the system was built up firstly by self-assembly of the cationic acceptor (sulfanylpropyl 4,4'bipyridinium) and in a second stage by self-organisation (metathesis) of the anionic donor (copper phthalocyanine-3,4',4'', 4'''-tetrasulfonate). The electrical properties of such a hybrid structure were investigated by STM using a gold tip and resulted in asymmetrical *I-V* characteristics with a rectification ratio in a range of 60-100 at ± 1V, see Figure 4.54. The illustrated rectifying behaviour was attributed to the model presented by Aviram and Ratner.[135]
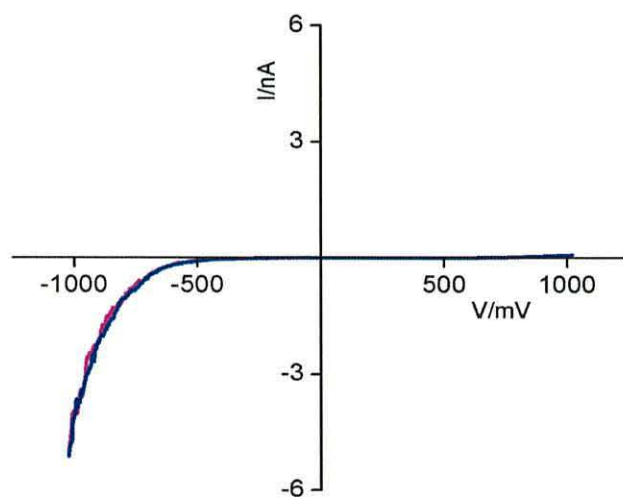
Figure 4.54 *I-V* characteristics for the complete $Au|BP^{2+}|CuPc(SO_3^-)_4(Na^+)_n$ structure.[207]

An even more radical improvement in electrical asymmetry was observed for Au-S-$C_{10}H_{20}$-A$^+$-π-D|D$^-$|Au rectifier systems.[2] Ionically coupled devices in which the bipyridinium unit was replaced with D-π-A molecules, presented in Figure 4.55, have been recently reported.
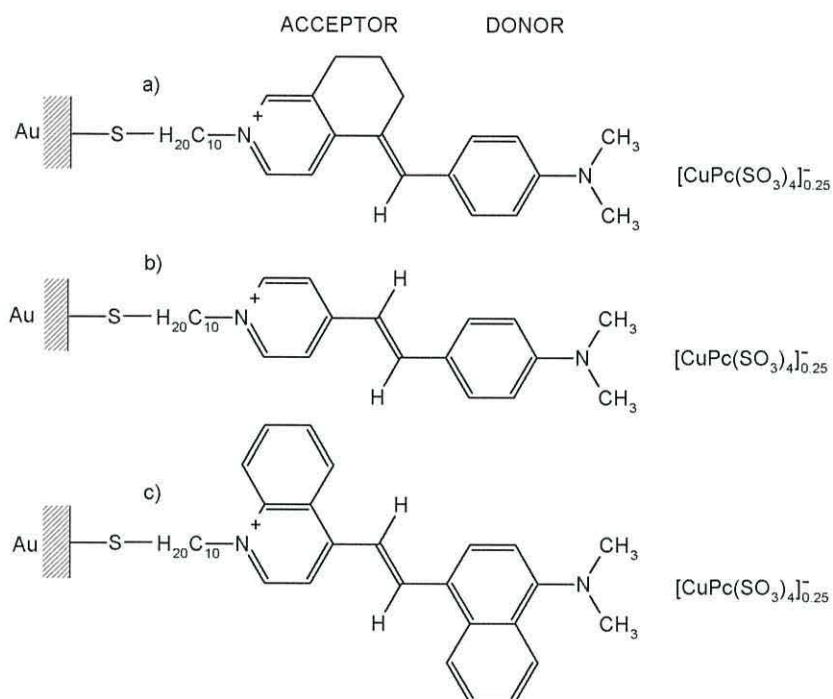
Figure 4.55 Molecular structures of mixed monolayers of cationic dye and phtalocyanine.

All three films were formed *via* a chemisorption process of a cationic dye and subsequently the ionic assembly of an anionic donor. The STM data for the hybrid **a** yielded rectifying behaviour with a rectification ratio of 3000 at ± 1 V, see Figure 4.56, being almost three orders of magnitude higher when compared to the results obtained from SAMs of the iodide salt of the same molecule.[193] Noteworthy is the fact that electrical asymmetry of the presented structure is on a par with that from metal-insulator-metal (MIM) system where such behaviour is attributed to metal oxide Schottky barriers. However, in this case electrical properties were determined by the cationic dye, particularly by steric hindrance which effectively maintained the separation of the donor and acceptor electroactive moieties. Therefore, the use of an unhindered cationic dye, see Figure 4.56, hybrid **b** would decrease electrical asymmetry. This behaviour was demonstrated by the hybrid **b** that exhibited *I-V*

characteristics with a much lower RR of 15-70 at $\pm$ 1 V. It was also reported, that the deposition of an anionic layer (phthalocyanine) enhanced the electron-donating capability of the device, hence an improvement in rectification ratio can be observed. Further supporting data for the rectifying behaviour being a result of the hybrid structure was obtained from structure **c**. The rectification ratio of such a system formed by ionic assembly was increased from values of 50-150 at $\pm$ 1 V, obtained for SAMs of the iodide salt of the same cationic moiety[196] to the value of 700-900 at $\pm$ 1 V.
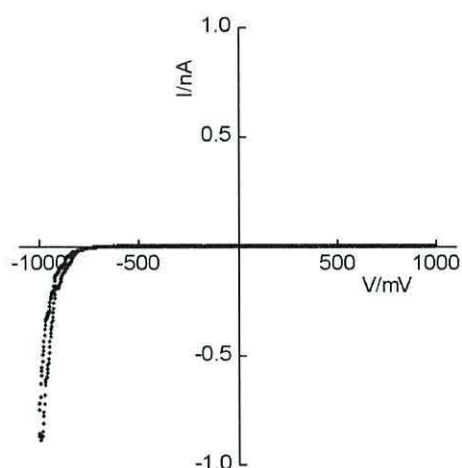
Figure 4.56 *I-V* characteristic of Au-S-$C_{10}H_{20}$-A$^+$-π-D|D$^-$|Au structure, where the cationic moiety was 5-(4-dimethylaminobenzylidene)-5,6,7,8 -tetrahydroisoquinolinioum, and the anionic donor (forming the second layer) was copper (II) phthalocyanine-3,4',4'',4'''-tetrasulfonate.[2]

These impressive results imply that rectifying junctions may be promising for the fabrication of future molecular electronic devices, and thus may successfully replace the already limited bulk inorganic technology.

The formation of organic rectifying junctions that incorporated a molecular wire were, for the first time, revealed by Ashwell *et al.*[208] In this report, the electronic behaviour of an arylene-ethynylene oligomer consisting of a 7nm long backbone, hexyloxy side-chains and teminal thiol groups located at both ends was discussed, see Figure 4.57.
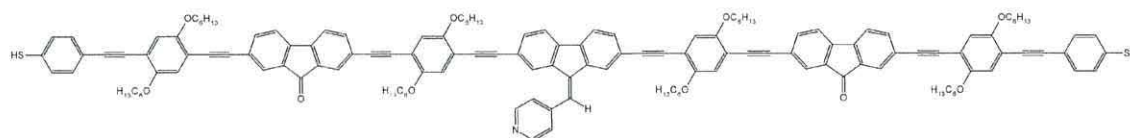
Figure 4.57 Molecular structure of the 7nm long backbone wire.

The 7 nm long wire, when deposited alone on a Au-coated substrate and investigated by STM using Au and PtIr probes, exhibited mainly symmetrical *I-V* characteristics, see Figure 4.58.
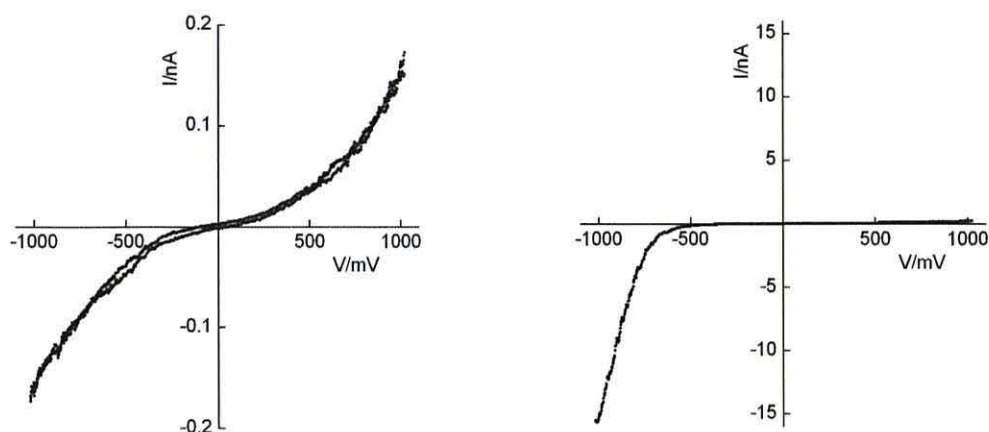
Figure 4.58 *I-V* characteristics of the 7 nm wire on the left and that of the hybrid incorporating 7 nm wire and phtalocyanine.[208]

However, the diode-like behaviour could be induced by protonating this wire molecule (exposure to HCl) and ionically coupling with an electron-donating phthalocyanine. Thus, the investigation of electrical properties of Au-WIRE$^+$[CuPc(SO$_3^-$)$_4$(Na$^+$)$_n$]$_{1/(4-n)}$ bilayer structures resulted in *I-V* characteristics being invariably asymmetrical with current ratio which varied from 20-80 at ± 1 V, see Figure 4.58. These variations in the rectification ratio might be caused by non-uniform alignment across the whole system.

4.3.10 Other approaches

Metzger *et al.* reported two examples of molecular rectifiers made from fullerenes.[209,212] The first system studied, was that of an azafullerene, composed of a weak electron donor, dimethylaniline, and a directly attached N-capped C$_{60}$ which acts as an electron acceptor,[209] see Figure 4.59.
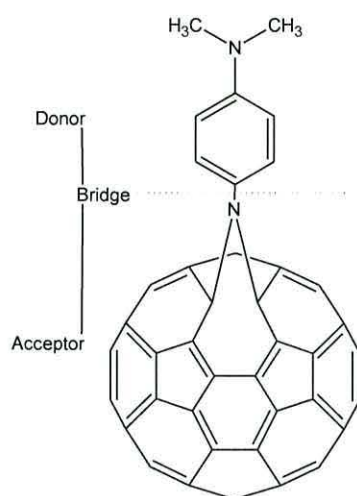
Figure 4.59 Stucture of azafullerene developed by Metzger.[210]

When SAMs of such a molecule were sandwiched between two gold electrodes, a high current was observed with tremendous rectification ratios. However upon much cycling of the bias the asymmetry decreased to give *I-V* characteristics with a rectification ratio of *ca*. 2. The reason for such behaviour in an azafullerene system was believed to result from gold stalagmites previously formed within the monolayer,[211] see Figure 4.60 and the subsequent destruction of those structures by cycling the voltage.
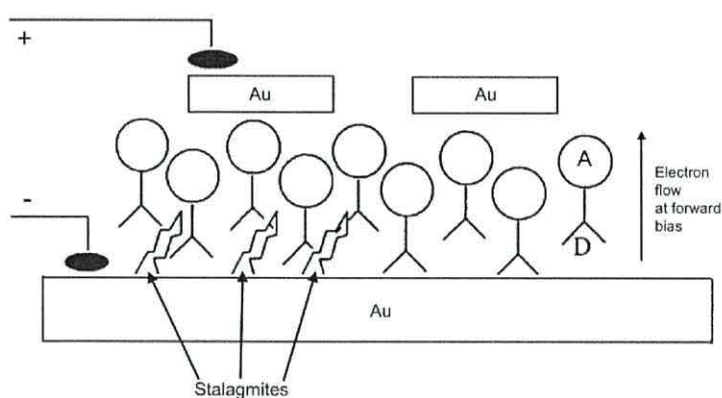
Figure 4.60 Schematic diagram of 'Blue fullerene' between electrodes on Au electrodes, including Au stalagmites with indicated direction of electron flow under forward bias. A-acceptor, D-donor.[212]

A more recent rectifier was an LB fullerene system, composed of two triphenylamine groups (electron donors) linked *via* a π-bridge with a weak electron acceptor moiety (fullerene),[212] see Figure 4.61.
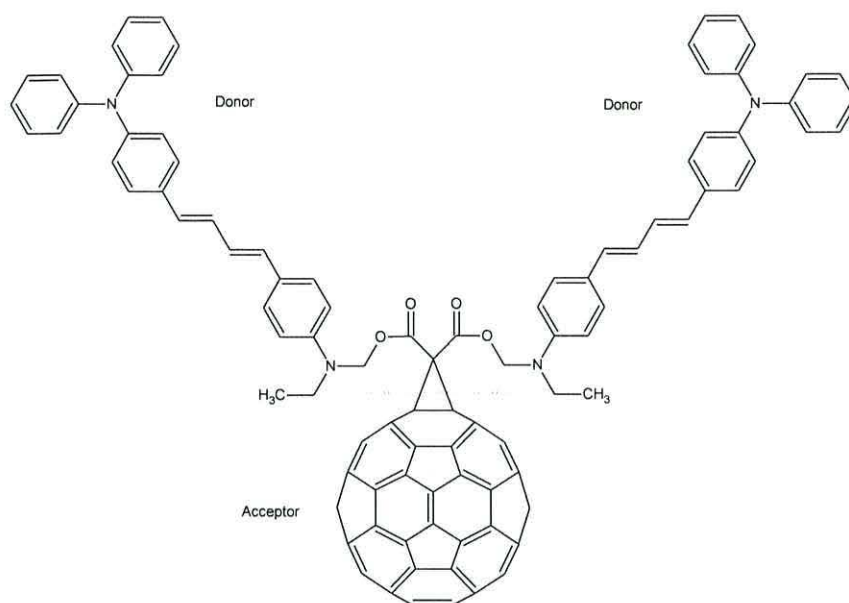
Figure 4.61 Fullerene-based LB rectifier.[210]

This system was built up by assembling a molecule to one of the gold electrode, while the latter electrode was evaporated on the top of monolayer. STM investigations of such a device gave only small rectification ratios, however its value did not decrease after cycling of the voltage, probably due to its tendency to form very dense and stiff LB monolayers. Although the presented results are not astounding, fullerene-based systems with strong rectification ratios could provide the solution to the stability problems relative to conventional LB rectifiers.

4.3.11 Molecular wires

Molecular wires have recently received much attention, as the simplest molecular devices which contribute to the successful miniaturisation process of the field of electronics. It is believed that the application of these components meets the requirement of connecting single molecule based devices to the macroscopic 'world'. Research in this area has been mainly focused on the most promising groups of molecular wires, such as: conjugated hydrocarbons, carbon nanotubes, porphyrin

oligomers and DNA in order to obtain the complete characterisation of the conduction mechanism of molecules.

Molecular wires, in order to fulfil their potential, must be linear and of defined length and constitution.[10] For this to be achieved, Tour and co-workers employed an alternative method of polymerisation, the Iterative Divergent/Convergent approach, to produce oligo(phenylene ethynylene) (OPE) molecules of different lengths among which the longest one was 16-mer with a length of 128Å,[213,214] see Figure 4.62.
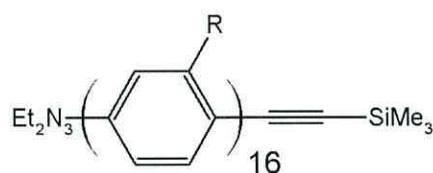
Figure 4.62 Schematic representation of the longest oligo(phenylene ethynylene) wire synthesised by Tour and co-workers.

However, the conductive properties of this molecule have not been determined and therefore study of its effectiveness as a molecular wire has been carried out on shorter molecules.

The investigation of the conductivity of the oligomers assembled onto a metallic surface has become possible with the development of the scanning tunnelling microscopy. Using the STM technique, Bumm *et al.* have been able to address single molecular wires that had been embedded into an insulating layer of dodecanethiol assembled onto a gold electrode,[215] see Figure 4.63. The random insertion of single conjugated molecules at defect sites occurred when the thioacetate group on such a molecule was deprotected to the thiol.
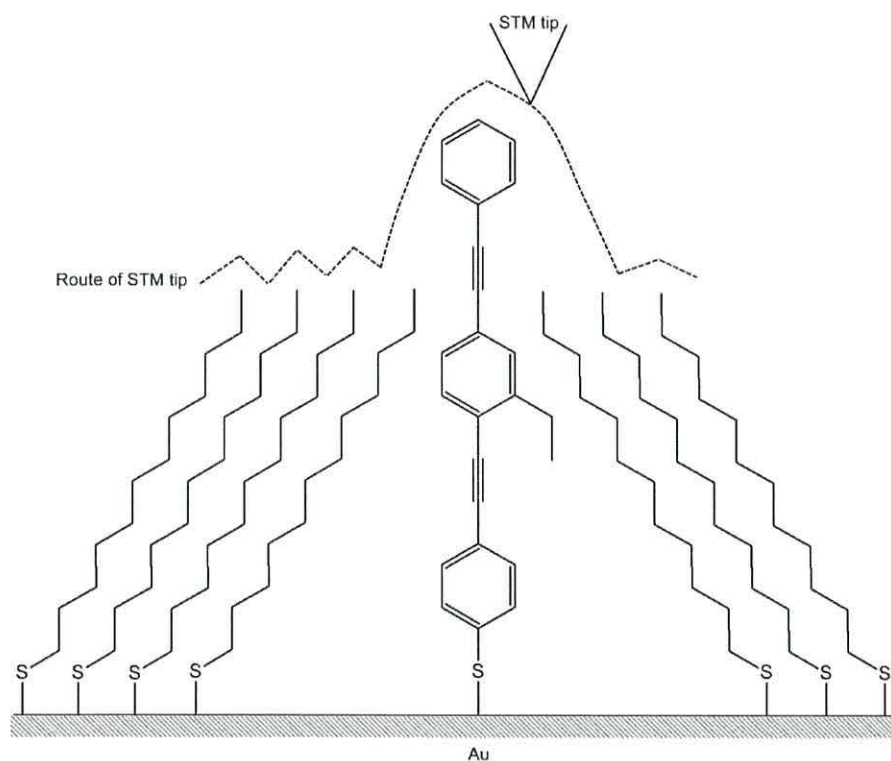
Figure 4.63 Mixed monolayer of molecular wire and n-dodecanethiol.

The STM measurements revealed that the conductivity of the conjugated molecules was greater when compared to that attributed to the alkanethiol surroundings. However, the obtained results were said to be intuitive considering the involvement of a tip-sample tunnelling gap. Therefore, this experimental value of the conductivity could not be unambiguous with its absolute value.

The technique for determining the conductance of molecular wire systems which utilises a nanopore array was developed by Zhou *et al.*[216] In this method, a SAM active region ~ 1000 molecules of conjugated molecular wire (4-thioacetylbiphenyl) in a 30 nm-diameter area was situated between a gold electrode at the bottom and a titanium top electrode, see Figure 4.64. The application of a nanoscale size device guaranteed a highly ordered and defect free arrangement of the adsorbates.
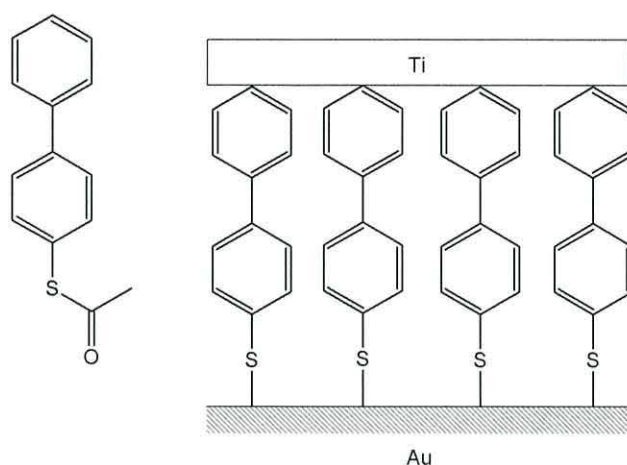
Figure 4.64 The representation of Tour wire junction in which the electrons flow occur only from Au/Ti electrode to the S-Au surface due to different metal-molecule interface of the Ti layer than the Au-S barrier.[217]

However, the behaviour exhibited by such a system was in contrary to the model of molecular rectification proposed by Aviram-Ratner,[135] as the observed current at +1 V was approximately 500 times higher compared to the current at -1 V. Therefore, it was reasonable to believe the obtained asymmetric *I-V* characteristics were a result of the generation of Schottky barriers resulting from the oxidisable titanium electrodes rather than being ascribed to the molecule itself.

Kushmerick *et al.* also reported the conductivity of oligo(phenylene ethynylene) (OPE) class of molecular wires.[218] The molecules presented in Figure 4.65 were used to demonstrate the influence of the affinity of the linking group to the electrode on the overall conductance.
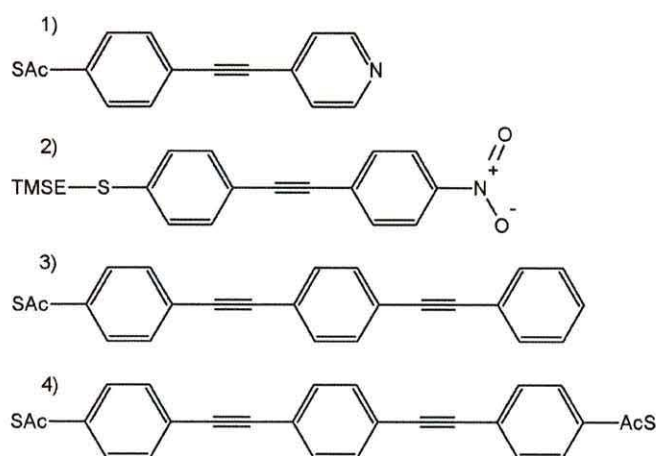
Figure 4.65 Molecular structures of oligophene-based rectifiers studied by Kushmerick.[218]

Molecules **2**, **4**, those with the best molecule-metal connection, exhibited no rectification. The conductance measurements for these molecules revealed the molecular wire behaved with identical characteristics in both directions, see Figure 4.66. However, molecules **1**, **3** whose rectification ratios were 1.75 at ± 1 V and 3.75 at ± 0.9 V, respectively, showed asymmetric characteristics caused by a low level of molecule-gold interactions.[218] There is also evidence that the higher rectification ratio of **c** results from different connections on either sides.[219]
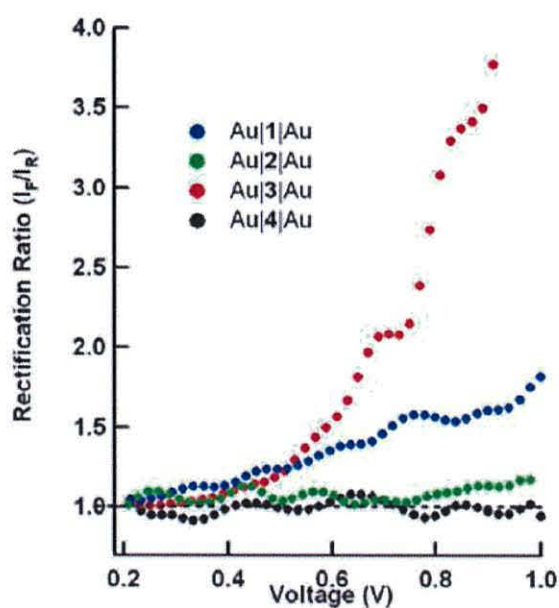
Figure 4.66 *I-V* characteristics exhibiting the dependence of the electrical behaviour on the molecular length and interaction with the gold.[218]

To find the most conductive system, Kushmerick *et al.* performed an investigation into the charge transport dependence as a function of the bond length of the molecule.[219] In these measurements, oligo(phenylene ethynylene) OPE molecules were compared to oligo(phenylene vinylene) (OPV) molecular wires. These two classes of molecular wire have lately attracted a lot of attention[215,220] and, according to results presented previously, the OPV molecule should display a higher conductivity due to better π-conjugation. The results obtained by Kushmerick *et al.* showed molecular conductance in agreement with earlier research. However, the enhanced conductivity of OPV was attributed smaller bond length variation in OPV molecules than in OPE rather than to the planarity of such molecules.[219]

In order to overcome the miniaturisation threshold of silicon devices, Ashwell *et al.*[221] designed and analysed a novel bottom-up method for molecular wire fabrication of precisely defined length. The reported technique relies on self-assembly of molecules between upper and lower gold electrodes separated by a predefined nano-scale gap. In the case of the presented study, the system was assembled in three steps by subsequent immersion of substrates in component solutions. Hence, a substrate was firstly coated only with the gold, whilst in the other two steps coated with the following layers: 4-[(3-mercaptophenylimino)-methyl]-benzaldehyde, 2,6-diaminoanthra-9,10-quinone. The resultant molecular structure of such a system expected as depicted in Figure 4.68 was simultaneously consistent with X-ray photoelectron spectroscopy (XPS) study.
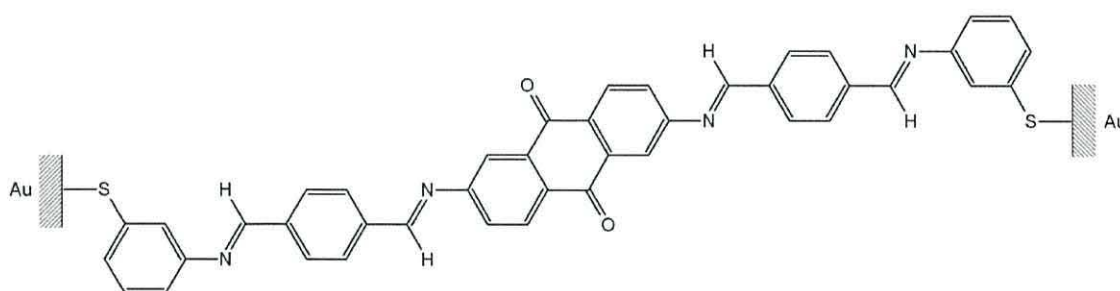
Figure 4.67 Molecular structure of the wire of defined length obtained from the three step process on planar gold-coated substrates.

The electrical properties of that stable platform linked to an insulating "mushroom" (the description of the mushroom device reported in ref. 221) exhibited almost identical

electrical behaviour to those obtained from STM studies, see Figure 4.68. It was concluded, that the observed symmetrical *I-V* characteristics mimicked those of self-assembled monolayers on planar substrates.
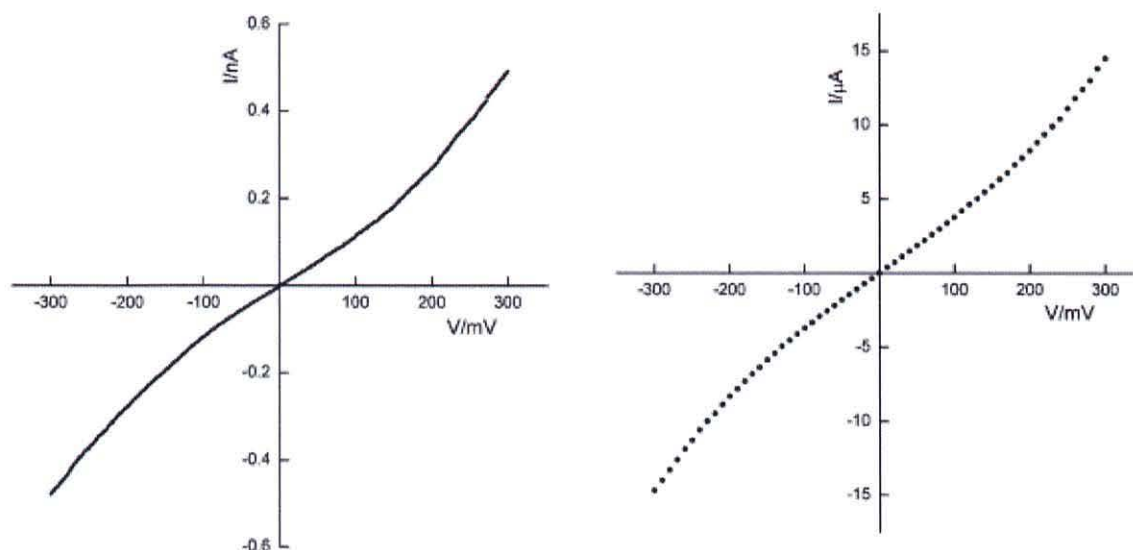
Figure 4.68 *I-V* characteristics of a SAM of the symmetrical molecular wire on the left, and that of the molecule inserted mushroom device.[221]

5 Experimental

5.1   Substrate preparation

The cleanliness of a substrate is of great importance for the success of the assembly processes (see section 2.1). In order for this to be achieved, the following procedure was performed.

1) 10 MHz AT-cut quartz crystals were placed into the plasma cleaner (*Gala Instrument, Plasma Prep 2*, see Figure 5.1), and the chamber evacuated.
2) After 3 min, nitrogen gas was pumped in for another 3 min.
3) The generator was switched on to form the plasma.
4) After a predetermined time the generator was automatically switched off.

Figure 5.1 Gala Instrument, Plasma Prep 2.

To perform SPR measurements, gold-coated glass slides were used as a substrate. However, prior to the deposition process, slides must have been thoroughly cleaned according to the procedure described below.

1) The hydrophobic BDH glass microscopic slides removed from the sealed packing were initially examined. Only slides without any surface defects, i.e. scratches and blemishes were selected.

2) The slides were ultrasonicated for 20 minutes in general grade chloroform and then in general grade isopropanol for another 20 minutes.

3) Both sides of the slides were then inspected and wiped in a single direction with dust and surfactant free tissues soaked in acetone in order to remove any grease and contamination from the surface.

4) Afterwards, the slides were successively ultrasonicated in ultrapure chloroform, isopropanol, ultrapure water and isopropanol for 20 minutes at the time.

5) The cleaned slides were immersed in isopopanol and stored in a fridge.

6) Prior to use, the slides were rinsed thoroughly with pure water and dried in a stream of dry air.

Highly oriented pyrolytic graphite (HOPG) was used in STM measurements, to reveal *I-V* characteristics of a studied molecule. The HOPG samples were purchased from *Aztech Trading*. The advantage of utilising graphite as a standard substrate is that the carbon atoms build up a multilayered structure, so that the surface of the HOPG can be easily prepared by peeling off the upper layers with a strong adhesive tape from both sides of a sample. Thus, the atomically flat and clean substrate surface beneath can be revealed. Any flakes that formed during this process can be removed by using tweezers.

Gold coating was performed on previously cleaned substrates. Both, hydrophobic glass slides and HOPG were coated with a gold film of a thickness being at ± 47 nm. Glass slides were used for SPR measurement, whilst HOPG substrates for STM studies during which the role of a Au film was to act as the electrode. The procedure was realised by using an *Edwards 360 A* unit and a gold wire (99.99%) purchased from *Sigma-Aldrich Chemicals Ltd.* being the coating material.

The predetermined mass of the gold wire was placed into a molybdenum boat connected to an electrical circuit. The substrates (slides or HOPG) were mounted upside down on a mask above the boat along with a quartz crystal microbalance, which monitored the rate of gold coating. Hence, the desired thickness of gold could be obtained. The coater chamber was sealed and the pressure was pumped down to 1.8 x 10^{-6} Torr. Then, a current was applied to the boat in order to melt the gold. The molybdenum boat was shielded during the initial heating to protect substrates against volatilised impurities in the gold melting process. After a few seconds, the shield was removed allowing the vapourised gold to evaporate on the substrate surfaces until the desired thickness was reached. The coating rate was kept as slow as possible to obtain a uniform gold film.

5.2　Monolayer preparation

5.2.1 Preparation of SAMs on gold-coated substrates.

The SAM film preparation was performed by exposure of the Au-coated substrate to a solution of the studied molecule. The substrate, quartz crystal, gold coated slide or Au-coated HOPG, was selected depending on which characteristic of the SAM was to be measured. The substrate was immersed into the solution for a set period of time (several short periods of time rather than one long period). After each interval of immersion, determined by the deposited species, the sample under study was thoroughly rinsed with pure solvent to remove any physisorbed layers. Afterwards, the film was dried in a stream of cold air. The completion of the adsorption process is dependent on the concentration of the solution and can take from several minutes up to several hours.

As the head sulfur of the investigated compound was protected by thioacetate group, few drops of ammonium hydroxide were added to the prepared solution to displace that group and thus increase the rate of adsorption process. In the case when terminal thiol groups were protected by cyanoethyl group(s), the deposition process was performed with the addition of sodium methoxide as a deprotecting agent. Once the deposition was completed, the measurements were taken.

5.3　Measurements techniques

5.3.1 QCM

The QCM measurements were performed using a gold-coated 10 MHz quartz crystal purchased from *International Crystal Manufacturing Co.* Prior to deposition, the crystal's surface was cleaned as described above and thoroughly washed with a sequence of pure solvents: methanol, chloroform, methanol, ethanol and subsequently dried in cold air to avoid any temperature distortion of the quartz crystal. The cleaned crystal was used immediately, as a stored one would need to be cleaned again. The initial frequency was measured. The cleaning procedure was repeated until a stable value of frequency, varying by less than ± 1 Hz, was achieved. After deposition, the

frequency of the quartz crystal with the adhered material was recorded again. Hence, the frequency shift between the initial and resultant value was assessed, and a relative area per molecule could be derived from the Sauerbrey equation (see section 3.1).[105]

The frequency during the overall deposition process was monitored using a Hewlett-Packard 53131A 225 MHz Universal Counter and a Thandar TS3021S, (power supplier) supplying a direct current of 1 mA at 9 V, see Figure 5.2.

Frequency counter   Quartz crystal holder   Power supply
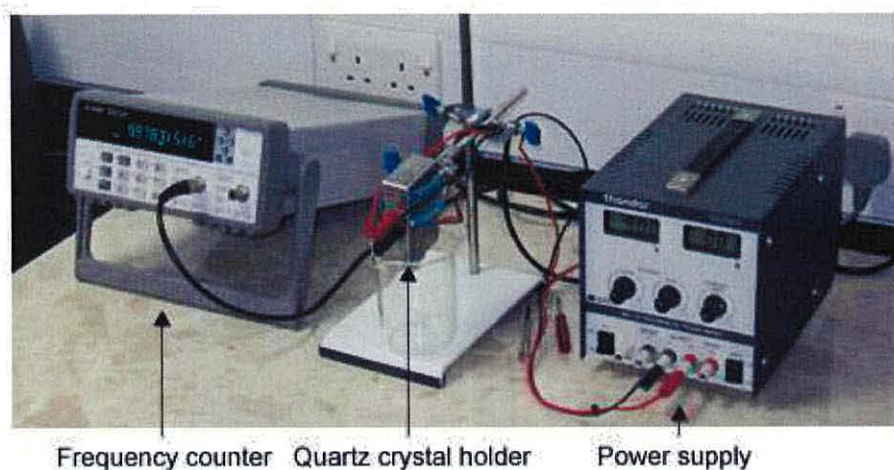
Figure 5.2 QCM set up.

5.3.2 SPR

The film thickness and dielectric permittivity were determined by SPR measurements. The layer system used in these studies comprised of a glass microscope slide with gold coated onto its surface. The metal thickness was monitored in the vacuum evaporation process, and was of approximately 47 nm. The self-assembled monolayer was deposited onto this substrate and the sample was fixed to a 60° BK7 crown glass prism. The good optical contact between the sample and the prism was ensured owing to the use of methyl benzoate whose refractive index matches that of the glass.

SPR measurements were performed employing the Kretschmann configuration, the illustration shown in Figure 5.3, with a p-polarised monochromatic light of two different laser beams, these being green and red lasers at wavelengths of 532 nm (*frequency doubled Nd:YAG laser*) and 632.8 nm (*HeNe laser*) respectively. The laser

beam was passed through a polarising filter plane (p-polarisor) in order to remove any vertical s-polarised light before passing the p-polarised light through a chopper (*Stanford research systems SR540*). The laser beam was then equally divided into two paths (sample and reference beams) by a beam splitter, with the reference part going to the reference detector and the sample one to a prism assembled on a rotation stage, so that the angle of incidence can be altered between 38° and 50°. This range was used due to the fact that the critical angle of a prism is about 41.3° for both lasers. The light reflected from the sample was detected by the sample detector. The signals from the sample and reference detectors were sent to the lock in amplifiers (*Stanford research systems SR830*) and their intensities were measured. The data at different angles were collected and resulted in a spectrum showing reflectivity variation as a function of the angle of incidence (see section 3.2). The spectrum obtained after deposition was compared with the one for the bare gold surface. The thickness and the real (ε_r) and imaginary (ε_i) dielectric permittivities of adsorbates were determined by a least squares error fit of the experimental measured curves to the theoretical predicted by the Fresnel equation.
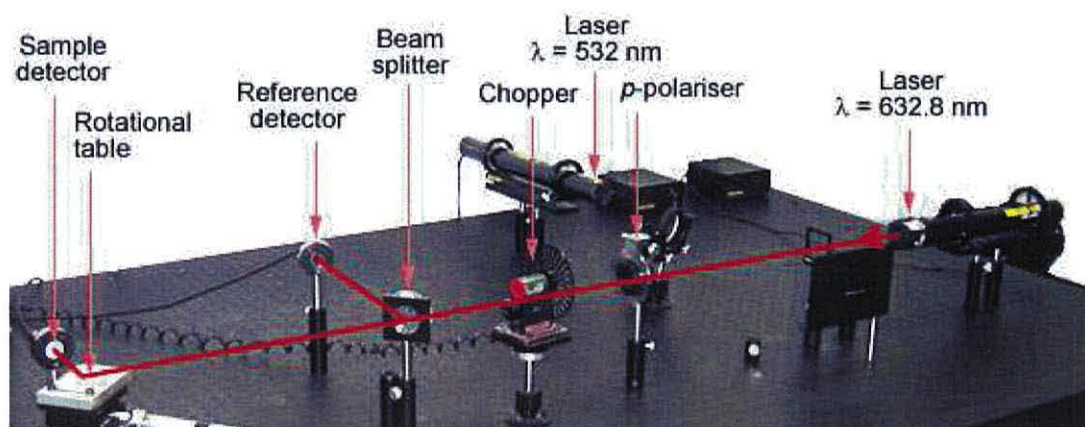
Figure 5.3 Illustration of the SPR setup incorporating two light sources. Red line shows propagation of laser beam through SPR system including polarisation, splitting and detection of the light.

5.3.3 STM

The STM measurements were performed by the use of a *Digital Instrument Nanoscope IV multimode STM by Veeco International* and recorded by a dedicated PC. The experimental set-up is illustrated in Figure 5.4.
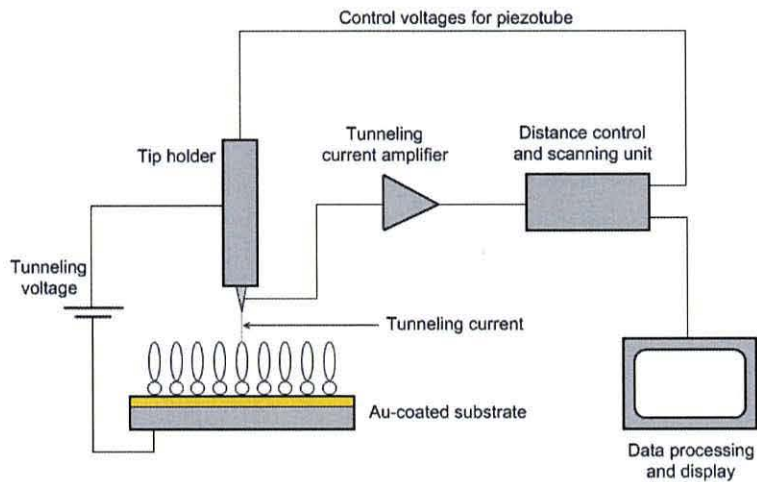
Figure 5.4 Schematic diagram of STM.

The instrument was placed on a vibration isolation stage (manufactured by *Table Stable, TS 150*) in order to prevent undesirable vibrations. For the characteristics of the studied material to be obtained, the tip was engaged at a current setpoint varying from 300 pA to 1000 pA and a voltage from 30 mV to 80 mV. Once the tip was successfully engaged, the surface under study was scanned providing an image. If the image revealed a smooth and even region of the surface, the tip was switched from the image mode to the STS IV mode. In this mode the feedback loop was used to maintain the tip position with respect to the surface. STS plots were taken in a sweep from 1024 mV to -1024 mV with 2mV increments whilst recording the tip-sample currents (providing the spectrum of the tunnelling current *I* versus the tunnel bias *V*). The measurements were also taken with the beginning value of this sweep being -1024 mV, in order to verify the same behaviour of the *I-V* curves. Each of *I-V* curves was obtained by averaging over 30 single scans, so that any noise was minimised. For the current jumps using the method of Heiss[5] (see section 3.3) to be revealed, STM measurements were performed in the

constant height mode. *I-V* characteristics were measured at different places of the sample to ensure that any obtained plots exhibiting rectification were confirmed. The effectiveness of the asymmetrical behaviour of molecules is defined as a rectification ratio (RR) that can be calculated from equation at the applied voltage V_0.

$$RR = \left| \frac{I(V_0)}{I(-V_0)} \right|$$

(4)

I-V characteristics of organic materials were recorded using PtIr (*Vecco International*) and mechanically cut gold tips. These types of tips were chosen due to improved atomic resolution and resistance to oxygen.

5.4   Chemical characterisation techniques

The organic compounds synthesised at Cranfield University were characterised by the following techniques to confirm structure and purity of the compounds:

UV-Vis spectra of products, usually dissolved in chloroform unless stated otherwise, were performed using a CECIL CE 9000 spectrophotometer. Data was recorded on a computer *via* Data stream software.

Differential scanning calorimetry (DCS) analyses were performed using a Melter Toledo DSC 822^e to determine the melting points and a purity of different compounds. Samples were heated from 25° to 400°C in 10°C steps.

The X-ray photoelectron spectroscopy (XPS) studies of molecules presented in this thesis were performed by Barbara Urasinska-Wojcik and Kym Ford at University of Queensland, Brisbane, Australia.

5.5   Synthetic methods

The reactions presented below were performed according to the procedure of Anne J. Whittam.[222]

5.5.1 Synthesis of thioacetic acid S-(4-iodo-propyl) ester

To a solution of sodium iodide (10.4 g, 69.4 mmol) in acetone (~ 300 mls) was added thioacetic acid S- (4-chloro-butyl) ester (2.99 mls, 22,7 mmol) in a 1:3 molar ratio. The mixture was refluxed overnight and then cooled. After cooling, the white solid (sodium chloride) was filtered off, whilst the solvent from the filtrate was reduced by rotary evaporation. The mixture was purified by column chromatography on silica gel (chloroform as an eluent-100 %) to yield the product-thioacetic acid S-(4-iodo-propyl) ester, as a dense yellow oil: yield 4.4 g.
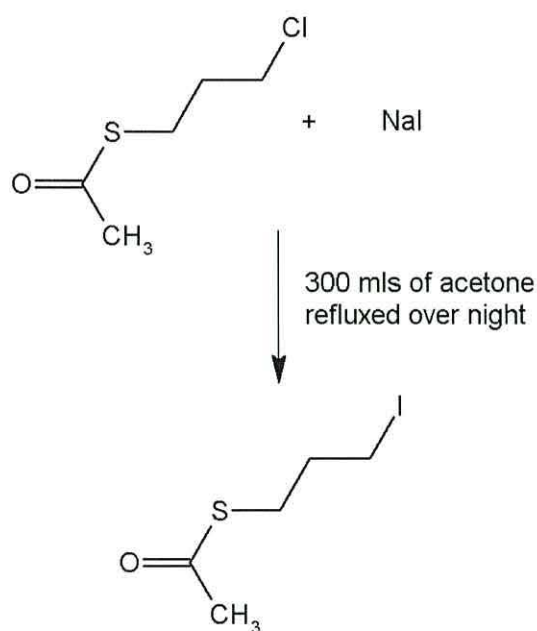
Figure 5.5 Synthesis of thioacetic acid S-(4-iodo-propyl) ester.

5.5.2 Synthesis of thioacetic acid S-[3-(4-formyl-phenoxy)-propyl] ester.

The recrystallised 4-hydroxybenzaldehyde (0.305 g, 2.5 mmol) was dissolved in distilled water, *ca.* 50 mls. To this solution was added sodium hydroxide pellets (202 g, 5.0 mmol) in a 1:2 molar ratio. The reaction was stirred for 3 hrs until the sodium salt of 4-hydroxybenzaldehyde was formed. A solution of thioacetic acid S-(4-iodo-propyl) ester (0.723 g, 3.0 mmol) in acetone (~20 mls) was added to the salt. This was refluxed and stirred for 12 hrs. After that time, a solvent extraction was performed by adding ~50 mls of chloroform. The bottom organic layer of the resultant mixture was extracted and washed with 3 x 50 mls of water. The water from that mixture was extracted and washed with 3 x 50 mls of chloroform. All chloroform fractions were combined and were dried by the addition of magnesium sulfate. Then the magnesium sulfate was filtered, whilst the solvent was removed by the rotary evaporator. The resulting was purified by column chromatography on silica gel (eluent: chloroform 100 %, and then hexane: ethyl acetate 60:40 %, respectively). Because there were still some impurities, the mixture was purified by prep-plate chromatography (eluent hexane:ethyl acetate 60:40 %) to yield the product, thioacetic acid S-[3-(4-formyl-phenoxy)-propyl] ester, a colourless oil: yield 0.128 g.
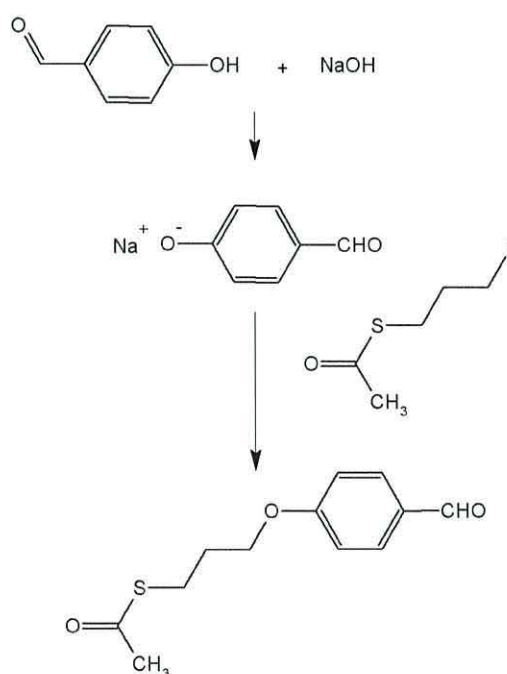
Figure 5.6 Synthesis of thioacetic acid S-[3-(4-formyl-phenoxy)-propyl] ester.
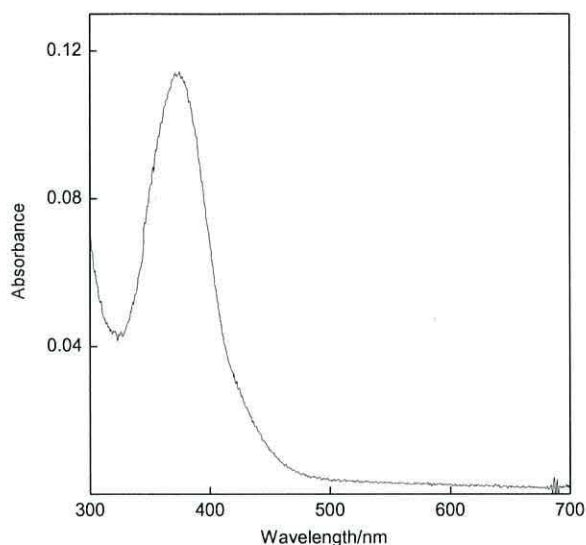
Figure 5.7 UV-Vis spectrum of thioacetic acid S-[3-(4-formyl-phenoxy)-propyl] ester in chloroform solution.

The UV-Vis spectrum depicted in Figure 5.7 exhibited a band of absorbance at 390 nm. The peak at this wavelength is expected to be recorded for such a colourless compound.

6 Results and discussion

Interest in developing components for use in the construction of nanoscale electronic devices brought molecular wires to the forefront of attention. They represent an important class of compounds for the realisation of molecular electronics, due to their ability to form a pathway for charge transfer through a tunnelling mechanism.[17,223,,224] Therefore, the investigation of the electrical properties of wire systems became a key challenge for research.

6.1 The wire of defined length

Organic components for electronic applications are produced mostly by traditional batch chemical syntheses. However, the following molecules were formed in a sequence of reactions at the surface. The idea of incorporating this type of method in building up the extended systems was chosen mainly due to the ability for the fabrication of molecular wires of a precisely defined length with fine control of the electrical properties.

Furthermore, this relatively easy process results in desired products being capable of forming spontaneous, well ordered films. The only requirement for this type of reaction to occur is the presence of an active group with an affinity to noble metal (preferably gold) in the compound hence, enabling the chemisorption to the metal surface (SA mechanism described in section 2.1).

The success in production of an ideal molecular rectifier would allow the elimination of complex syntheses yielding very often only small amounts of desired products. Moreover, the reaction at the surface enables avoiding problems encountered with the purification process (removal of the product from excess reactants or other impurities whose presence may cause the inhibition of physical properties of the product), which additionally requires a substantial energy input and adds significant cost to the overall process. Additionally, some chemicals appear to be difficult to synthesise or are poorly soluble. Thus, in an attempt to overcome the synthetic problems, this section presents a novel method towards the fabrication of molecular wire systems excluding traditional chemical reactions.

6.1.1 Deposition of a weak donor (thioacetic acid S–[3 –(4–formyl–phenoxy)–propyl] ester) on the surface of a gold-coated substrate

SAM films on the quartz crystals were fabricated by immersion of the gold-coated substrate into 0.1 mg cm^{-3} chloroform solutions of this component to which a few drops of ammonium hydroxide were added to facilitate displacement of the acetyl group, see Figure 6.1.
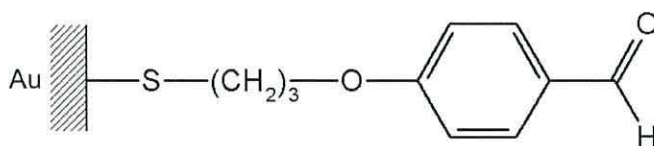
Figure 6.1 Molecular structure of thioacetic acid S-[3 -(4-formyl-phenoxy)-propyl] ester (**SAM 1**) linked to the gold substrate.

Optimum deposition was obtained by repeated immersions at 5 min intervals and thoroughly rinsed with a subsequent sequence of pure solvents: chloroform, methanol, pure water and ethanol to remove any physisorbed material from the surface. The film was then dried in a stream of cold air. The rate of the monolayer growth was monitored throughout the deposition from the frequency change (for a clean crystal and that after each reading) revealing the equilibrium of the process being reached after 105 min, see Figure 6.2. The calculated mean area 0.3 ± 0.03 nm^2 molecule^{-1} was characteristic for all of the studied samples and correlated well with the molecular cross-section. It must be noted, that this molecular area value provided the limiting area for all subsequent reaction steps.
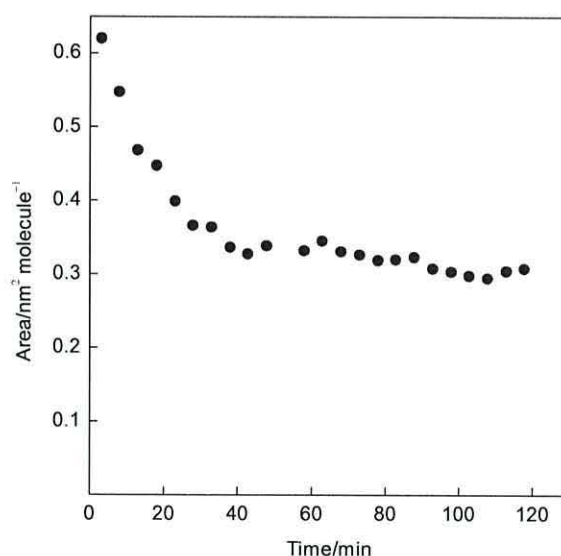
Figure 6.2 Molecular area of SAM 1 versus time for deposition of *via* chemisorption onto a QCM.

Evidence verifying the initial chemisorption onto Au-coated substrate, was provided by XPS studies. The spectra exhibited a doublet at 162.8 eV (S 2p$_{3/2}$) and 164 eV (S 2p$_{1/2}$) that corresponds to the binding energies of Au-thiolate link. S

ulphur doublet characteristc to the thiol group of the unbound sulphur-containg parent compound was stronger, at 164.5 eV and 165.1 eV.

In order to perform the electronic investigations, the monolayer film was formed *via* chemisorption on the Au-coated HOPG substrate in the same manner as for QCM characterisation. SAMs were studied at several locations across the surface using plain

PtIr probes and the recorded *I-V* plots were averaged from 35 scans to assure the obtainment of relatively noise free characteristics. An example of *I-V* characteristics is depicted in Figure 6.3. All of the curves were symmetrical, which was consistent with the non electron-accepting nature of the molecule (a weak donor), thus the observed behaviour was expected. It was found that the symmetry was unaffected by variation of initial set point conditions. They appeared to only affect the magnitude of the tunnelling current by influencing the tip-surface distance.
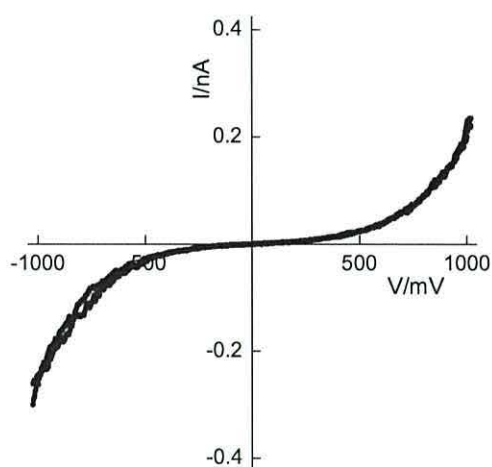
Figure 6.3 *I-V* characteristics of thioacetic acid S-[3-(4-formyl-phenoxy)-propyl] ester monolayer.

6.1.2 D – A deposition

The second step was realised by immersion of the pre-formed **SAM 1**, see Figure 6.1 on the 10 MHz quartz crystal into an ethanol solution of 2,6-diaminoanthra-9,10-quinone (0.1 mg cm^{-3}) to which 2 drops of acetic acid were added in order to assist the molecular wire formation at the Au-coated substrate surface.
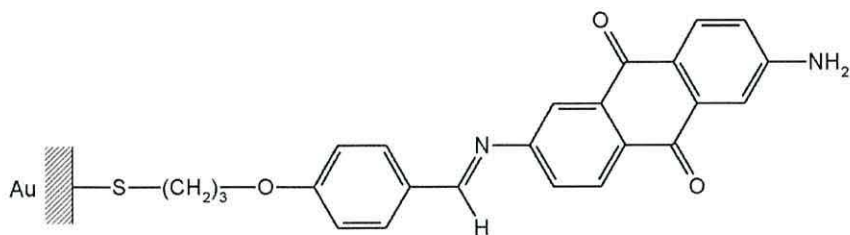
Figure 6.4 Molecular structure of self- assembled monolayer of 2,6-diaminoanthra-9,10-quinone (**SAM 2**) built up on the surface of **SAM 1** (thioacetic acid S-[3-(4-formyl-phenoxy)-propyl] ester) linked to the gold substrate.

The condensation of the surface aldehydes and solution-based amino substituents that yields molecular wire formation *via* imine group, see Figure 6.4, was observed through the frequency change during QCM characterisation. The frequency saturated to a constant value after 382 min of total immersion. Hence, the contact area derived from the Sauerbrey analysis of 0.35 ± 0.03 nm^2 molecule $^{-1}$ provides larger cross-section. This suggests that 2,6-diaminoanthra-9,10-quinone is combined with *ca.* 80% of molecules, see Figure 6.14 (frequency change of each stage *vs.* total molecular mass). The reaction seemed to be accomplished independently on the addition of acetic acid confirming the alignment of the molecule within monolayer. However the condensation process was not consistent in the absence of acetic acid and, as depicted in Figure 6.5, provided characteristics of monolayer growth were quite irregular. Thus, further measurements were performed in the presence of catalyst due to significant influence on the reaction facilitation.

XPS analysis on D-A wire yielded asymmetric nitrogen peaks resolved into two separate bands with binding energies of 399.3 and 400.7 eV, which corresponded to the surface-based imino (N=CH) and amino (NH$_2$) groups.
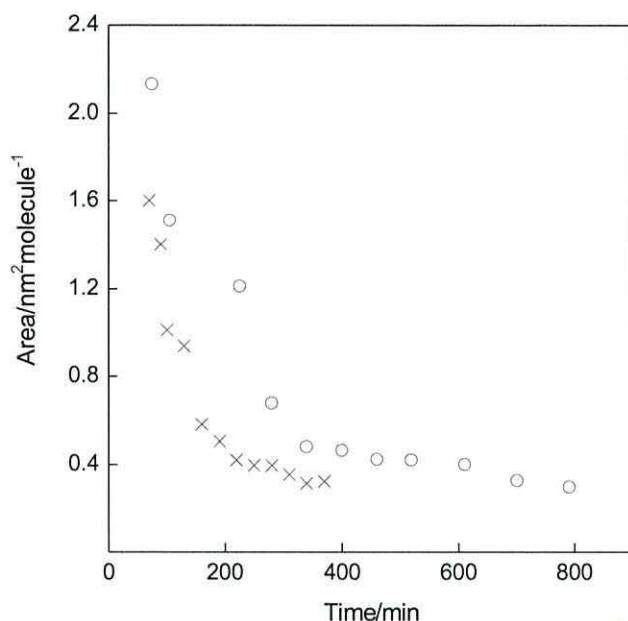
Figure 6.5 Molecular area versus time for 'step by step' deposition of D-A molecule *via* chemisorption onto a QCM in chloroform solution with (x) and without (o) addition of acetic acid.

Electrical measurements were performed by STM. The sample was contacted by a PtIr tip at different locations across the sample exhibiting reproducible rectifying behaviour with rectification ratios of *ca.* 5 at ± 1 V. The asymmetry recorded in the positive quadrant of the *I-V* plot, see Figure 6.6, indicated the electron flow from the probe to the Au coated HOPG at forward bias. Thus, electrons tunnel from (cathode) to 2,6-diaminoanthra-9,10-quinone acceptor on one side and from the tiolate-linked end of a weak donor molecule to the substrate (anode) on the other. The observed behaviour, verifies the theory that the electrical asymmetry arose from the designated donor-acceptor sequence. The direction at forward bias consistent with the Aviram and Rathner mechanism,[135] confirms the electron-accepting character of 2,6-diaminoanthra-9,10-quinone moiety. It may suggest that the electron-donating character of NH_2 group was either effectively neutralised by adsorbtion to the Au probe or resonantly attached to molecule's ring.

Moreover, the profile of *I-V* characteristics for molecular wire system recorded *via* STS was in agreement with that determined by theoretical calculations (see publication I,

section 9) assuming that Au-S assembly causes the tilt of vertically aligned molecular wire at an angle of 120°.
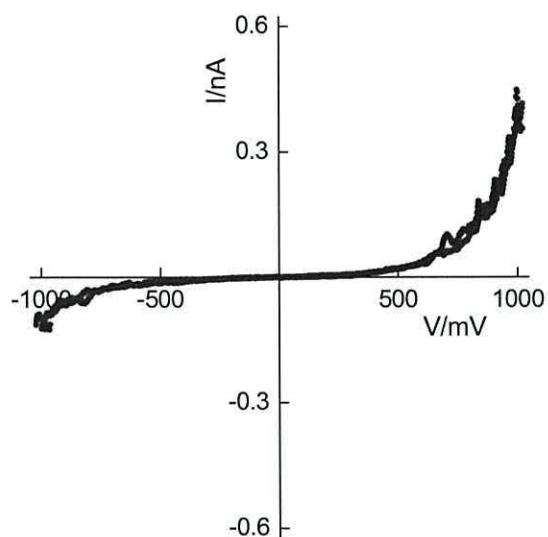
Figure 6.6 The example of the *I-V* curve obtained for D-A molecule.

6.1.3 D – A – A deposition

The final fabrication step, see Figure 6.7, of the molecular device of defined length was realised in a presence of acetic acid to assist the same type of condensation reaction, to which nitro-terminated aldehyde was added. The formation of the molecular wires was controlled by the immersion time.
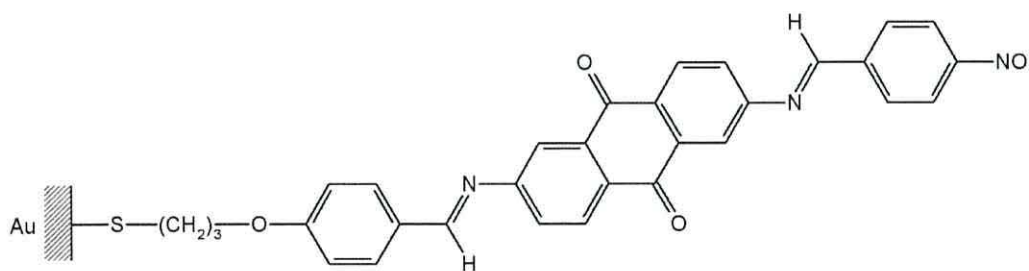
Figure 6.7 Molecular structure of self-assembled molecule (**SAM 3**) composed of D-A-A moieties linked to the gold substrate.

The mean area occupied by the terminal self-assembled molecule determined from the Sauerbrey equation was of 0.33 ± 0.03 nm^2 molecule^{-1} with the value being

characteristic for the whole molecule fabricated by the docking of successive molecules. The close packing of the molecule was obtained after the total immersion period of *ca.* 1300 min. Irregularity of the characteristic of monolayer growth and significantly longer time required to accomplishment of the reaction may indicate some rearrangements within the monolayer.
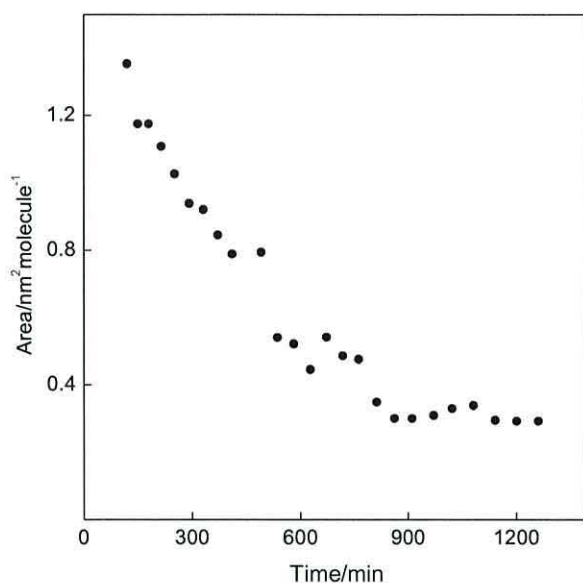
Figure 6.8 The characteristic for the D-A-A molecule built up during the 'step by step' deposition.

To verify the packing density of each layer involved in the assembly of the molecular wire, a plot demonstrating the dependence of the number of moles of each monolayer as a function of immersion time was calculated, see Figure 6.9. Hence, the packing density of the second layer depicted in Figure 6.9 did not project beyond the limit assigned by the initial chemisorbed monolayer. Therefore, the arisen assemblies seemed to be free from physisorbed materials and any random adsorbates. The slightly greater number of moles falling to **SAM 3** is more likely attributed to a solvent being trapped in the lattice.
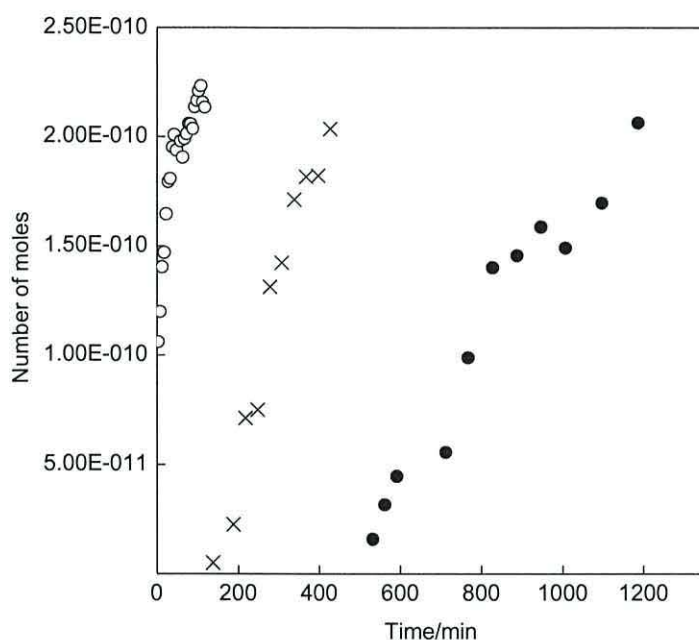
Figure 6.9 Number of moles as a function of immersion of a QCM in thioacetic acid S-[3-(4-formyl-phenoxy)-propyl] ester (**SAM 1**), 2,6-anthraquinone(**SAM 2**) and 4-nitrobenzaldehyde (**SAM 3**); o) representation of **SAM 1**, x) **SAM 2** and •) **SAM 3**.
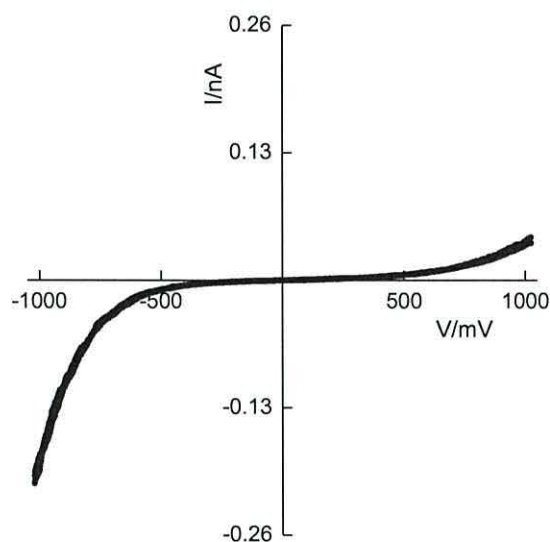
Figure 6.10 *I- V* curve obtained for D-A-A molecule.

STM studies of the molecule revealed reproducible asymmetrical characteristics with maximum rectification ratios of *ca.* 19 at ± 1 V when contacted by a PtIr probe. However, the enhancement of the current in the negative quadrant, see Figure 6.10 was inconsistent with the Aviram and Ratner rectification mechanism, which anticipated an

asymmetry in the positive quadrant for the ground state molecule. The observed rectifying behaviour would indicate a suppression of molecule's electron-accepting properties caused by the protonation of the terminal NO_2 group. The resultant structure acting as an electron-donor is shown in Figure 6.11. This might have caused a reversal in the direction of electrons tunnelling through the molecular wire system, when sandwiched between two electrodes. Consequently, the asymmetric characteristics could be observed in the opposite quadrant of the *I-V* plot instead of the one initially expected, see Figure 6.10.
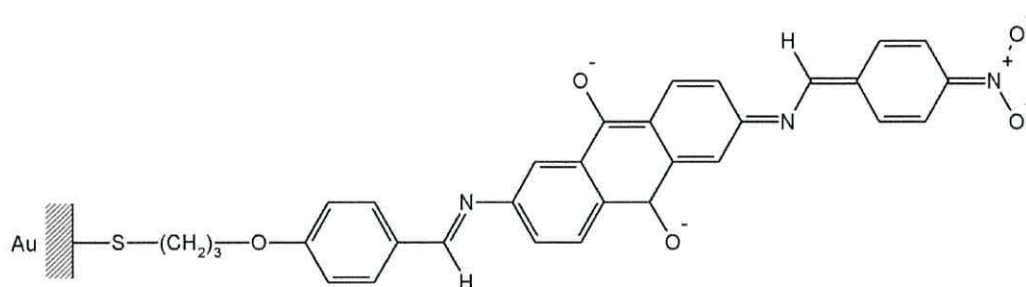
Figure 6.11 The assumed molecular structure of self-assembled molecule composed of D-A-D moieties linked to the gold substrate.

However, obtained results are less likely to stem from the protonation process, as otherwise to reported elsewhere,[132,196] the investigated D-A-A molecule was only exposed to a weak, acetic acid that was employed to facilitate the reaction. Due to incorporated difficulties in controlling of behaviour of 4-nitrobenzaldehyde within the junction, such a molecule, with a strong electron-withdrawing character, may not be suitable candidate for controlled assembly within the junction.

6.1.4 D – A – D deposition

Due to the unexpected behaviour of the D-A-A system induced by an electron-accepting upper layer, the terminal molecule was replaced with 4-dimethylaminonaphtalaldehyde, demonstrating electron-donating character, see Figure 6.12. The SAM from D-A-D molecular wire was characterised by QCM and STM techniques.
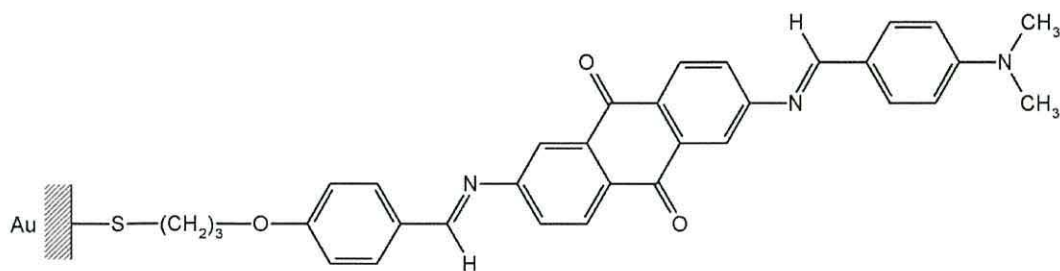
Figure 6.12 The trilayer self-assembled system (**SAM 4**) composed of D-A-D moieties deposited on the gold coated substrate.

The **SAM 4** was formed once the first two layers (donor and acceptor respectively) were already deposited onto planar gold-coated substrates. The final stage of the reaction was accomplished by the immersion of either the quartz crystal or HOPG coated with both, **SAM 1** and **SAM 2**, into the ethanol solution of the terminal component. The rate of condensation of the surface amine and the aldehyde-based solution monitored by QCM revealed that the well ordered layer of SAM4 was achieved after an immersion period of *ca.* 100 min. The frequency shift of 30 Hz (recorded by QCM) with respect to the initial frequency of this stage determined the molecular area of 0.30 ± 0.03 nm^2 molecule^{-1}, see Figure 6.13. The obtained results of cross-section area would suggest that **SAM 4** combines with a nearly 1:1 ratio to D-A wire, see Figure 6.14.
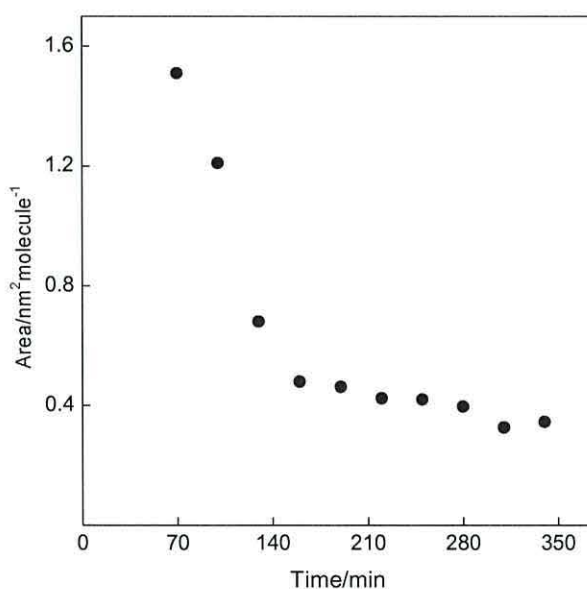
Figure 6.13 The QCM derived molecular area for **SAM 4**.

The XPS spectra of the molecular wire formed after the third step of deposition process, exhibited slightly asymmetric N 1s peaks at *ca.* 399.2-399.5 eV with shoulders on the high energy side that correspond to the surface-based amino substituents.
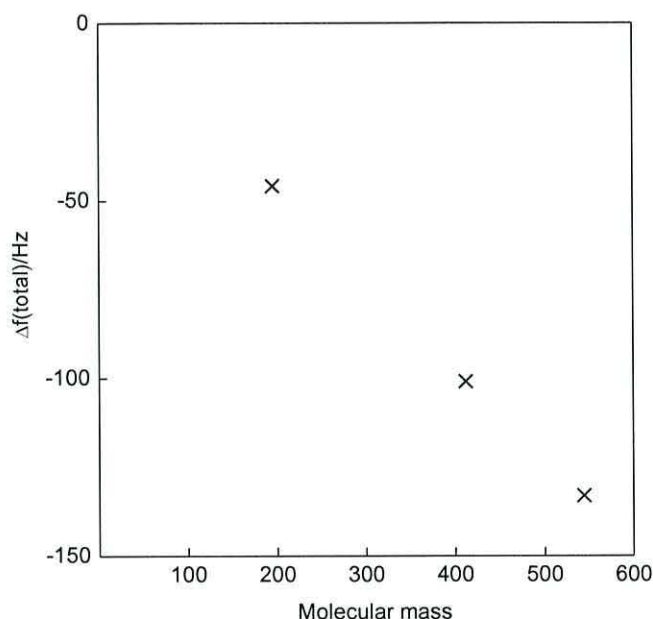
Figure 6.14 Frequency change from each stage of the process *vs.* molecular mass of the wire as it is assembled in first step **SAM 1** (x at lowest value of molecular mass) and elongated in next two steps (**SAM 2, SAM 4**). Lower values of a frequency change are observed for each subsequent step.

STM analysis was conducted on Au-coated HOPG as well as quartz crystal substrates. The recorded *I-V* characteristics of the whole system when contacted by the plain PtIr tip demonstrated rectifying behaviour. This time, all of the measured *I-V* curves exhibited a high current in the negative quadrant as shown below in Figure 6.15. Rectification ratios calculated from 6 samples were in the range of 5-13 at ± 1V. This data stems from the fact that, the dialkylaminonaphtaldehyde moiety is far stronger donor than thiolate group and although donor-acceptor-donor sequence, different behaviour of the resultant wire to that observed for **SAM 1** is logical. Thus, the functional molecular wire formed after final step of three-stage process, may be considered as having an Au-wire-A-π-D structure. Following the consistency with Aviram and Ratner prediction, the electron flow through the investigated system at forward bias is from the cathode to the electron-accepting side of the system and from the stronger of two donors to the opposite side of the device.
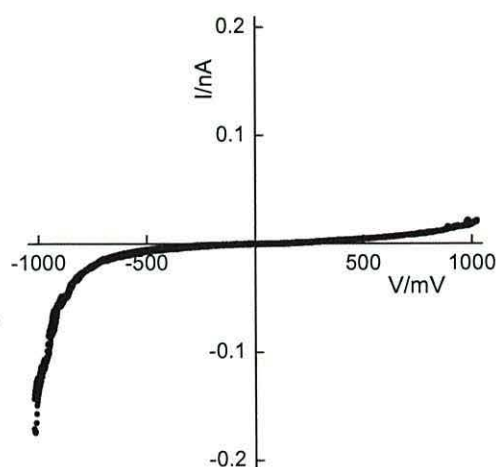
Figure 6.15 *I-V* plot for the complete D-A-D system.

It can be concluded that rectification occurs when both, electron-donating and electron-accepting, moieties are incorporated within the structure of the molecular wire and the bias for rectification may be reversed depending on the donor and acceptor sequence, see Figure 6.16. This provides the evidence that altering asymmetric *I-V* characteristics are molecule-induced.
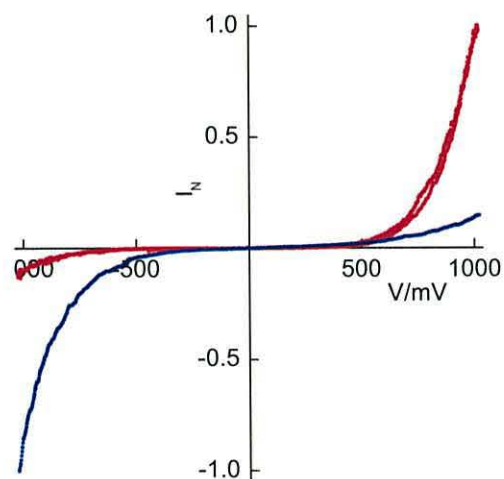
Figure 6.16 Normalised data following reaction with 2,6-diaminoanthra-9,10-quinone (red) and 4-dimethylaminobenzaldehyde (blue). The data were collected by STS and the sign corresponds to the substrate electrode.

6.1.5 Summary

Electrical analysis of D-A-D wire formed from sequentional assembly of donor-acceptor components demonstrated that the properties of molecular wire systems could be tuned by altering the donor-acceptor sequence. Rectification was recorded when one end of the wire was electron-donating and the other, electron-accepting (for example D-A step). Consequently, the bias for rectification was reversed for the resultant wire-like structure composed of D-A-D sequence. This also provided the evidence that the rectifying behaviour was molecular in origin. Additionally, the direction of electron flow at forward bias for each step followed the Aviram-Ratner model; from cathode to acceptor on one side and from donor to anode on the opposite side. The exception to that model was observed only for D-A-A molecule, but that was due to an uncertain rearrangement within the film probably caused by a strong electron-accepting character of NO_2 substituent.

Presented work reports on the three-stage process, but incorporation of this method in formation of elongated structures is significant due to the ease of the process yielding very complex systems of defined length with fine control of electrical properties.

6.2 Conjugated molecular wire systems with redox-active core units

In an attempt to explore the importance of molecular wires for electronic applications, this part of the reported research is focused upon oligo(arylene) compounds with incorporated redox-active units into their backbones. Investigated molecular wires were designed to create Au-WIRE-Au junctions. All of the investigated molecules whose results are revealed in this section were synthesised by the Bryce group, School of Chemistry at the Durham University.

6.2.1 Molecular wire with an electron-donating core unit in the backbone.

The first molecule under study belonging to the oligo(arylene)s family, presented in Figure 6.17 is composed of a 1.9 nm long backbone with thioacetyl-protected termini groups.
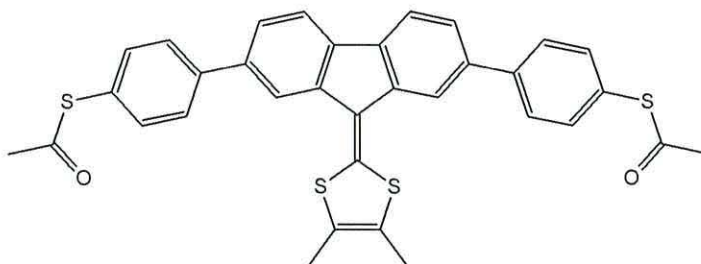
Figure 6.17 Molecular structure of the molecular wire with an electron-donor moiety [9-(1,3-dithiol-2-ylidene)fluorene in the backbone (**WIRE 1**).

The molecular film was successfully generated by immersion of the Au-coated substrate in a tetrahydrofuran (THF) solution of the precursor (with concentration of 0.05 mg cm^{-3}), to which a few drops of ammonium hydroxide were added in order to facilitate the deposition process. The rate of the monolayer growth was monitored by frequency change during chemisorption onto a quartz crystal, whose value became constant after *ca.* 380 mins. Hence, the mean area occupied by molecules determined from Sauerbrey analysis was 0.8 ± 0.04 nm^2 molecule^{-1}, see Figure 6.18. The data was similar to that obtained when the protecting agent (ammonium hydroxide) was omitted, but the time required for the complete assembly of the latter was almost twice as long, see Figure 6.18.

The monolayer was characterised by XPS, and studies provided evidence confirming self-assembly occurrence. The spectra exhibited an S 2p peak at 162 eV that corresponds to the binding energy of the Au-thiolate link [225] and another at 164eV being characteristic to the 1,3-dithiol-2-ylidene unit and unbound thiolate group.[226]
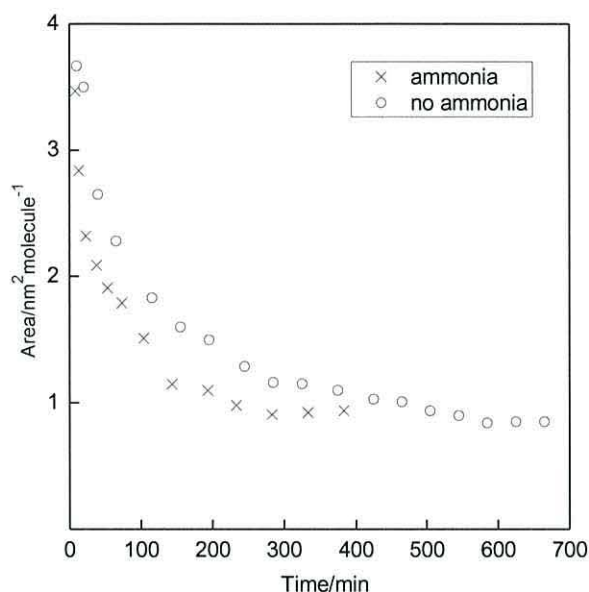
Figure 6.18: Molecular area *versus* time *via* chemisorption onto a QCM for SAM of **WIRE1**. Comparison of monolayer growth characteristics with the addition of deprotective agent to when omitted.

The electrical properties were measured by STM using an Au tip at the initial set point of *ca.* 400-600 pA at 30 mV. In each case, the monolayer film was investigated at several locations across each of the SAM. The relatively noise free plots, which can be seen in Figure 6.19 were the averaged *I-V* measurements from 30 scans at each side. *I-V* characteristics were recorded for different set-point conditions and studies revealed mainly symmetrical behaviour independent of the application of deprotecting agent. Although there were slight differences in the shape of the recorded *I-V* characteristics, the general profile of the curves was not affected. However, the altered set point parameters which determine the distance between the tip and the substrate influenced the magnitude of the tunnelling current. This behaviour was reported for STM studies on other wire-like molecules.[208]

Infrequently, slight asymmetry with higher current in the negative quadrant of the *I-V* plot could be observed (the current ratio of *ca.* 1.8 at ± 1 V). Since the redox-active unit has been incorporated into the backbone of **WIRE 1**, it was feasible that recorded behaviour was molecular in origin, as analogues with lack of electroactive central moiety by comparison are completely symmetric.[227] Thus, direction of electrons flow at forward bias indicated a vertical alignment of the molecule with electron-donating

moiety, 1,3-dithiol-2-ylidene, being tilted towards the Au tip. The latter confirmed the chemisorption of **WIRE 1** onto Au-coated substrate *via* sulphur atom.
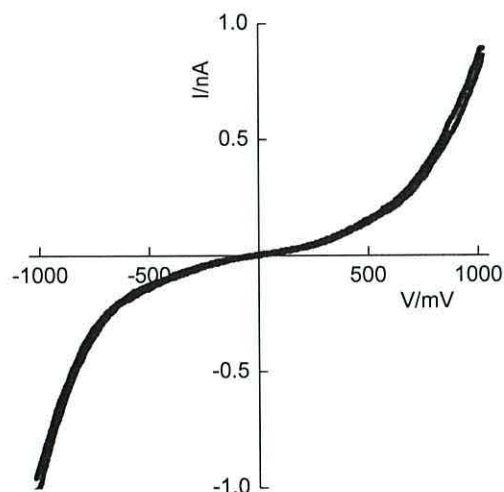
Figure 6.19 *I-V* characteristics of a SAM of the symmetrical molecular wire, when the sample was treated with tetrahydrofuran and with omitting it.

The measurements of single molecule conductivity in this study were performed using the *I(t)* method of Haiss *et al* [5] (see section 3.3). The samples for study were prepared in the same manner as for the *I-V* characterisation and probed by the gold tip. Although Haiss *et al.* stated that the current jumps cannot be observed on clean gold surfaces,[5] the coverage of the surface was verified by *I-V* measurements. During measurements the tip was positioned at a suitable distance from the sample surface. This tip-substrate separation was determined by the tunnelling parameters at relatively high values (300 mV), so that the molecule from initially flat-lying phase could form a molecular bridge, observed as a current jump. The magnitude of the event is proportional to the applied tip-substrate potential.[5] The tip-sample gap was maintained constant and the tunnelling current was monitored as a function of time. The electrical contact between electrodes was guaranteed by both thiol termini groups of the molecule (strong Au-S interactions, see section 2.1). The characteristic STM current jump of the **WIRE 1** is illustrated in Figure 6.20 a, below, whereas the large number of contact events recorded at different locations on a sample yielded the histogram plot, see Figure 6.20 b. As can be seen, the adsorption persisted for *ca.* 80 to 100 ms for the most recorded events with almost 50% of all current jumps exhibiting values of 0.105 ± 0.05 nA for a surface bias of 300mV.

Moreover, the histogram constructed from all recorded events indicates predominantly the single-molecule contact centred about 0.11 nA. Thus, adsorbtion *via* single thiolate link to the gold tip can be confirmed.
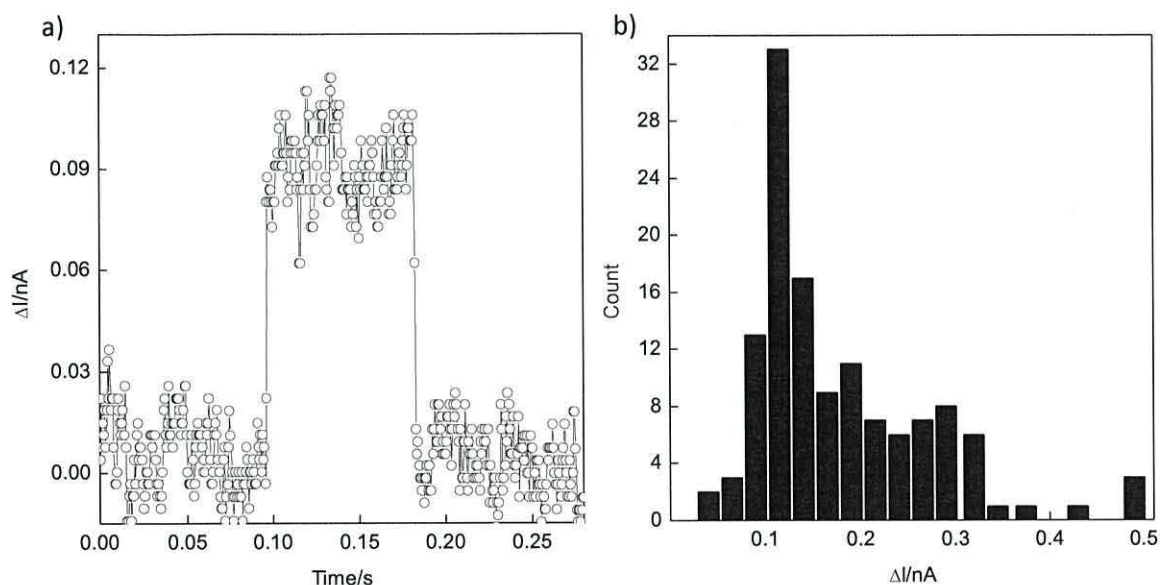
Figure 6.20 The representation of a) current jump and b) histogram of 132 current jumps at a sample bias of 300 mV.

The comparison of the data obtained by the application of Haiss' method to those displayed by *I-V* characteristics lead to the conclusion that the single molecule current of the latter is about 2 times higher at the same voltage. The observed behaviour can be explained by the initial set point parameters that influence the tip-substrate separation while the sample is probed for *I-V* characterisation.

6.2.2 Molecular wire with an electron-accepting core unit in the backbone.

The analogue of **WIRE1** shown in Figure 6.21 with the same backbone length, but in contrary, with a central electron-acceptor moiety, revealed unexpected behaviour when deposited onto Au-coated substrates and characterised by QCM and STM.
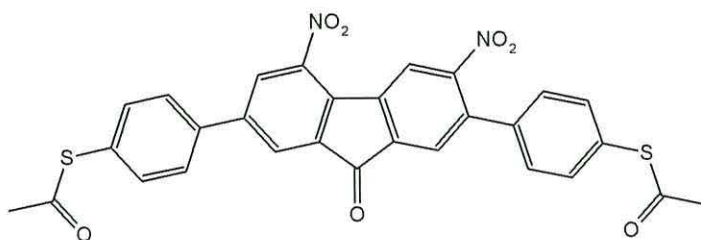
Figure 6.21 The molecular structure of the oligo(arylene) molecular wire with protected thiolate termini groups and an electron-accepting core moiety in the backbone(**WIRE 2**).

The monolayer from **WIRE 2** was prepared in the same manner as for the **WIRE 1**, where the deposition occurred in tetrahydrofuran solution of the precursor with a concentration of 0.05 mg cm^{-3} in the case of the presence and absence of deprotecting agent (ammonium hydroxide). QCM studies were performed on five crystals for each case and revealed consistent time data for the formation of the complete monolayer. The frequency saturated to a constant value after *ca.* 300 min and 380 min when with ammonium hydroxide and without it, respectively. This means that the mean area derived from Sauerbrey equation was almost identical for both cases, of *ca.* 1.1 nm^2 molecule^{-1}, see Figure 6.22.
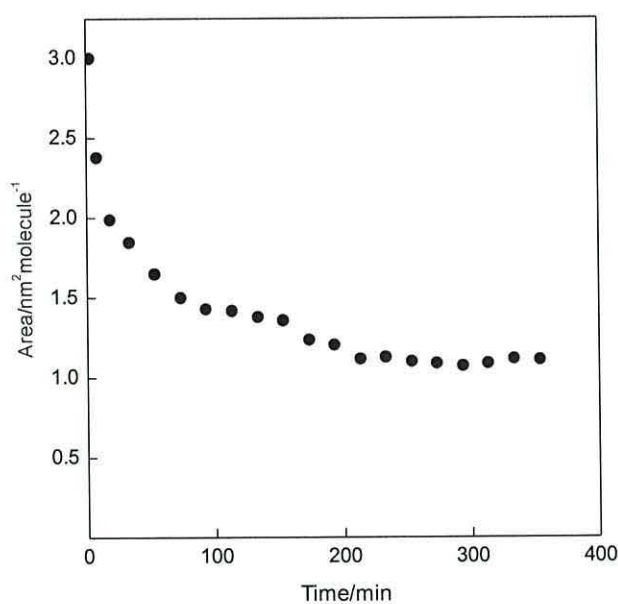
Figure 6.22 Area *versus* immersion time for **WIRE 2.**

The value obtained for the area per molecule was significantly different when compare to that of the analogue, **WIRE 1**. However, the area is consistent with van der Waals dimensions for molecular wires, but only if different alignment of the molecules within the monolayer is considered. Thus it was assumed that the molecule was attached to the Au-coated substrate by nitro substituents. It was reported elsewhere[228] that nitro groups enhance significantly the electron-withdrawing character of fluorenone derivatives. On the other hand these electron-acceptor substituents decrease the rate of conventional assembly.[229] Thus, phenomenon can be explained by weakening of the Au-S interactions[230] due to very electron deficient dinitrofluorene core in favour of physisorbtion *via* NO_2 groups. Moreover, XPS studies on **WIRE 2** provided evidence that monolayer film formation was ambiguously dominated by chemisorption *via* the sulphur atom. The spectra exhibited a sulphur doublet, at 161.9 eV ($S2p_{3/2}$) and 163.1 eV ($S 2p_{1/2}$), characteristic to the binding energies of sulphur atom to Au, whereas the unbound component exhibited a far stronger doublet, at 163.4 and 164.6 eV. A single N 1s peak exhibited at 405.6 eV, characteristic of the NO_2 groups, was found in monolayer samples formed in the presence and absence of the deprotecting agent. Additionally, the chemical instability reported by Stapleton et al.[231] when nitro-substituted oligo(phenyleneethynylene) thiolate molecules were assembled in the presence of ammonium hydroxide, was not observed. Otherwise the N spectra would yield two additional peaks at, 402.1 and 399.3 eV, characteristic of NH (OH) and NH_2 that stemmed from thiolate-nitro redox processes.

The phenomenon of the assembly *via* competitive Au-thiolate / NO_2-Au interactions was also supported by quantitative analysis (results are due to be published, see publication III, section 9). The analysis suggested formation of the SAM under basic condition *via* Au-S link in 40-65% with a remainder assembled *via* nitro substituents, see Figure 6.23.
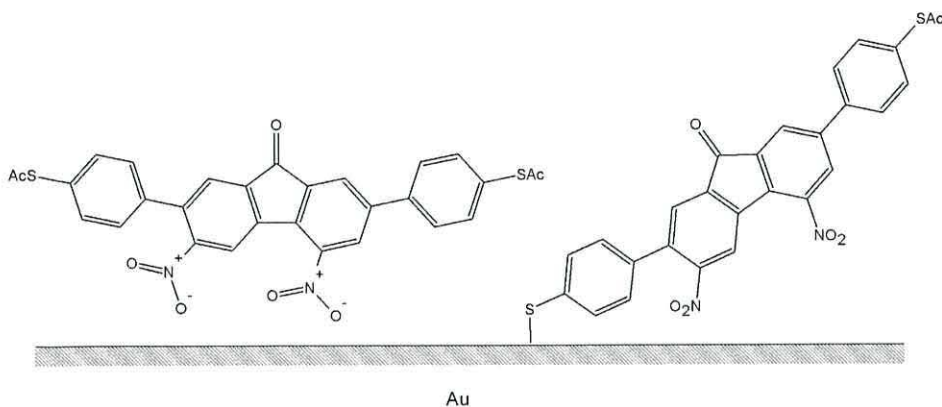
Figure 6.23 Schematic representation of assembly of **WIRE 2** *via* competing Au-S/NO₂-S assembly.

Moreover, the electrical studies of such a molecular wire recorded the repetitive asymmetric *I-V* characteristics with the higher current in the negative quadrant, see Figure 6.24, and maximum rectification ratio being of *ca.* 5 at ± 1 V.
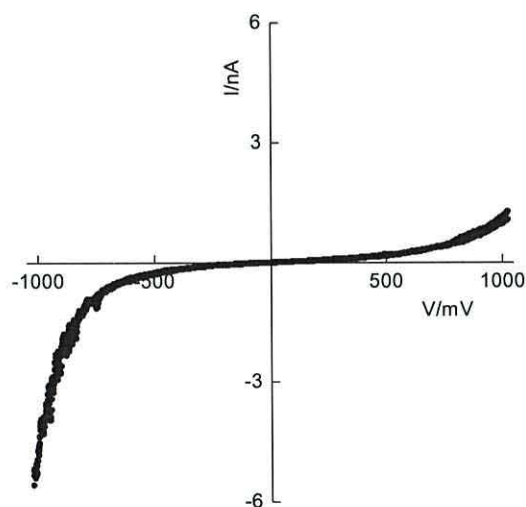
Figure 6.24 Representation of *I-V* characteristic obtained for **WIRE 2** deposited on gold, suggesting an electron-accepting character of the molecule.

The observed rectifying behaviour, unlikely for these wire-like molecules, would suggest an electron-accepting character of the SAM that could have stemmed from the contact between the nitrogen group and a gold electrode. Furthermore, when considering the consistency of the rectification mechanism with the Aviram and Ratner model, the enhancement of the current in the negative quadrant of *I-V* plot indicates the flow of electrons from the substrate to the LUMO of the acceptor on one side and from the HOMO of the donor to the tip on the other. This suggests the parallel alignment of

the molecule with nitrogen atoms of the central moiety being anchored to the Au-coated substrate.

Further electrical measurements were performed employing the *I(t)* technique of Haiss *et al.*[5] The samples were prepared identically as presented for the **WIRE 1** and resulted in the occurrence of spontaneous adsorption and desorption with abrupt changes in the tunnelling current at the sample bias of 300 mV, see Figure 6.25a. As shown in Figure 6.25 a, the adsorption (of sulphur and nitrogen groups in this case or only one of them) event lasted for *ca.* 100 ms with *ca.* 40 % falling within the range of 0.28 ± 0.05 nA. The analysis of hundred-seventy-four current jumps recorded at different locations on the substrate yielded the histogram shown in Figure 6.25 b, which also revealed double molecule contact centred about 0.4 nA, 10 % to the total recorded events. This can be explained by the fact that for smaller tip-sample separations, the probability of multiple contacts is increased.[5]

It must be noted that the conductivity for **WIRE 2** is higher than that of **WIRE 1**, probably implying influence of different conformation within a junction. According to report of Haiss *et al*,[5] observed behaviour could stem from greater tilt angle towards the substrate and thus better coupling between Au electrodes and a molecule. The same report also imply that the conductivity enhancement is due to end phenyl group-Au substrate interactions at angles beyond 50°. This would also confirm assembly via NO_2 groups, but since the assembly is competing, the controlled coupling of thiolate molecules, with strong electron-acceptor character, in the junction is difficult.
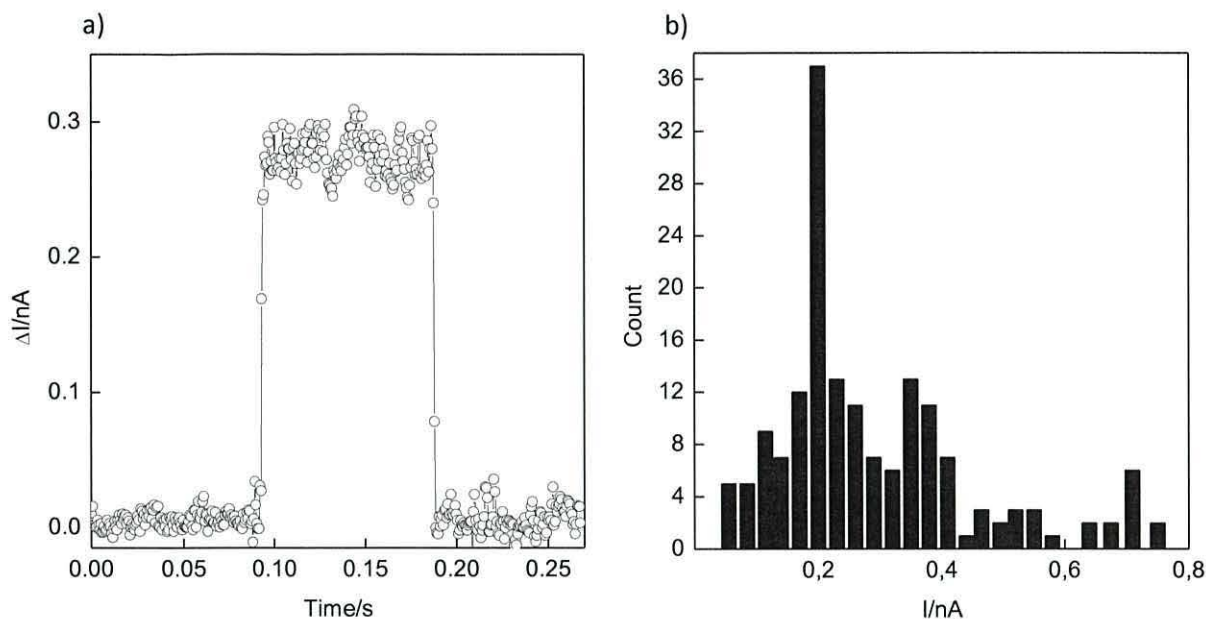
Figure 6.25 The representation of a) current jump and b) histogram of 174 current jumps at a sample bias of 300 mV.

In an attempt to provide evidence supporting the foregoing assumption regarding the alignment of the molecular wire **2** within the monolayer, further investigations were performed on 2,7-dibromo-3,5-dinitrofluorenone (**MOL1**) presented in Figure 6.26. Such a molecule, like molecular wire **2**, is composed of two nitrogen groups that have an affinity to gold. Thus if any electrical asymmetry occurs, such behaviour will be more likely induced by a molecule attached by nitrogen atoms to the gold electrode, as there is a lack of sulphur atoms in the structure of the molecule.
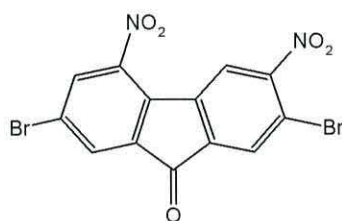
Figure 6.26 The molecular structure of **MOL1.**

In order to verify the growth of the monolayer on the gold-coated substrate surface, the QCM studies were executed in the first instance. An illustration of the characteristic of the growth of the molecular film is presented in Figure 6.27. The mean area occupied by the molecule was 0.5 ± 0.05 nm^2 molecule^{-1}.
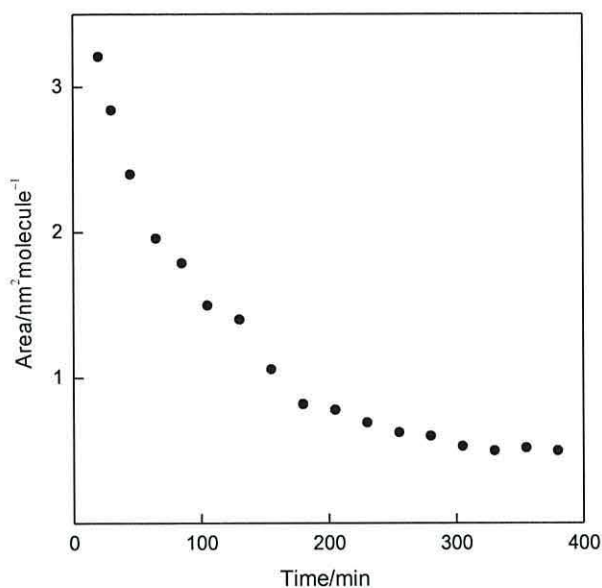
Figure 6.27 Kinetics of SAM deposition on QCM. Mean area occupied by the molecule was 0.5 nm^2 molecule^{-1}.

Relying on the QCM measurements indicating the presence of the monolayer on the Au surface, STM investigations were performed. The electrical studies yielded reproducible rectifying behaviour with the higher current in the negative quadrant of the *I-V* plot, see Figure 6.28. The rectification ratio calculated from several samples was of *ca.* 3.0 at ± 1 V. Taking into consideration the lack of terminal thiol groups in the structure of the molecule, the provided data confirmed the initial assumption regarding the alignment of such a molecule on a gold coated substrate.
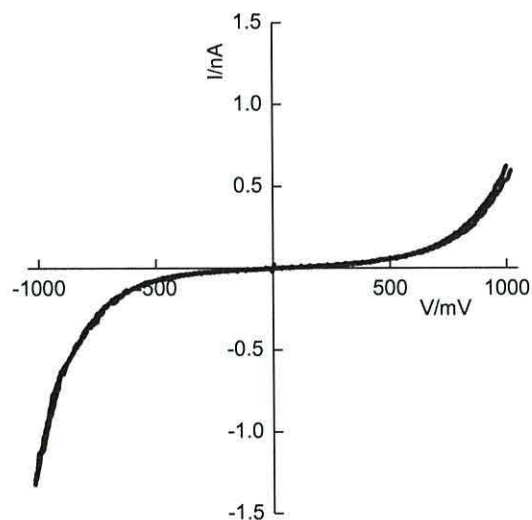
Figure 6.28 The example of *I-V* characteristic suggesting the molecule's attachment by nitrogen group.

6.2.3 Summary

The investigation of two oligo(arylene) analoques with incorporated different redox-active building blocks in their backbones exhibited significantly different results. Electrical analysis revealed symmetrical and asymmetrical *I-V* curves for **WIRE1** and **WIRE2**, respectively, despite wire-like stuctures of both molecules. This suggested different modes of assembly of **WIRE1** and **WIRE2**. Additional evidence was provided by XPS data which also confirmed coupling of **WIRE2** to Au electrode *via* competing S-Au/NO$_2$-Au interactions. The observed bahaviour was explained to be due to weakened S-Au adsorbtion as a consequence of the very electron deficient dinitrofluorenone core of **WIRE 2**, which was in conjugation with the thiolate group. Contrary, **WIRE1** was assembled *via* conventional Au-S chemisorption.

Provided data led to the conclusion that, thiolated molecules with a strong electron-accepting group in their central core, in particular those with nitro substituents, might not be suitable for controlled assembly within the junction.

6.3   Extended π-conjugated molecular wire system

Molecular electronic systems with integrated oligo(phenyleneethynylene)s (OPE) have drawn a lot of attention[232,233] due to rigid-rod and length-persistent structures. However, it must be noted that, at room temperature, the phenylene rings are freely rotating meaning that rotation with respect to each other will cause the reduction of the conductance. The investigated π-conjugated molecular wire whose results are revealed in this section was synthesised by the Bryce group, School of Chemistry at the Durham University.

This molecular wire (**WIRE 3**) with an extended backbone (3.9 nm long) and 1,3-dithiol-2-ylidene (electron donor) pendant substituent on the central fluorene moiety was studied in order to examine its potential for incorporation into an electronic circuit. The almost linear backbone of such an oligomer, see Figure 6.29, has hexyloxy side-

chains to ensure its solubility in organic solvents and terminal thioacetate protecting groups.
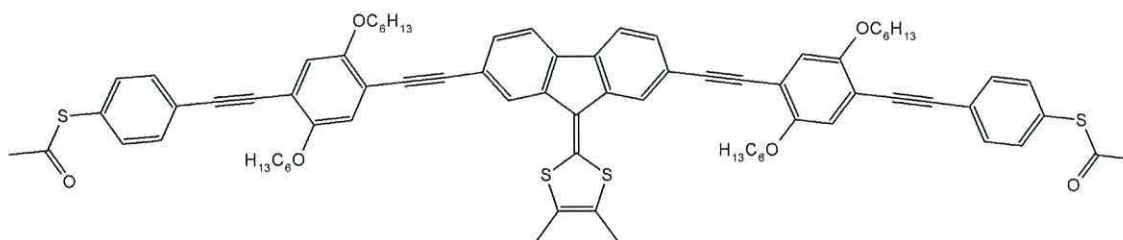
Figure 6.29 Molecular structure of the molecular wire with a 3.9 nm long backbone (**WIRE 3**).

Monolayers were formed by immersing Au-coated 10MHz quartz crystals in a tetrahydrofuran solution of **WIRE 3** (0.1 mg cm^{-3}) to which ammonium hydroxide (NH_4OH) was added to displace acetyl groups. Substrates were repeatedly immersed for 10-15 min intervals and thoroughly rinsed to remove any physisorbed material from the surface. The QCM studies revealed that independently on the treatment with deprotecting agent (ammonium hydroxide); the monolayer growth characteristics under both sets of conditions exhibited almost identical shape and took the same time for completion of the deposition process. Monolayer formation indicated from the frequency change, which saturated to a constant value after *ca.* 2h, and subsequent Sauerbrey analysis yielded a mean area of *ca.* 1.2-1.5 nm^2 molecule^{-1} for the chemisorbed wire, see Figure 6.30. The calculated value, which constitutes an average of eight measurements (four for each case) was consistent with the van der Waals cross section of the molecular wire on the assumption that the tilted molecules were partially overlapped. Obtained results suggested occurrence of monolayer without the formation of disulfides, as otherwise, the limiting area would be considerably reduced.
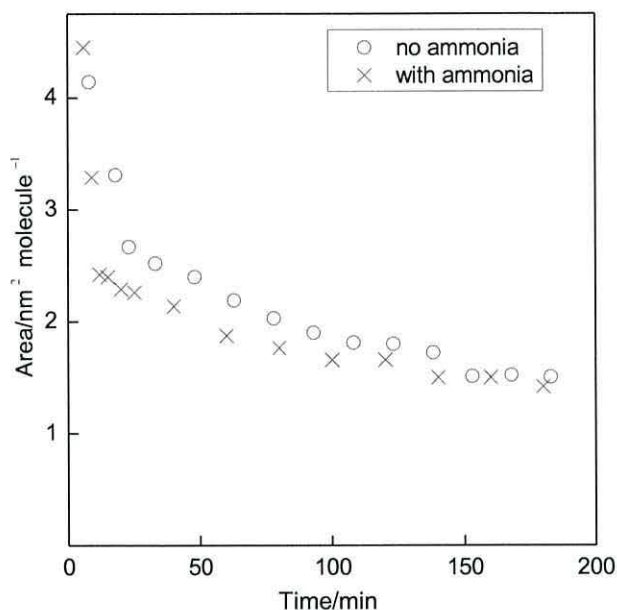
Figure 6.30 Kinetics of SAM deposition for **WIRE 3** monitored with QCM technique; crosses indicate the molecular area for the molecule when used deprotecting agent, while dots with omitting it.

In order to study the electrical measurements, SAMs were chemisorbed onto Au-coated HOPG under basic conditions to ensure removal of the protecting groups at both termini, as these could act as a barrier to conduction if retained. Films assembled on planar substrates were monitored by STM using various set-point current and voltage conditions to land the gold probe. The STM measurements were performed at several locations across the sample and revealed symmetrical *I-V* plots as anticipated for symmetrical wire-like molecules contacted by gold electrodes. Although slight asymmetry in the negative quadrant of the *I-V* plot was observed, see Figure 6.31, such behaviour was recorded infrequently and the provided rectification ratios were of *ca.* 1.5 at ± 1 V. Thus, the occurrence of electrical asymmetry was associated with more extreme set-point conditions.
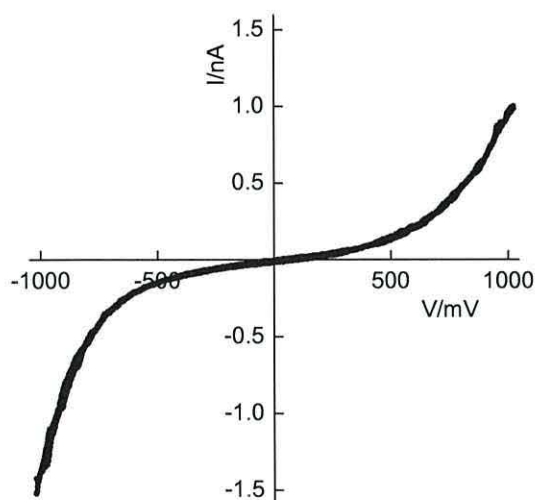
Figure 6.31 *I-V* characteristic observed for wire-like molecule (**WIRE 3**).

Electrical conductivity of a single molecule was performed by monitoring the current as a function of time, *I(t)* method of Haiss *et al.*[5] The same samples, as for the *I-V* characterisation were used to perform these measurements. Probing (at different locations) across the sample with the gold tip located at a fixed height just above the SAM at the sample bias of 300 mV gave series of current jumps among which the one shown in Figure 6.32 a, represents the lowest recorded current. The adsorption of the terminal thiol group to the Au probe manifested by the enhancement of the current persisted for *ca.* 50-100 ms with *ca.* 30 % of all events within the range of 0.12 ± 0.03 nA at 300mV, see Figure 6.32 b. The histogram revealed the simultaneous attachment of multiple molecules, with two events centred about 0.24 ± 0.03 nA and another centred about 0.36 ± 0.03 nA. The demonstrated behaviour may be attributed to different contact geometry.[234] It can be concluded that for molecules of this length, it is rather difficult to bridge the gap between probe and substrate.[244] Thus, the observed conductivity may not relate to the current along Au-S-wire-S-Au junction but to the contact of the tip to the body of chromophore. This would also explain no significant difference in the electrical study of this molecule to that of **WIRE 1,** although the decrease of the current for a larger tip-substrate gap should be observed.[133]
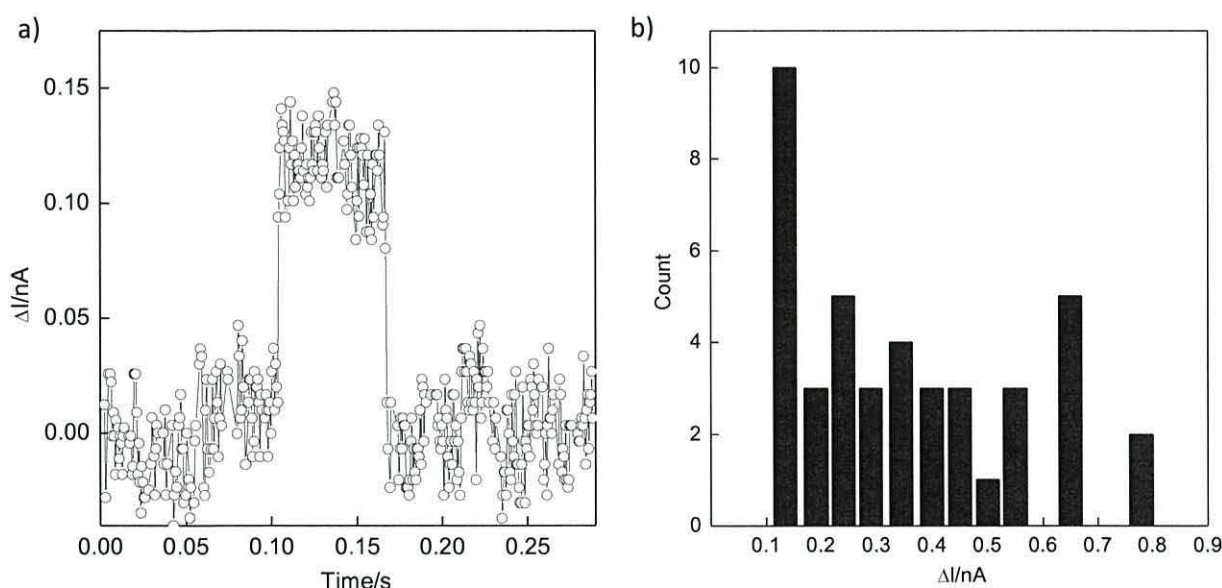
Figure 6.32 The representation of a) current jump and b) histogram of 50 current jumps at a sample bias of 300 mV.

Noteworthy is the fact that the value of the single molecule current obtained from *I(t)* technique of Haiss[5] is about 3 times larger to that manifested by *I-V* characteristics at the same voltage. However, similarly to the demonstrated dependence by molecular **WIRE 1**, such behaviour stems from the initial set point conditions influencing the distance between the tip and the substrate surface while the sample is probed for *I-V* characterisation.[5]

6.3.1 Summary

Most desired systems as candidates for applications in electrical circuits are these with a precise control of electrical properties while conjugated within a molecular junction. In this regard, the incorporation of redox-active groups into molecular wires is a promising solution that enables the system conductance to be tuned.

Analysis of **WIRE3** revealed a great potential of such structures, however in order to detect a dramatic change in the conductivity, adjustments of side group properties would be required. This could be achieved by geometrical or chemical manipulations. Thus, further investigation on such oligo(aryleneethynylene) derivatives must be performed.

6.4   Banana-shaped series of wires

In the context of potential applications of single molecular electronics in future technology, banana-shaped molecular wires were investigated. Studies on a series of three analogues with different backbones length were performed to determine the influence of the S-S distance on the electrical properties of the junction. The molecular wires with incorporated central dihexylofluorene moieties, whose results are presented in this section, were synthesised at Durham University.

6.4.1 BWIRE 1

The shortest molecular wire (intramolecular S-S distance *ca.* 2.5 nm) with long chains ($C_{16}H_{13}$) attached to the central moiety core of the backbone, whose sole purpose is to enable solubility in organic solvents, is presented in Figure 6.33. The presence of cyanoethyl-protected terminal thiols allows assembly onto gold electrodes and thus makes them ideal for single-molecule device fabrication.
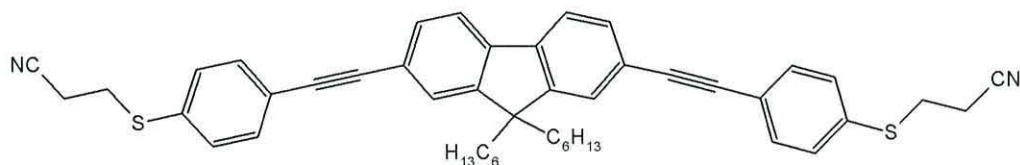
Figure 6.33 Molecular structure of banana-shaped molecular wire 1, **BWIRE 1**.

Monolayers were fabricated by immersing gold-coated substrates in a tetrahydrofuran solution of the wire (0.05 mg cm^{-3}) to which a deprotecting agent was added (sodium metoxide) in order to facilitate the chemisorption process. The rate of monolayer growth was monitored with the QCM throughout the deposition process. Self-assembly was improved by multiple short intervals (10 min), rather than one long and thorough rinsing with pure solvents to remove any physisorbed material. The measurement performed on several crystals revealed optimum deposition time lasting of *ca.* 400 min with the mean area reaching value of *ca.*1.24 ± 0.05 nm^2 molecule^{-1}, see Figure 6.34. Similar data were obtained in the absence of sodium metoxide, see Figure 6.34. Both characteristics exhibited similar shapes suggesting the same alignment within molecular

film independently on the addition of a deprotecting agent. The calculated value was consistent with the cross section of the molecular wire assuming partial overlap of tilted molecules within the film.
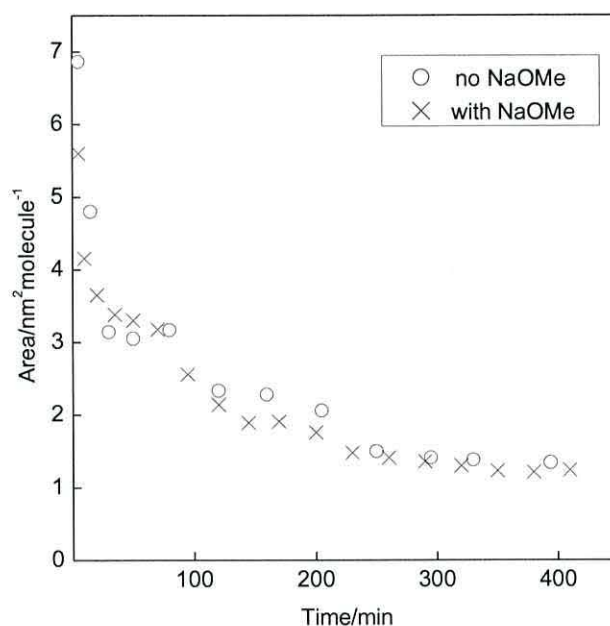
Figure 6.34 Molecular area *versus* immersion the total immersion time for banana-shaped **BWIRE 1**.
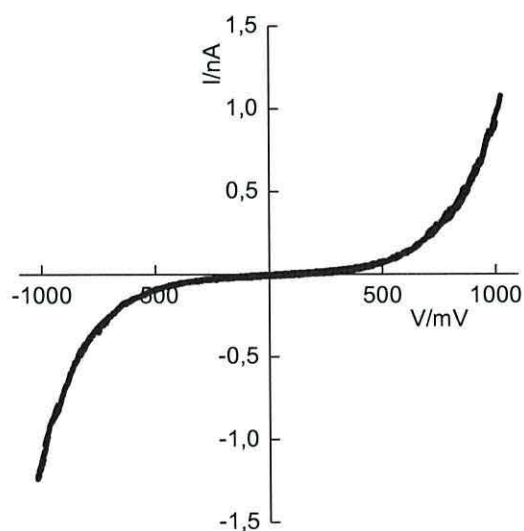
Figure 6.35 Symmetrical *I-V* characteristic of the molecular **BWIRE 1** chemisorbed to the gold-coated substrate and contacted with a gold probe; set-point current of 800pA at 30 mV.

I-V characteristics were determined by STS using Au tips with the position initially set to provide current of 800 pA at 30 mV. The investigations of SAMs at several locations

across the surface, exhibited symmetrical behaviour, see Figure 6.35, as anticipated for wire-like molecules located between Au contacts. The relatively noise-free characteristics were obtained by averaging the data from 30 scans. It was also found that different set point conditions have rather minimal effect on the profile of *I-V* curves. They only affected the magnitude of tunnelling current by influencing the substrate-tip distance. Moreover, such behaviour has been reported on other wire-like molecules.[132,208]

The conductivity of a single-molecule was determined by monitoring the single molecule current as a function of time using the method of Haiss *et al.*[5] For this purpose the Au tip was located above the sample but within contacting distance of the surface by fixing the tunnelling current at relatively high values. The data from current jump studies observed at 300 mV are presented in Figure 6.36 a, with the number of recorded current jumps resulting in the histogram shown in Figure 6.36 b. As can be seen the adsorption event persisted for *ca.* 40 ms within the range of 0.085 ± 0.005 nA which constituted 30 % of all current jumps. The histogram also revealed double and triple molecule contact centred about 0.16 and 0.24 respectively. However, as found elsewhere[5], for the smaller tip-substrate separation the attachment of multiple molecules is more possible.
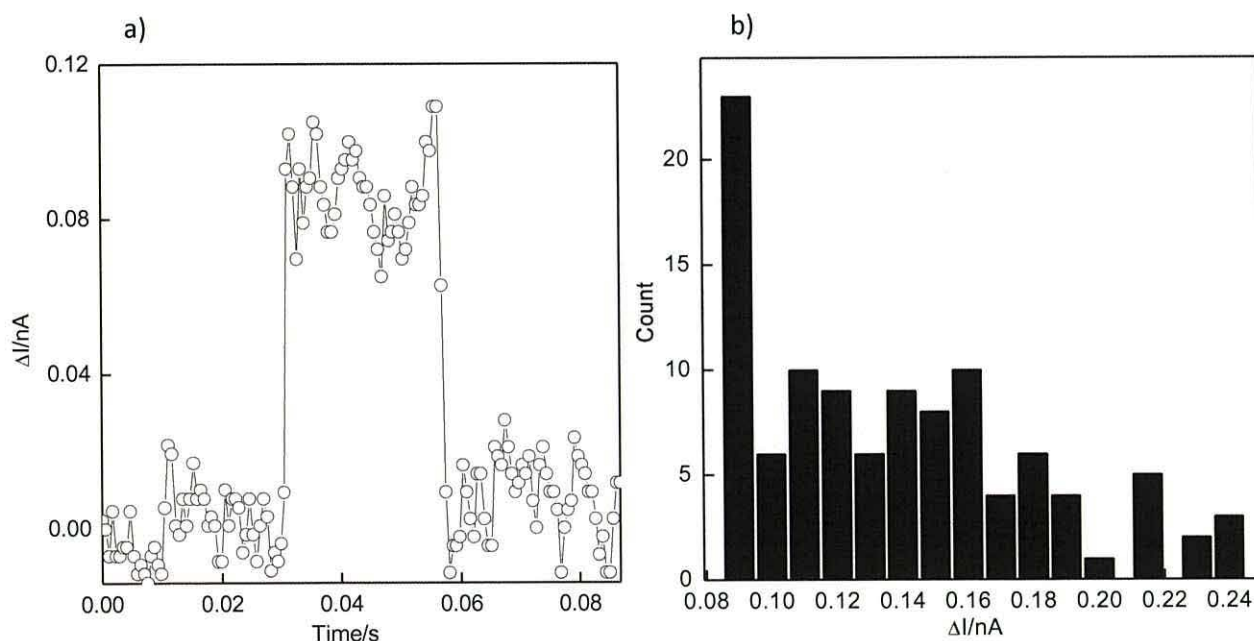
Figure 6.36 The representation of a) current jump on the left and b) histogram of 107 current jumps at a sample bias of 300 mV.

When comparing the single-molecule current, see Figure 6.36, to that displayed by the *I-V* plot, see Figure 6.35, at the same voltage, a significant difference can be discovered. However, it can be explained by dependence of the latter on the set point conditions which can influence the tip-sample separation. In the case of single-molecule conductivity measurements, the STM set-point current induces the formation of stochastic molecular wire bridges between both the tip and substrate, see Figure 3.6 b in section 3.3. The molecule is anchored to both electrodes by thiol terminated groups within defined molecular tunnelling bridges and thus the value of the contact gap separation is independent of the initial set point current.

6.4.2 BWIRE 2

The longer analogue of the molecular wire **BWIRE 1**, depicted in Figure 6.37 was investigated in the same manner as the **BWIRE 1**.
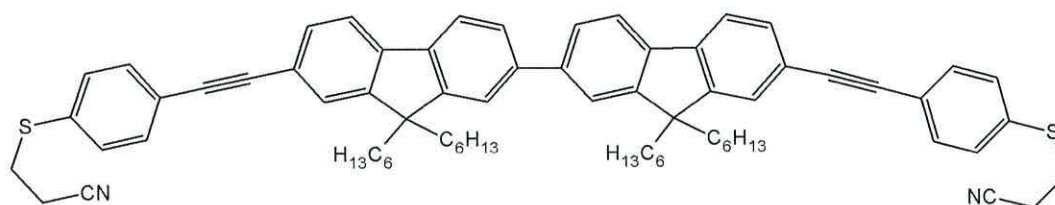
Figure 6.37 Molecular structure of **BWIRE 2.**

QCM analysis performed on several samples provided an average area per molecule of 1.6 ± 0.02 nm^2 molecule^{-1} with the time needed for the monolayer completion being of *ca.* 270 min. Noteworthy is the fact that the shape of the growth characteristic of recent molecular wire is similar to that of **BWIRE 1,** see Figure 6.38. This would signify the same alignment within the monolayer film. However the rate of monolayer growth of **BWIRE 2** appeared to be shorter suggesting better ordering on the gold surface. Assuming partial overlap of the tilted molecular wire, the calculated area is consistent with the molecular cross-section.
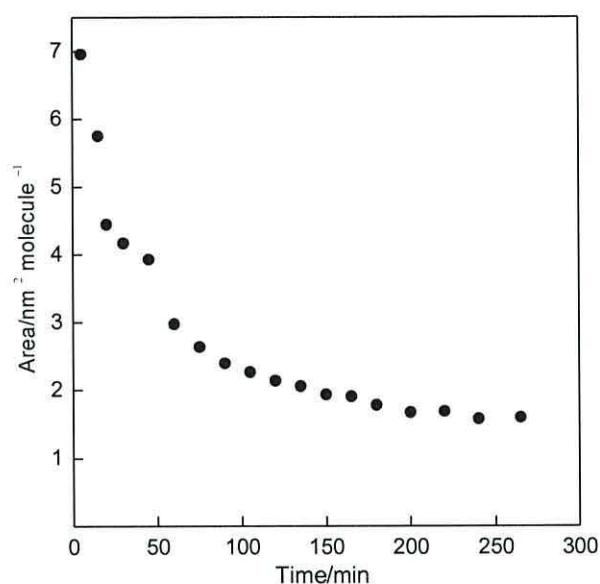
Figure 6.38 Monolayer growth characteristic of **BWIRE 2**. Mean area occupied by the molecule was 1.6 nm^2 molecule^{-1}.

STM investigation yielded typical behaviour for wire-like molecules located between Au electrodes. The reproducible symmetrical *I-V* characteristics were obtained by using a tip initially set to provide a tunnelling current of *ca.* 800 pA at 30 mV with further investigations performed across a broad range of set-point values. Although the slightly higher current in the negative quadrant was observed, see Figure 6.39, such behaviour was found to be relatively small compared to the inherent properties of the film. Moreover, such behaviour was found to be a common feature of wire-like molecules.[208]
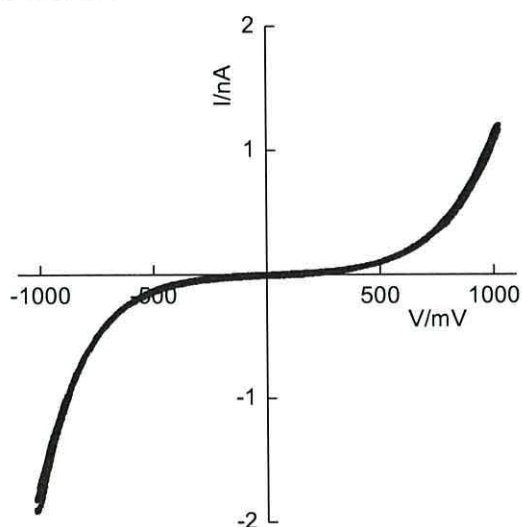
Figure 6.39 *I-V* characteristic from a SAM of the symmetrical molecular wire 2 on gold-coated substrate contacted by a gold tip.

Further investigations of **BWIRE 2** were performed using the method of Haiss *et al.*[5] The measurement of the tunnelling current as a function of constant tip-substrate separation resulted in a series of current jumps, the jump shown in Figure 6.40 a represents the adsorption event lasting for 40 ms. As seen from the histogram, see Figure 6.40 b, most of the recorded events fall within the range of of 0.5 ± 0.05 nA. Thus, the observed data are predominantly attributed to the single molecule attachment. Noteworthy is the fact that as the length of the molecular wire increased, the conductivity of a single molecular wire decreased.
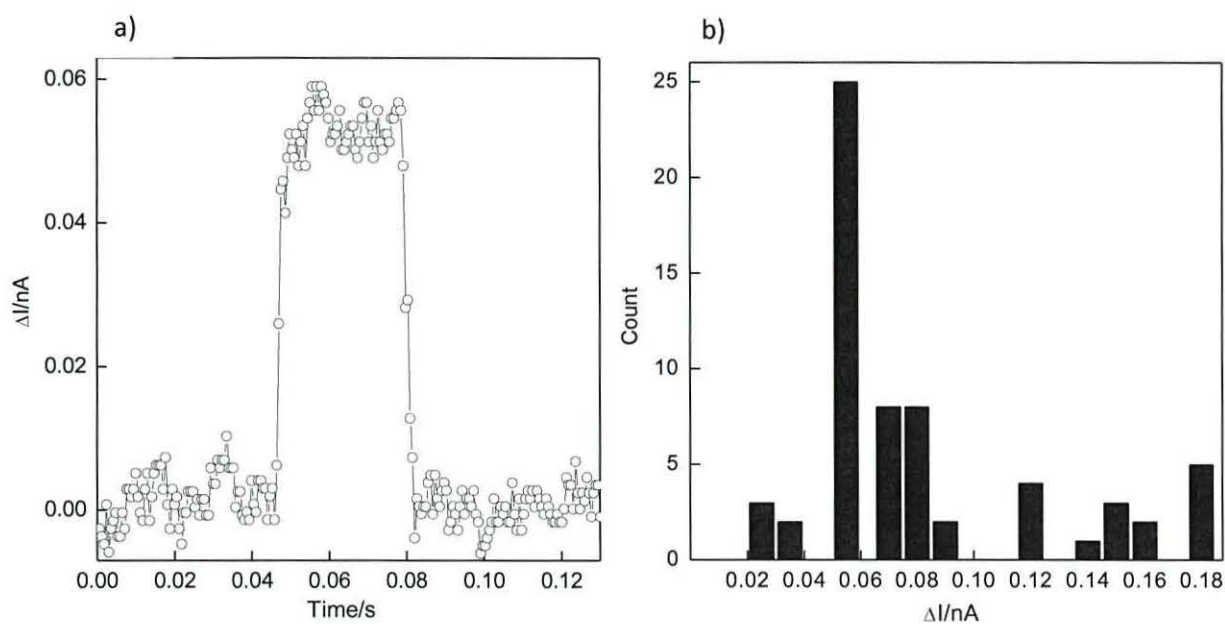
Figure 6.40 a) The representation of 63 current jumps, b) Histogram of current jumps at a sample bias of 300 mV.

6.4.3 BWIRE 3
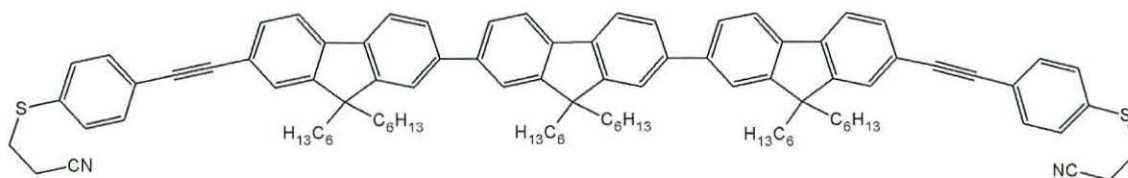
Figure 6.41 Molecular structure of **BWIRE 3.**

The QCM studies of the molecular wire **BWIRE 3,** see Figure 6.41, incorporating an even longer backbone provided a mean area of *ca.* 2.2 nm^2 molecule^{-1} with the time required to obtain this highly ordered monolayer film being of *ca.* 330 min. The QCM studies performed on several quartz crystals yielded the repetitive monolayer growth characteristic with a second slope observable at around 50th minute of the deposition, see Figure 6.42. However, it can be concluded that such behaviour reflects the typical monolayer growth kinetic for this series of molecules, as is reproducible by all three analogues, see Figures 6.34, 6.38, 6.42.
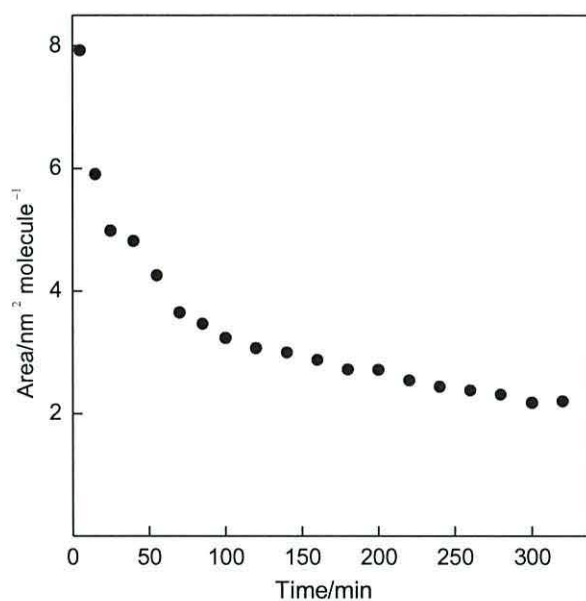
Figure 6.42 Monolayer growth characteristic of molecular **BWIRE 3**. Mean area occupied by the molecule was 2.2 nm^2 molecule^{-1}.

STM studies were executed on quartz crystals using a gold tip. An example *I-V* plot of **BWIRE 3** chemisorbed onto a gold substrate is presented in Figure 6.43. All curves were symmetrical independent on the applied potential and current. The varied set point parameters affected only the magnitude of the current (within the range of 0.1-0.2 nA) by influencing the probe-surface contact distance, whereas the general shape of the curve remained the same.
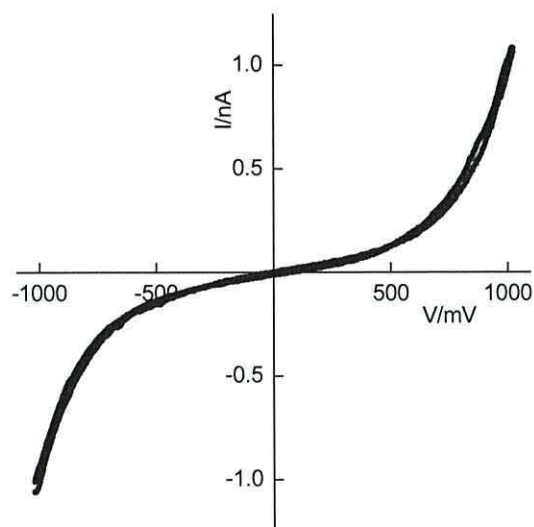
Figure 6.43 *I-V* characteristic of the **BWIRE 3** deposited on a gold-coated substrate and contacted by a gold probe with a set point current of 800 pA and sample bias of 30 mV.

In an attempt to examine the influence of the length of the backbone on the tip-sample separation and thus single molecule conductivity, further measurements employing the method of Haiss *et al.*[5] were performed. To ensure the occurrence of single molecule contact, the constant height mode was used in which molecules spontaneously attached and detached from the STM tip. The representation of a current jump resulting from the incorporation of a molecular wire in the gap is shown in Figure 6.44 a. whereas a large number of current jumps measured at different locations across the substrate surface were analysed to yield the histogram depicted in Figure 6.44 b. As can be seen, the adsorption event lasted for 30 ms with almost 45 % of all recorded current jumps at 300 mV within the range 0.15 ± 0.05 nA. In this case, there is no evidence on the histogram plot of any multiple contacts.
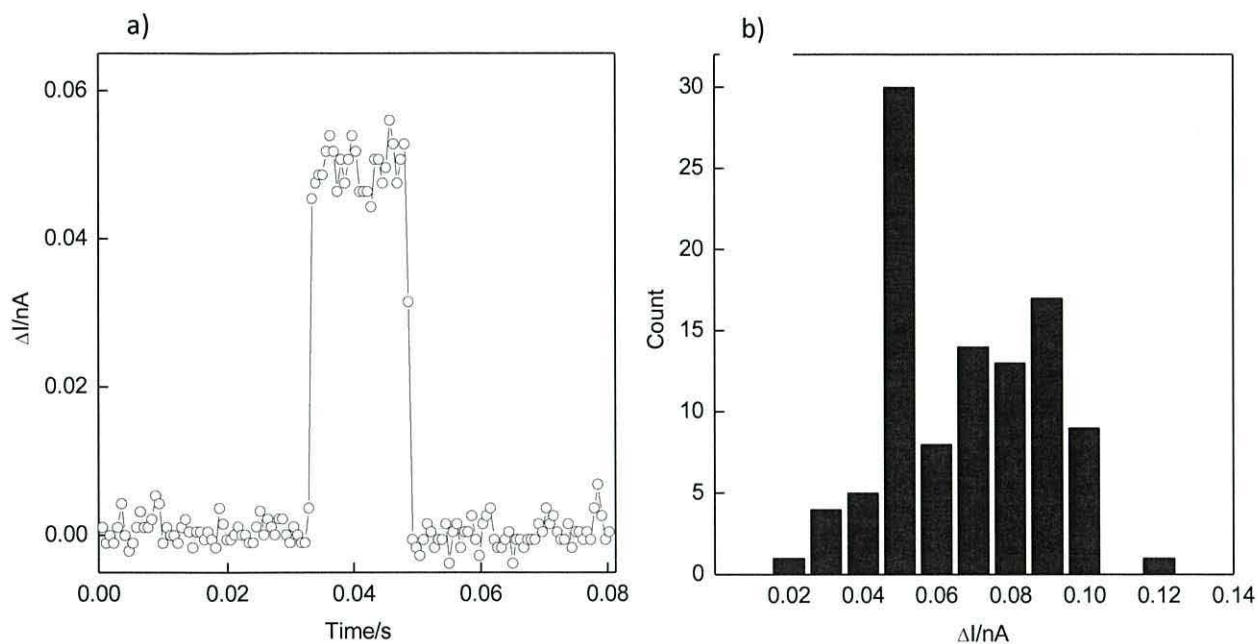
Figure 6.44 The representation of a) current jump and b) histogram of 102 current jumps at a sample bias of 300 mV.

6.4.4 Summary

Electrical analysis revealed the symmetrical behaviour for all of **BWIRE** analogues, as expected for conventional wire-like molecules, although slightly asymmetrical *I-V* characteristics were recorded, but infrequently. The latter was ascribed to the varying set point conditions, rather than being molecular in origin. Measurements of single molecule conductivity performed using the method of Haiss *et al.*[5] disclosed a decrease of the conductivity with increasing length of a molecular wire.

6.5   Chevron-shaped molecules

Another class of materials upon which this research focused, was a group of chevron-shaped molecules. The name for such molecules originates from their bent structure and stems from the central core that causes the *ca.* 120° bending angle of the arm moieties. This unconventional configuration of compounds motivated investigations of their alignment and electrical properties. The understanding of the correlation between the structure's organisation within the monolayer and its impact on the rectifying behaviour also became challenging.

The following experiment presents the study on two chevron-shaped molecules composed of central electron-acceptor group and two, fixed, donor moieties terminated with anchoring groups, which allow for either vertical or horizontal alignment of the D-A-D chromophore at the substrate surface. However only horizontally aligned SAM with donor groups of such D-A-D system projected towards either the lower electrode or the higher would provide the electrical asymmetry, as anticipated by the Aviram and Ratner model of rectification.

The following results reveal the nature of chevron-shaped molecules, shown below in Figure 6.45, that spontaneously adsorb on the gold coated substrates (quartz crystal, Au-coated glass slides and HOPG) and self-organise into two-dimensional assemblies. Both of compounds were synthesised by Andy Stipetic from Liquid Crystals and Advanced Organic Materials Group at Hull University.
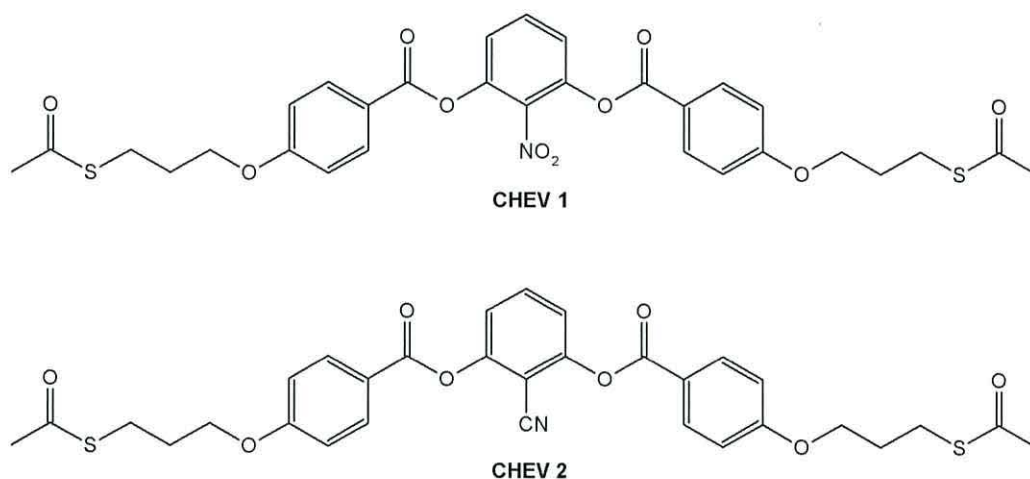
Figure 6.45 The structures of chevron-shaped compounds, **CHEV 1** and **CHEV 2**.

Monolayers of both investigated molecules were accomplished by immersion of Au-coated substrates into precursor materials. For thin films of both analogues to be formed, two separate solutions were prepared; of **CHEV 1** and **CHEV 2**, dissolved in chloroform giving concentrations of 1.05 mg/ml and 0.98 mg/ml respectively to which a few drops of ammonium hydroxide were added. Substrates were repeatedly immersed for 10-15 min intervals and thoroughly rinsed each time with pure solvents (chloroform, methanol, and ethanol) to remove any physisorbed materials. QCM studies revealed that

the addition of ammonia, with the aim of facilitating the deposition process caused a decrease in the resonant frequency to only half of the anticipated value. This was observable as a slope at 50th and 100th minutes of **CHEV 1** assembly and at 150th minutes of **CHEV 2**, see Figure 6.46, suggesting rearrangements within monolayer. The characteristic of monolayer growth also indicated the continuous frequency drop, possibly solvent trapping in the lattice, see Figure 6.46. Thus, further measurements were carried out without the addition of a deprotecting group. The limited area per molecule derived by use of the Sauerbrey equation was found to be of 1.04 nm^2 molecule^{-1} after *ca.* 400 mins (for both chevrons) of total deposition, see Figure 6.47.
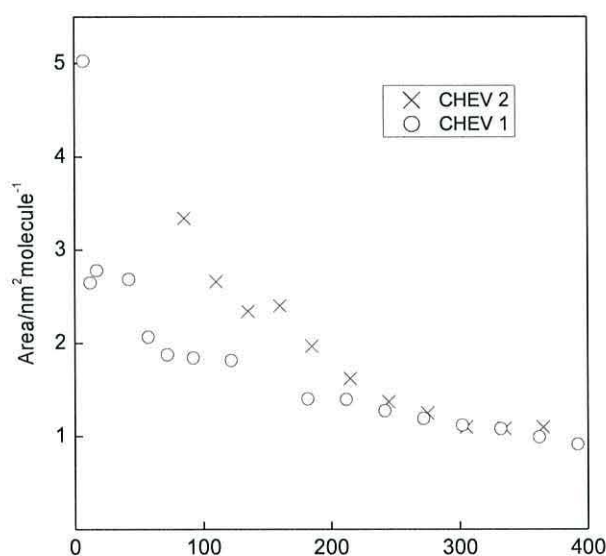
Figure 6.46 QCM measurement of two investigated chevron-shaped molecules. The process was performed with the addition of ammonia; dots indicate the molecular area of **CHEV 2**, while crosses, of **CHEV 1**.

The value of the area per molecule correlates with a horizontal orientation of chevrons with respect to the substrate surface that resulted from the assembly *via* two anchoring groups located at opposite ends of the D-A-D chromophore. The obtained results imply that chemisorption *via* Au-S linkage is preferable interaction than packing through physisorbtion (*via* nitro substituents). Assuming that molecule with a strong electron-accepting group decrease the rate of Au-S assembly by weakening the interaction between Au and sulphur, as reported elsewhere,[229,230] the observed behaviour may stem from formation of two strong Au-S bonds.
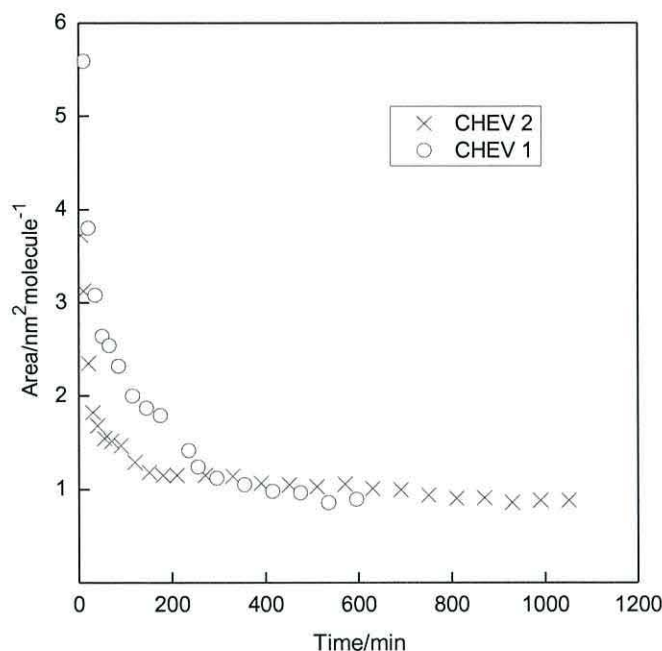
Figure 6.47 QCM measurement of two investigated chevron-shaped molecules, dots indicate the molecular area of **CHEV 1**, while crosses that of **CHEV 2**.

In order to verify the molecular alignment, SPR analysis was realised. The **CHEV 1** film spontaneously assembled onto the gold coated glass slide yielding monolayer thicknesses of 0.82 – 1.07 nm and 1.0 ± 0.2 nm, achieved from the green (532 nm) and red (632.8) laser respectively. The coherent results for **CHEV 2** chemisorbed to the gold were gained only from the red laser, and it was indicated to be 0.96-1.18 nm. Both sets of data correspond to the presumed orientation of the molecules within the monolayer.

I-V characteristics of those films formed on the gold-coated HOPG were obtained using the Nanoscope IV STM when contacted with the PtIr tip. For the molecular nature of observed rectification to be confirmed, several different locations across the monolayer surface were scanned. Examples of resultant asymmetrical plots for both molecules are depicted in Figure 6.48.
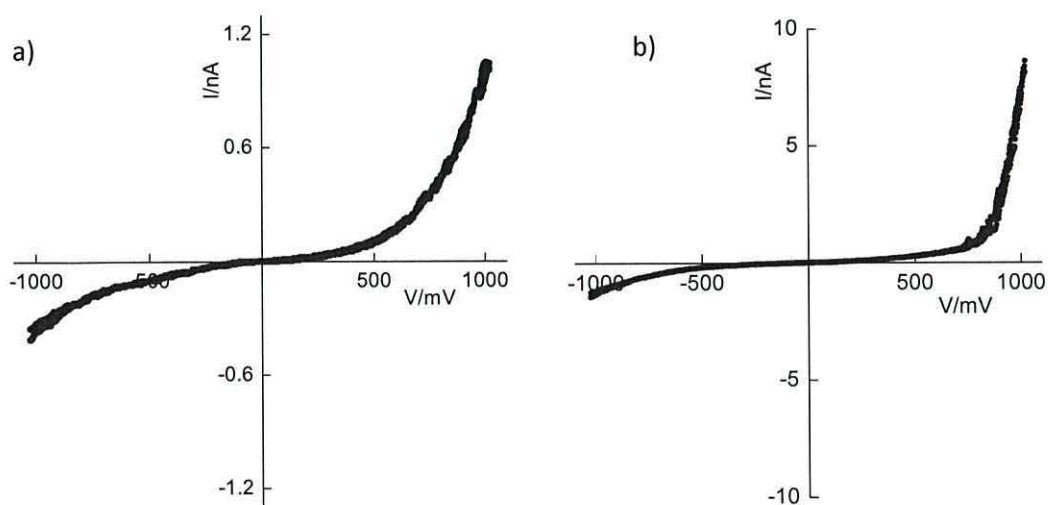
Figure 6.48 a) slightly asymmetrical *I – V* curve of **CHEV 2** with rectification ratio of *ca.* 4 at ± 1V), b) *I – V* characteristic of **CHEV 1** with a maximum rectification ratio of *ca.* 13 at ± 1V recorded for this molecule.

As shown in the figure 6.48, above, under forward bias, rectification invariably occurs in the negative quadrant of the *I-V* plot for both chevrons; however the shapes of both characteristics exhibited significant differences, the rate of the asymmetries also varied. Moreover, among the number of plots taken from the substrate coated with **CHEV 2**, only 40 % of recorded curves displayed the enhancement of the current in an appropriate quadrant, presented in Figure 6.48. In order to explain such behaviour, the molecular structure of those molecules must be considered. Hence, the slight asymmetry observed for the **CHEV 2** molecule more likely stems from the nature of the –CN group which is only a weak electron-acceptor, whereas the –NO$_2$ group has a strong electron-accepting character.

However, in both cases, the STS plots signify the electrons flow from the contacting tip via the molecule to the gold coated substrate indicating consistency with the Aviram and Ratner theory,[135] which predicts electrons flow from the cathode to the acceptor at one side (A$^+$ → A^0) and from the donor to the anode at the other side (D^0 → D$^+$). The demonstrated direction confirms that the acceptor is placed adjacent to the tip with donor groups attached to the gold surface, with the top centre of the chevron being an acceptor moiety, and arms of the chevron being donor moieties.

Once the direction of electrons flow through the molecules was determined and thus the alignment, the same samples were probed to image the SAMs. The images with the well ordered topography were obtained only for the SAM of **CHEV 1**. The image of low-resolution (of *ca.* 100 nm) was taken in the first instance and zoomed into an area of *ca.* 22 nm, as presented below in Figure 6.49. The increased resolution image revealed that the adjacent molecules are parallel to each other with a uniform bent direction constituting the "zigzag" shape. There are also noticeable bright spots which might have been attributed to the aromatic parts of the molecule due to their large electronic density resulting in higher contrast than that of the alkyl chains. The molecular arrangement and area occupied by chevron molecules seen in the figure below corroborates to the data given by QCM and SPR.
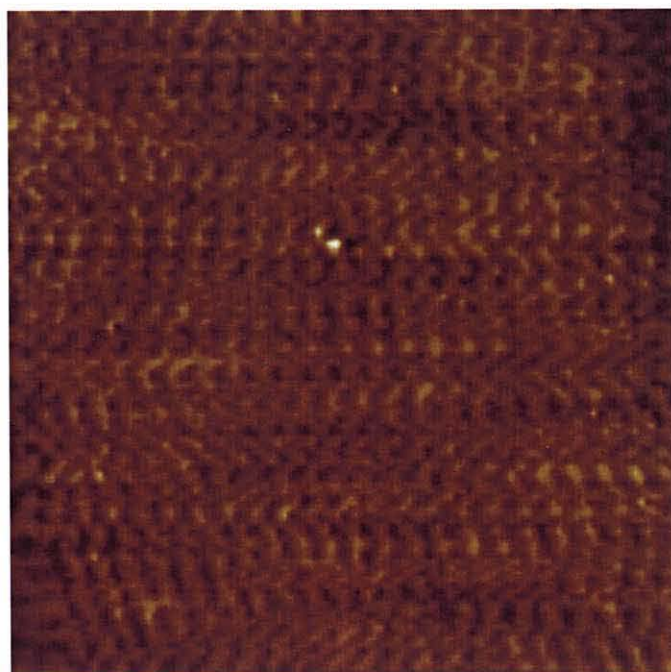
Figure 6.49 20 nm x 20 nm STM image of gold coated HOPG with **CHEV 1**.

6.5.1 Summary

The molecular structure of **CHEV1** and **CHEV2** implies three possible alignments within the monolayer film; Au-S chemisorption *via* only one thiolate link , Au-S

assembly *via* two thiolate groups located at both termini or coupling between central electron-withdrawing group and Au-coated substrate (physisorbtion). QCM measurements and electrical analysis correlated however with a horizontal alignment with respect to the substrate surface. Additionally, occurrence of the rectification in the negative quadrant provided the evidence that conventional Au-S chemisorption was preferred over physisorbion *via* R-Au (R-CN or NO$_2$). Contrary to results of **WIRE2** (see section 6.2), assembly *via* competing S-Au/R-Au interactions was not observed for **CHEV1** and **CHEV2**. The exception to the behaviour reported elsewhere,[229,230] possibly stemmed from attachment of chevron-shaped analogues *via* two Au-S linkages instead of one.

7   Conclusions and recommendations

The results provided by the study presented in this thesis demonstrate different types of organic molecule based devices with potential application in molecular electronics. However the majority of research was focused upon molecular wire systems, especially those involving a multi-step modular chemistry approach. The surface based synthesis of such complex structures with precisely defined length on Au-coated electrodes was monitored with QCM. The QCM measurements providing the limiting values of molecular areas for all subsequent reaction steps verified the occurrence of condensation reactions between successive reagents and the alignment within the monolayer. The plot of calculated area versus number of moles indicated that the resultant structure was free from physisorbed materials and any random adsorbates.

The STM investigations performed in order to characterise electrical properties of the systems also gave information of the monolayer composition. The results obtained from STM exhibited rectification only when one end of the wire was electron-donating and the other was electron-accepting. The symmetrical nature of **SAM 1** (weak donor) determined symmetrical *I-V* characteristics. As the direction of electron flow at forward bias was from the cathode to the acceptor and from the donor to the anode, the bias for rectification of the wire could be reversed by altering the sequence and thus their

asymmetric *I-V* plots. However, the results obtained for a **D-A-A** molecule revealed the enhancement of the current in the unexpected quadrant to that predicted by the Aviram and Ratner theory. Nevertheless, the behaviour of **SAM 3** was believed to stem from the protonation of the terminal group of the molecule that might have caused it to switch its electron-accepting character to an electron-donating one. On the other hand, the protonation occurs under exposure to HCl vapour, unlikely to conditions of the reaction of condensation. Due to difficulties associated with controlled assembly of nitro-terminated aldehyde, further investigations were performed on a **D-A-D** system, in which the failed electron-accepting group was replaced by an electron-donating group. The results taken from STS measurement agreed with the Aviram and Ratner model, although in proposed rectification mechanism, donor and acceptor moieties are separated by σ-bridge.

The step-by-step method of forming functional molecular wires with extended lengths by sequencing chemical building blocks has a great potential in developing assemblies for molecular electronic applications. It is used to overcome difficulties in precisely controlling the component length to connect molecular wires across prefabricated nano-sized electrode gap structures[221,235] and permits the arrangement of functional groups with predetermined donor-acceptor sequences for rectification. It was proved that by altering the sequence of molecular components, reproducible control of *I-V* characteristics can be achieved, confirming that recorded behaviour is molecule induced. The ability to tune properties of self-assembled monolayers in metal-molecule-junctions by sequential coupling of components provides a better understanding of molecular electronic systems and a promising tool for designing future electronic devices. Research on development of such a method is of a great importance, as incorporation of redox-active groups into molecular wires (in order to tune transport properties) *via* classical synthetic chemistry is experimentally very demanding, especially at single-molecule level. Thus, more advanced studies on multi-step modular chemistry approach are required.

The STM studies of a series of molecular wires, π-conjugated oligo(arylene)s (OPE) and banana-shaped, demonstrated symmetrical behaviour, as expected for wire-like molecules when deposited between two metal electrodes. Moreover, the general profile

of all recorded curves was not affected by the alteration of set point parameters; they only influenced the magnitude of the tunnelling current. Further measurements allowed observations of current jumps of π-conjugated molecular wire systems (**WIRE 1**, **WIRE 3**) and that of banana-shaped molecule which revealed the dependence on backbone length. It was found that the single molecule conductivity decreased exponentially with their length which was consistent with the Haiss' proposal.[5]

Despite the symmetrical character of the molecular wires, STM measurements of **WIRE 2** exhibited the enhancement of the current in the negative quadrant of the *I-V* plots suggesting an electron-accepting character of such a wire. Considering the consistency of the occurrence of electrons flow at the forward bias with the Aviram and Ratner rectification mechanism, the observed behaviour could contribute to the molecule being anchored to the Au-coated substrate by nitrogen groups. Assembly of the terminal nitro group to the top electrode has already been reported,[218] but otherwise to this phenomenon, NO_2-Au interaction occurred once the thiol group had initially been adsorbed onto the bottom electrode. The competing S-Au/NO_2-Au interactions were ascribed to weakening of conventional Au-S assembly[228,229] and thus formation of a disordered monolayer. The latter implies that thiolate molecules with strong electron-accepting substituents, in particular nitro groups, may not be suitable for controlled assembly in junctions. However, further research on this system could be performed in order to find a way of controlling such a phenomenon, even though currently the most promising way of incorporation of a single molecule into electronic circuit is *via* Au-thiolate linkage.[50]

Noteworthy is the fact that measurements employing the method of Haiss *et al.*[5] provided results indicating single molecule contact despite the method being applied so far only to molecular wires chemisorbed to the gold contacts by thiol groups.

Further research was focused upon chevron-shaped molecules; molecules whose planar structure comprises a central unit that induces a bending angle of two arms fixed to the head moiety. **CHEV 1** and **CHEV 2** yielded molecular diode-like behaviour when deposited onto the gold coated substrate and probed by STM. SAMs were prepared to verify the alignment within the monolayer, as the presence of two thiol terminal groups located at both ends of the chromophore allowed for either vertical or horizontal

attachment to the gold surface. SPR analysis supported the results taken from QCM indicating the horizontal orientation of both chevrons. Moreover, the enhancement of the current in the negative quadrant of the *I-V* plot that signified the electrons flow from the contacting tip to the gold-coated substrate provided even more evidence. Thus, adhering to the Aviram and Ratner theory the acceptor moiety should be adjacent to the tip, whereas the donor moiety is anchored to the gold surface. It can be concluded that both arms have an electron-donating character due to the presence of thiol groups enabling the chemical bonding with the gold. Although in both cases (**CHEV 1, CHEV 2**) the higher current occurred in the negative quadrants of the *I-V* plot, **CHEV 2** showed lower rectification ratio, more likely due to the weak nature of its electron-acceptor group. The data given by former measurements also corroborated to the molecular arrangement revealed by STM images.

In summary, results presented in this thesis deal with a major challenge in developing components for use in molecular-scale electronics. The particular emphasis has been placed on the understanding of the alignment, electrical properties of the molecules assembled and ability to tune of these properties in metal-molecule-metal junctions. The significance of redox-active subunits incorporation in organic material to modulate the conductance in metal-molecule-metal junctions has also been shown. In order to continue contribution in realisation of molecular electronics in the way to overcome the impeding threshold of silicon devices, further research on single molecule conductance and its dependence on various factors, must be performed.

The ability to organise the donor-acceptor systems on electrodes is significant for molecular scale electronics and the method of building such systems, presented in section 6.1, is highly versatile. Sequential synthesis combines the ease of complex system fabrication with fine control of their functionalities. Moreover, this type of systems can be extended with the precise control of a molecular wire length and recently successful assembly of elongated molecule on nanoparticulate TiO_2 was demonstrated.[236] This phenomenon enables building components for photovoltaic applications by the use of step-by-step deposition. In order to realise that synthesis, nanoparticulate TiO_2 must be modified by a surface modifier consisting of carboxylate and NH_2 /CHO functional groups ($COOH-R-NH_2/CHO$). This approach is to be used

due to a strong affinity of TiO_2 to carboxylate group of a linker molecule.[237, 238] Moreover, a presence of NH_2 or CHO group at the end of that linker molecule facilitates a successful binding of aldehyde or amino-substituted units to TiO_2 film. Consequently, the molecular wire can be elongated to a specified length on TiO_2 nanoparticulate. Application of sequentional synthesis of donor and acceptor moieties in photovoltaics can impart performance either in terms of efficiency or stability due to electroactive units being isolated at opposite ends of the molecule. However, in order to achieve a (desired) charge separation that would yield an improved conductivity in comparison to result obtained for Au-S-wire-A-π-D system (see section 6.1), more effective barrier between donor and acceptor moieties must be incorporated (for example, as originally proposed by Aviram and Ratner[135], composed of a few -CH_2- groups). The purpose of that is to sufficiently decouple the molecular orbitals of both, donor and acceptor units, so that they would be essentially non-interacting.

In the other approach, a complex molecule composed of donor and acceptor sequences can be assembled as a three-dimensional network on Au-coated substrate, to form cluster aggregates. The development of such a system may have a great potential in the enhancement of photoconversion efficiency.

8 Publications

I. G. J. Ashwell, P. Wierzchowiec, L. J. Philips, C. J. Collins, J. Gigon, B. J. Robinson, C. M. Finch, I. R. Grace, C. J. Lambert, P. D. Buckle, K. Ford, B. J. Wood, I. R. Gentle, Functional Molecular Wires, *Phys. Chem. Chem. Phys.*, **10**, 1859, 2008.

II. C. Wang, M. R. Bryce, J. Gigon, G. J. Ashwell, I. Grace, C. J. Lambert, Synthesis and Properties of Functionalized 4 nmScale Molecular Wires with Thiolated Termini for Self-Assembly onto Metal Surfaces, *J. Org. Chem.*, **73**, 4810, 2008.

III. X. Zeng, C. Wang, A.S. Batsanov, M. R. Bryce, J. Gigon, B. Urasinska-Wojcik, G. J. Ashwell, Synthesis and Properties of Functionalized Oligo(arylene) Molecular Wires with Thiolated Termini: Competing Thiol-Au and Nitro-Au Assembly, in preparation.

9   References

[1] G. Cao, *Nanostructures and Nanomaterials: synthesis, properties and apllications.* Imperial College Press, London, 2004.

[2] G.J. Ashwell, B. Urasinska, W.D. Tyrrell, *Phys. Chem. Chem. Phys.*, **8**, 3314, 2006.

[3] J.M. Tour, *Acc. Chem. Res.*, **33**, 791, 2000.

[4] J.G. Kushmerick, J. Naciri, J.C. Yang, R. Shashidhar, *Nano Lett.*, **3**, 897, 2003.

[5] W. Haiss, R.J. Nichols, H. van Zalinge, S.J. Higgins, D. Bethell and D.J. Schiffrin, *Phys. Chem. Chem. Phys.*, **6**, 4330, 2004.

[6] G.E. Moore, *Electronics*, **38**, 114-117, 1965.

[7] S. Thompson, International Devices Meeting, IEDM Technical Digest, 61, 2002.

[8] R.M. Ramanathan and R. Willoner, Technical report at Technology@ Intel Magazine, Intel Corporation, 2006.

[9] C.C. Mann, *Technology Review*, **103**, 42, 2000.

[10] J. M. Tour, *Chem. Rev.*, **96**, 537, 1996.

[11] C. Joachim, J.K. Gimzewski, A. Aviram, *Nature*, **408**, 541, 2000.

[12] M.R. Brycs, M.C. Petty, D. Bloor, *Molecular Electronics,* Oxford University Press, New York, 1995.

[13] http://www.intel.com/technology/mooreslaw/index.htm

[14] K.S. Kwok, J.C. Ellenbogen, , *Materials Today*, **5**, 28, 2002.

[15] R.P. Feynman, *Miniaturization;* Gilbert, H.D, Ed.; Reinhold: New York, 282, 1961

[16] J.M. Tour, M. Kozaki, J.M. Seminario, *J. Am. Chem. Soc.*, **120**, 8486, 1998.

[17] G. Maruccio, R. Cingolani, R. Rinaldi, *J. Mat. Chem.*, **14**, 542, 2004.

[18] M.R. Stan, P.D. Franzon, S.C. Goldstein, J.C. Lach, M.M. Ziegler, *IDEE*, **91**, 1940, 2003.

[19] J. R. Heath, M. A. Ratner, Molecular electronics, *Physics Today*, **56(5)**, 43, 2003.

[20] A.E. Ghosh, P. S. Damle, S. Datta, A. Nitzan, *MRS Bulletin*, **29**, 391, 2004.

[21] S. Roth, S. Blumentritt, M. Burghard, E. Cammi, K. Liu, J. Muster, G. Philipp, T. Rabenau, D. Carroll, S. Curran, G. Dusberg, *Synthetic Met.*, **94**, 105, 1998.

[22] W. C. Bigelow, D.L. Pickett, W.A. Zisman, *J. Colloid. Sci.*, **1**, 513, 1946.

[23] R.G. Nuzzo, D.L. Allara, *J. Am. Chem. Soc.*, **105**, 4481,1983.

[24] N. Tillman, A. Ulman, J.S. Schildkraut, T.L. Penner, *J. Am. Chem. Soc.*, **110**, 6136, 1988.

[25] D.L. Allara, R.G. Nuzzo, *Langmuir*, **1**, 45, 1985.

[26] D.L. Allara, R.G. Nuzzo, *Langmuir*, **1**, 52, 1985.

[27] N.E. Schlotter, M.D. Porter, T.B. Bright, D.L. Allara, *Chem. Phys. Lett.*, **132**, 93, 1986.

[28] P.E. Laibinis, G.M. Whitesides, D.L. Allara, Y.-T. Tao, A.N. Parikh, R.G. Nuzzo, *J. Am, Chem. Soc.*, **113**, 7152, 1991.

[29] N.P. Prince, D.L. Seymour, D.P. Woodruff, R.G. Jones, W. Walter, *Surface Science*, **215**, 566, 1989.

[30] L.H. Dubois, R.G. Nuzzo, *Ann. Rev. Phys. Chem.*, **43**, 437, 1992.

[31] A. Ulman, *An Introduction to Ultrathin Organic Films: From Langmuir-Blogett to Self-Assembly*, Academic Press Inc, New York, 1991.

[32] R.R. Birge, Ed., Molecular and Biomolecular Electronics, American Chemical Society, Washington, DC, 1991.

[33] P. Fenter, P. Eisenberger, J. Li, N. Camillone, S. Bernasek, G. Scoles, T.A. Ramanarayanan, K. S. Liang, *Langmuir*, **7**, 2013, 1991.

[34] F. Schreiber, *Progress in Surface Sci.*, **65**, 151, 2000.

[35] A. Eberhardt, P. Fenter and P. Eisenberg, *Surface Sci.*, **397**, L285-L290, 1998.

[36] G.E. Poirier, E.D. Pylant, *Science,* **272**, 1145, 1996.

[37] F. Schreiber, *J. Phys.: Condens. Matter*, **16**, 881, 2004.

[38] A. Kumar, H.A. Biebuyck, G. M. Whitesides, *Langmuir*, **10**, 1498, 1994.

[39] H.X. He, H. Zhang, Q. G. Li, T.Zhu, S.F.Y. Li, Z.F. Liu, *Langmuir*, **16**, 3846, 2000.

[40] D.J. Olbris, A. Ulman, Y.J. Shnidman, *J. Phys. Chem.*, **99**, 6865, 1995.

[41] F.P. Zamborini, R.M. Crooks, *Langmuir*, **14**, 3279, 1998.

[42] R.M. Nyquist, A.S. Eberhardt, L.A. Silks, Z. Li, X. Yang, B.I. Swanson, *Langmuir*, **16**, 1793, 2000.

[43] D.J. Revell, J.R. Knight, D.J. Blyth, A.H. Haines, D.A. Russell, *Langmuir* , **14**, 4517, 1998.

[44] C.D. Bain, E.B. Troughton, Y.-T. Tai, J. Evall, G.M. Whitesides, R.G. Nuzzo, *J. Am. Chem. Soc.*, **111**, 321, 1989.

[45] D.L. Allara, A.N. Parikh and F. Rondelez, *Langmuir*, **11**, 2357, 1995.

[46] J. Sagiv, *J. Am. Chem. Soc.* **102**, 92, 1980.

[47] M.M. Walczak, C. Chung, S.M. Stole, C.A. Widrig and M.D. Porter, *J. Am. Chem. Soc.*, **113**, 2370, 1991.

[48] S. Lee, J. Park, R. Ragan, S. Kim, Z. Lee, D.K. Lim, D.A.A. Ohlberg, R.S. Williams, *J. Am. Chem. Soc.*, **128**, 5745, 2006.

[49] M.L. Chabinyc, X. Chen, R.E. Holmlin, H. Jacobs, H. Skulason, C.D. Frisbie, V. Mujica, M.A. Ratner, M.A. Rampi, G.M. Whitesides, *J. Am. Chem. Soc.,* **124**, 11730, 2002.

[50] J. C. Love, L. A. Estroff, J. K. Kriebel, R.G. Nuzzo, G.M. Whitesides, *Chem. Rev.,* **105**, 1103, 2005.

[51] C.D. Bain, G.M. Whitesides, *J. Am. Chem. Soc.*, **111**, 7164, 1989.

[52] R.K. Smith, P.A. Lewis, P.S. Weiss, *Progress in Surface Science*, **75**, 1, 2004.

[53] G.E. Poirier, *Chem. Rev.*, **97**, 1117, 1997.

[54] R.G. Nuzzo, F.A. Fusco, D.L. Allara, *J. Am. Chem. Soc.*, **109**, 2358, 1987.

[55] R.G. Nuzzo, B.R. Zegarski, L.H. Dubois, *J. Am. Chem. Soc.*, **109**, 733, 1987.

[56] A. Ulman, *Chem. Rev.,* **96**, 1533, 1996.

[57] M. Hasan, D. Bethell, M. Brust, *J. Am. Chem. Soc.*, **124**, 1132, 2002.

[58] H.A. Biebuyck, C.D. Bain, G.M. Whitesides, *Langmuir*, **10**, 1825, 1994.

[59] L. Strong, G. M. Whitesides, *Langmuir*, **4**, 546, 1988.

[60] C.D. Bain, H.A. Biebuyck, G.M. Whitesides, *Langmuir*, **5**, 723, 1989.

[61] H.A. Biebuyck, G.M. Whitesides, *Langmuir*, **9**, 1766, 1993.

[62] M.D. Porter, T.B. Bright, D.L. Allara, C.E.D. Chidsey, *J. Am. Chem. Soc.*, **109**, 3559, 1987.

[63] R.G. Nuzzo, L.H. Dubois, D.L. Allara, *J. Am. Chem. Soc.*, **112**, 558, 1990.

[64] M. Buck, F. Eisert, J. Fisher, M. Grunze, F. Träger, *Appl. Phys. A*, **53**, 552, 1991.

[65] D.S. Karpovich, G.J. Blanchard, *Langmuir*, **10**, 3315, 1994.

[66] R. Yamanda, K. Uosaki, *Langmuir*, **14**, 855, 1998.

[67] K. Tamada, M. Hara, H. Sasabe, W. Knoll, *Langmuir*, **13**, 1558, 1997.

[68] M. Kawasaki, T. Sato, T. Tanaka, K. Takao, *Langmuir*, **16**, 1719, 2000.

[69] E.B. Troughton, C.D. Bain, G.M. Whitesides, R.G. Nuzzo, D.L. Allara, M.D. Porter, *Langmuir*, **4**, 365, 1988.

[70] C.-J. Zhong, M.D. Porter, *J.Am. Chem. Soc.*, **116**, 11616, 1994.

[71] J. Noh, H. S. Kato, M. Kawai, M. Hara, *J. Phys. Chem.*, **106**, 13268, 2002.

[72] J.B. Schlenoff, M. Li, H. Ly, *J. Am. Chem. Soc.*, **117**, 12528, 1995.

[73] H. Takiguchi, K. Sato, Y. Ishida, K. Abe, K.Yase, K. Tamada, *Langmuir*, **16**, 1703, 2000.

[74] C.-J. Zhong, M. D. Porter, *Langmuir*, **15**, 518, 1999.

[75] M.W.J. Beulen, B. -H. Huisman, P.A. van der Heijden, F.C.J.M. van Veggel, M.G. Simons, E.M.F.G. Biemond, P.J. de Lange, D.N. Reinhoudt, *Langmuir*, **12**, 6170, 1996.

[76] M.C. Leavy, S. Bhattacharyya, W.E. Cleland, C.L. Hussey, *Langmuir*, **15**, 6582, 1999.

[77] J. Noh, T. Murase, K. Nakajima, H. Lee, M. Hara, *J. Phys. Chem. B*, **104**, 7411, 2000.

[78] C.D. Bain, J. Evall, G.M. Whitedes, *J. Am. Chem. Soc.*, **111**, 7155, 1989.

[79] R. Yamanda, . Wano, K. Uosaki, *Langmuir*, **16**, 5523, 2000.

[80] E. Delamarche, B. Michel, H. Kang, C. Gerber, *Langmuir*, **10**, 4103, 1994.

[81] D.M. Jaffey, R.J. Madix, *J. Am. Chem. Soc.*, **116**, 3012, 1994.

[82] D.N. Batchelder, S.D. Evans, T.L. Freeman, L. Haeussling, H. Ringsdorf, *J. Am. Chem. Soc*, **116**, 1050, 1994.

[83] R.S. Clegg, S.M. Reed, J.E. Hutchison, *J. Am. Chem. Soc.*, **118**, 2486, 1996.

[84] H. Fukushima, S. Seki, T. Nishikawa, H. Takiguchi, K. Tamada, K. Abe, R. Colorado, M. Graupe, O.E. Shmakova, T.R. Lee, *J. Phys. Chem. B*, **104**, 7417, 2000.

[85] T. Ishida, H. Fukushima, W. Mizutani, S. Miyashita, H. Ogiso, K. Ozaki, H. Tokumoto, *Langmuir*, **18**, 83, 2002.

[86] J.Lahiri, L. Isaacs, J. Tien, G.M. Whitesides, *Anal. Chem.*, **71**, 777, 1999.

[87] S. Kossek, C. Padeste, L.X. Tiefenauer, H. Siegenthaler, *Biosens. Bioelectron.*, **13**, 31, 1998.

[88] F.A. Armstrong, H.A. Heering, J. Hirst, *Chem. Soc. Rev.*, **26**, 169, 1997.

[89] B. Franklin, *Royal Society of London*, **64**, 445, 1774.

[90] A. Pockels, Surface tension, *Nature*, **43**, 437, 1891.

[91] Lord Rayleigh, *Philosophical Magazine*, **48**, 321, 1899.

[92] I. Langmuir, *J. Am. Chem. Soc.*, **39**, 1848, 1917.

[93] K. B. Blodgett, *J. Am. Chem.*, **56**, 495, 1934

[94] M.C. Petty, *Langmuir-Blodgett films. An introduction*, Cambridge University press, 1996, Cambridge.

[95] W.D. Harkins, *The Physical Chemistry of Surface Films,* Reinhold, New York, 1952.

[96] B.P. Binks, *Adv. Colloid Interface Sci.*, **34**, 343-432, 1991.

[97] K.B. Blodgett, *J. Am. Chem.*, **57**, 1007, 1935.

[98] S. Allen et al., *Proc. Soc. Photo-Opt. Eng.*, 682, 97, 1987.

[99] S.R. Kowel, L.M. Haydn, R.H. Selfridge, *Proc. Soc. Photo-Opt. Eng.*, 682, 103, 1987.

[100] S.K. Pollack, J. Naciri, J. Mastrangelo, C.H. Paterson, J. Torres, M. Moore, R. Shashidar, J.G. Kushmerick, *Langmuir*, **20**, 1838, 2004.

[101] M.D. Ward, D.A. Buttry, *Science*, **249**, 1000-1007, 1990.

[102] C.F. Brockelsby, *J. Sci. Instr.* **40**,153, 1963.

[103] C.K. O'Sulivan, G.G. Guibault, *Biosens. Bioelectron.,* **14**, 663, 1999.

[104] M.R. Deakin, D.A. Buttry, *Analytical Chemistry*, **61**, 1147A, 1989.

[105] G. Sauerbrey, *Z. Phys.,* **155**, 206, 1959.

[106] A.Wajid, *Sens. Actuators A*, **63**, 41, 1997.

[107] H. Raether, Surface plasma oscillations and their applications, in: G. Hass, M.H. Francombe, R.W. Hoffman (Eds.), Physics of Thin Films, Advances in Research and Development, Academic Press, New York, **9,** 145, 1977.

[108] W.L. Barnes, J.R. Sambles, *Surface Sci.*, **183**, 189, 1987.

[109] J.N. Wilde, M.C. Petty, J. Saffell, A. Tempore, L. Valli, *Measurement and Control*, **30**, 269, 1997.

[110] I. Pockrand, J.D. Swalen, J.G. Gordon, M.R. Philpott, *Surface Sci.*, **74**, 237, 1977.

[111] L. E. Bailey, D. Kambhampati, K.K. Kanazawa, W. Knoll, C.W. Frank, *Langmuir*, **18**, 479, 2002

[112] R.W. Wood, *Phil. Magm.*, **4**, 396, 1902.

[113] B. Liedberg, I. Lundström, E. Stenberg, *Sens. Actuators B,* **11**, 63, 1993.

[114] Z. Kretschmann, *Zeitschrift Für Physik*, **241**, 313, 1971.

[115] E. Kretschmann, H. Raether, *Z. Naturforsch.*, **23A**, 2135, 1968.

[116] K.-S. Chang, C. Chou, C.-H. Lin, *Applied Optics*, **32**, 2957, 1993.

[117] R.D. Young, Surface Microtopography, *Physics Today,* **24**, 42, 1971.

[118] G. Binning, H.Rohrer, *IBM J.Res. and Dev.,* **44**, 279, 2000.

[119] J. K. Gimzewski, C. Joachim, *Science,* **283**, 1683, 1999.

[120] R. Heinz, A. Stabel, J. P.Rabe, g. Wegner, F.C. De Schryver, D. Corens, W. Dehaen, C. Süling, Angew. *Chem., Int. Edn Engl.* **33**, 2080, 1994.

[121] B. McCarthy, J.N. Coleman, R. Czerw, A.B. Dalton, H.J. Byrne, D. Tekleab, P. Iyer, P.M. Ajayan,W.J. Blau and D.L. Carroll, *Nanotechnology,* **12**, 187, 2001.

[122] N.D. Lang, *Phys. Rev. Lett.*, **55**, 230, 1985.

[123] J.A. Kubby, J.J. Boland, *Surf. Sci. Rpts.*, **26**, 61, 1996.

[124] R. Wiesendanger, *Scanning Probe Microscopy and Spectroscopy, Methods and Aplications,* 1998, Cambridge University Press.

[125] D.M. Cyr, B. Venkataraman, G.W. Flynn, *Chem. Mater.,* **8**, 1600, 1996.

[126] B. Li, H. Wang, J. Yang, J. G. Hou, *Ultramicroscopy,* **98**, 317, 2004.

[127] P. Samori, J.P. Rabe, *J. Phys.Condens. Matter.,* **14**, 9956, 2002.

[128] Institute of Bio and Nanosystems, http://www.fz-uelich.de/ibn/index.php?index=218

[129] L.J. Whitman, J.A. Stroscio, R.A. Dragoset , R.J. Celotta, *Science,* **251**, 1206, 1991.

[130] M.F. Crommie, C.P. Lutz, D.M. Eigler, *Science,* **262**, 218, 1993.

[131] Ph. Avouris, *Acc. Chem. Res.* **28**, 95, 1995.

[132] G.J. Ashwell, B. Urasinska, C. Wang, M.R. Bryce, I. Grace and C.J. Lambert, *Chem. Comm.,* **15**, 4706, 2006.

[133] W. Haiss, H. Zalinge, S. J. Higgins, D. Bethell, H. Höbenreich, D.J. Schiffrin, R.J. Nichols, *J. Am. Chem. Soc.,* **125**, 15294, 2003.

[134] A. Aviram, Molecular electronics-science and technology, *Angew. Chem. Int. Ed.,* **28**, 520, 1989.

[135] A. Aviram, M.A. Ratner, Molecular Rectifiers, *Chem. Phys. Lett.,* **29**, 277, 1974.

[136] D.M. Chapin, C.S. Fuller, G.L. Pearson, *J. Appl. Phys.,* **25**, 676, 1954.

[137] A. Aviram, M. Ratner, M. Pomerantz, *Chem. Phy. Lett.,* **146**, 490, 1988.

[138] R.M. Metzger, *J. Am. Chem. Soc.,* **119**, 10455, 1997.

[139] M.R. Bryce, A. Green, J. Moore, D.F. Perepichka, A.S. Batsanow, J.A.K. Howard, I. Ledoux-Rak, M. Gonzalez, N. Martin, J.L. Segura, J. Garin, J. Orduna, R. Alcala, B. Villacampa, *Eur. J. Org. Chem.,* **2001**, 1927, 2001.

[140] R.M. Metzger, *Synthetic Met.,* **137**, 1499, 2003.

[141] Y.J. Zhang, Y. Li, Q. Liu, J. Jin, B. Ding, Y. Song, L. Jiang, X. Du, Y. Zhao, T.J. Li, *Synth. Metals,* **128**, 43, 2002.

[142] S. Zhou, Y. Liu, W. Qiu, Y. Zu, X. Huang, Y. Li, L. Jiang,D. Zhu, *Adv.Func. Mater.* **12**, 65, 2002.

[143] J.C. Ellenbogen, J.C. Love, *Proc. IEEE,* **88**, 386, 2000.

[144] W.R. Hertzler, *J. Org. Chem.,* **41**, 1412, 1976.

[145] C.A. Panetta, J. Baghdachi, R.M. Metzger, *Mol. Cryst. Liq. Cryst.,* **107**, 103, 1984.

[146] R.M. Metzger. R.R. Schumaker, M.P. Cava, R.K. Laidlaw, C.A. Panetta, E. Torres, *Langmuir,* **4**, 298, 1988.

[147] M.R. Bryce *J. Mater. Chem.*, **10**, 589, 2000.

[148] D.F. Perepichka, M.R. Bryce, C. Pearson, M.C. Petty, E.J.L. McInnes, J.P. Zhao, *Angew. Chem. Int. Ed.*, **42**, 4636, 2003. Supporting Information is available on www.wiley-vch.de/contents/jc_2002/2003/z51876_s.pdf.

[149] H. Rohrer, Scanning tunneling microscopy: a surface science tool and beyond, *Surface Science*, **299/300**, 956, 1994.

[150] A. Aviram, C. Joachim, M. Pomerantz, *Chem. Phys. Lett.*, **146**, 490, 1988.

[151] R.M. Metzger, C.A. Panetta, *J. Mol. Electron.*, **5**, 1, 1989.

[152] S. Scheib, M.P. Cava, J.W. Baldwin, R.M. Metzger, *J. Org. Chem.*, **63**, 1198, 1998.

[153] S. Scheib, M.P. Cava, J.W. Baldwin, R.M. Metzger, *Thin Solid Films*, **327**, 100-103, 1998.

[154] R.M. Metzger, C.A. Panetta, N.E. Heimer, A.M. Bhatti, E. Torres, G.F. Blackburn, S.K. Tripathy, L.A. Samuelson, *J. Mol. Electron.*, **2**, 119, 1986.

[155] R.M. Metzger, *Mater. Sci. Eng.*, **C3**, 277, 1995.

[156] N.J. Geddes , J.R. Sambles, D.J. Jarvis, W.G. Parker, D.J. Sandman, *Appl. Phys. Lett.*, **56**, 1916, 1990.

[157] N.J. Geddes, J.R. Sambles, D.J. Jarvis, W.G. Parker, D.J. Sandman, *J. Appl. Phys.*, **71**, 756, 1992.

[158] G. Ho, J.R. Heath, M. Kondratenko, D.F. Perepichka, K. Arseneault, M. Pézolet, M.R. Bryce, *Chem. Eur. J.*, **11**, 2914, 2005.

[159] G.J. Ashwell, J.R. Sambles, A.S. Martin, W.G. Parker, M. Szablewski, *Chem. Comm.*, **70**, 1374, 1990.

[160] A.S. Martin, J.R. Sambles, G.J. Ashwell, *Phys. Rev.Lett.*, **70**, 218, 1993.

[161] J.R. Sambles, A.S. Martin, *Physical Scripta*, T49, 718, 1993.

[162] A.S. Martin, J.R. Sambles, G.J. Ashwell, *Thin Solid Films* , 210-211, 313-316, 1992.

[163] G.J. Ashwell, E. J. C. Dawnay, A. P. Kuczynski, M. Szablewski, *Materials Research Society Symposium Proceedings*, **173**, 507, 1990.

[164] T. Xu, I. R. Peterson, M.V. Lakshmikantham, R.M. Metzger, *Angew, Chem, Int. Ed.,* **40**, 1749, 2001.

[165] N. Okazaki, J.R. Sambles, International Symposium on Organic Molecular Electronics, Nagoya, Japan, p.66, 2000.

[166] N. Okazaki, J.R. Sambles, M.J. Jory, G.J. Ashwell, *Appl. Phys. Lett.,* **81**, 2300, 2002.

[167] T. Xu, T.A. Morris, G.J. Szulczewski, R.M. Metzger, M. Szablewski, *J. Mat. Chem.,* **12**, 3167, 2002.

[168] G.J. Ashwell, R. Hamilton, L.R.H. High, *J. Mat. Chem.,* **13**, 1501, 2003.

[169] G.J. Ashwell, G.A.N. Paxton, *Aust. J. Chem.,* **55**, 199, 2002.

[170] A.C. Brady, B. Hodder, A.S. Martin, J.R. Sambles, C.P. Ewels, R. Jonem, P.R. Briddon, A. M. Musa, C. A. Panetta, D. L. Mattern, *J. Mat. Chem.,* **9**, 2271, 1999.

[171] R. M. Metzger, B. Chen, U, Höpfner, M. V. Lakshmikantham, D. Vuillaume, T. Kawai, X. Wu, H. Tachibana, T. V. Hughes, H. Samurai, J. W. Baldwin, C. Hosch, M. P. Cava, L. Brehmer, G.J. Ashwell, *J. Am. Chem. Soc.,* **119**, 10455, 1997.

[172] B. Chen, R. M. Metzger, *J. Phys. Chem. B,* **103**, 4447, 1999.

[173] D. Vuillaume, B. Chen, R.M. Metzger, *Langmuir,* **15**, 4011, 1999.

[174] B. Siffert, R.M. Metzger, *Colloids Surf.,* **53**, 79, 1991.

[175] S.A. Contera, H. Iwasaki, *Ultramicroscopy,* **91**, 231, 2002.

[176] S.C. Chang, Z.Y. Li, C.N. Lau, B. Larade, R.S. Williams, *Appl. Phys.Lett.,* **83**, 3198, 2003.

[177] R. McCreery, J. Dieringer, A.O. Solak, B. Snyder, A.M. Nowak, W.R. McGovern, S. DuVall, *J. Am. Chem. Soc.,* **125**, 10748, 2003.

[178] G.J. Ashwell, J.S. Bonham, L.E. Lyons, *Aust. J. Chem.,* **33**, 1619, 1980.

[179] J.G. Simmons, *J. Phys. D: Appl. Phys.,* **4**, 613, 1971.

[180] R. McCreery, J. Dieringer, A.O. Solak, B. Snyder, A.M. Nowak, W.R. McGovern, S. DuVall, *J. Am. Chem. Soc.,* **126**, 6200, 2004.

[181] J.O. McCaldin, T.C. McGill, *Annu. Rev. Mat. Sci.,* **10**, 65, 1980.

[182] R.M. Metzger, T. Xu, I.R. Peterson, *J. Phys. Chem. B,,* **105**, 7280, 2001.

[183] G.J. Ashwell, D.S. Gandolfo, *J. Mat. Chem.,* **11**, 246, 2001.

[184] G.J. Ashwell, D.S. Gandolfo, *J. Mat. Chem.*, **12**, 411, 2002.

[185] G.J. Ashwell, D.S. Gandolfo, R. Hamilton, *J. Mat. Chem.*, **12**, 416, 2002.

[186] G.J. Ashwell, M.A. Amiri, *J. Mat. Chem.*, **12**, 2181, 2002.

[187] J.W. Baldwin, R.R. Amaresh, I.R. Peterson, W.J. Shumate, M.P. Cava, M.A. Amiri, R. Hamilton, G.J. Ashwell, R.M. Metzger, *J. Phys. Chem. B*, **106**, 12158, 2002.

[188] C. Krzeminski, C. Delerue, G. Allan, D. Vuillaume, R.M. Metzger, *Phys. Rev. B, 64*, 085405-1-6, 2001.

[189] A.S. Martin, J.R. Sambles, G.J. Ashwell, *Phys. Rev. Lett.*, **70**, 218, 1993.

[190] P.E. Kornilovitch, A.M. Bratovsky, R.S. Williams, *Chem. Rev. B, 66*, 165436, 2002.

[191] G.J. Ashwell, R.J. Stokes, *J. Mater. Chem.*, **14**, 1228, 2004.

[192] G.J. Ashwell, A. Chwialkowska, L.R.H. High, *J. Mater. Chem.*, **14**, 2389, 2004.

[193] G.J. Ashwell, W.D. Tyrrell, A.J. Whittam, *J. Mater. Chem.*, **13**, 2855, 2003.

[194] G.J. Ashwell, W.D. Tyrrell, A.J. Whittam, *J. Am. Chem. Soc.*, **126**, 7102, 2004.

[195] G.J. Ashwell, A. Mohib, J.R. Miller, *J. Mater. Chem.*, **15**, 1160, 2005.

[196] G.J. Ashwell, A. Mohib, *J. Am. Chem. Soc.*, **127**, 16238, 2005.

[197] G.J. Ashwell, B.J. Robinson, M.A. Amiri, D. Locatelli, S. Quici, D. Roberto, *J. Mater. Chem.*, **15**, 4203, 2005.

[198] Y. Okahata, K. Ariga, H. Nakahara, K.J. Fukuda *J. Chem. Soc. Chem. Comm.*, 1069, 1986.

[199] G.J. Ashwell, M. Berry, *J. Mater.Chem.*, **15**, 108, 2005.

[200] G.J. Ashwell, G.S. Bahra, C.R. Brown, D.G. Hamilton, C.H.L. Kennard and D.E. *J. Mat. Chem.*, **6**, 23, 1996.

[201] G.J. Ashwell, J. Ewington, K. Moczko, *J. Mater. Chem.*, **15**, 1154, 2005.

[202] G.J. Ashwell, A. A. Maxwell, A. Green, *J. Mater. Chem.*, **12**, 2192, 2002.

[203] G.J. Ashwell, M. Sujka, A. Green, *Faraday Discussions*, **131**, 23, 2006.

[204] G.J. Ashwell, A. Chwialkowska, *Chem. Comm.*, **13**, 1404, 2006.

[205] C.M. Fisher, M. Burghard, S. Roth, *Synthetic Metals*, **71**, 1975, 1995.

[206] B. Mukherjee, J.A. Pal, *Chem. Phys. Lett.*, **416**, 289, 2005.

[207] G.J. Ashwell, J. Ewington, B.J. Robinson, *Chem. Comm.*, **6**, 618, 2006.

[208] G.J. Ashwell, W.D. Tyrrell, B. Urasinska, C. Wang, M.R. Bryce, *Chem. Comm.*, 1640, 2006.

[209] R.M. Metzger, J.W. Baldwin, W.J. Shumate, I.R. Peterson, P. Mani, G.J. Mankey, T. Morris, G. Szulczewski, S. Bosi, M. Prato, A. Comito, Y. Rubin, *J. Phys. Chem. B*, 107, 1021, 2003.

[210] J.R. Miller *Analysis of rectifying molecular thin films. PhD thesis.* Cranfield University 2005.

[211] G. Philipp, C. Müller-Schwanneke, M. Burghard, S. Roth, K. v. Klitzing, *J. Appl. Phys.*, **85**, 3374, 1999.

[212] A. Honciuc, A. Jaiswal, A. Gonsh, K. Ashworth, C.W. Spangler, I.R. Peterson, L.R. Dalton, R.M. Metzger, *J. Phys. Chem. B*, **109**, 857, 2005.

[213] D.L. Person, J.M. Tour, *J. Org. Chem.*, **62**, 1376, 1997.

[214] L. Jones, J.S. Schumm, J.M. Tour, *J. Org. Chem.*, **62**, 1388, 1997.

[215] L.A. Bumm, J. J. Arnold, M.T. Cygan, T.D. Dunbar, T. P. Burgin, L. Jones II, D.L. Allar, J.M. Tour, P.S. Weiss, *Science*, **271**, 1705, 1996.

[216] C. Zhou, M.R. Deshpande, M.A. Reed, L. Jones II, J.M. Tour, *Appl. Phys. Lett.*, **71**, 611, 1997.

[217] M.A. Reed, C. Zhou, M.R. Deshpande, C.J. Muller, T.P. Burgin, L. Jones II, J.M. Tour, The electrical measurement of molecular junction, in Molecular Electronics: Science and Technology, Annals of the New York Academy of Sciences, **852**, 133, 1998.

[218] J.G. Kushmerik, C.M. Whitaker, S.K. Pollack, T.L. Schull, R. Shashidhar, *Nanotechnology*, **15**, S489, 2004.

[219] J.G. Kushmerick, B.D. Holt, S.K. Pollack, M.A. Ratler, J.C. Yang, T.L. Schull, J. Naciri, M.H. Moore, *J. Am. Chem. Soc.*, **124**, 10654, 2002.

[220] H.D. Sikes, J.F. Smalley, S.P. Dudek, A.R. Cook, M.D. Newton, C.E.D. Chidsey, S.W. Feldberg, *Science*, **291**, 1519, 2001.

[221] G.J. Ashwell, P. Wierzchowiec, C.J. Bartlett, P.D. Buckle, *Chem. Comm.*, 1254, 2007.

[222] A.J. Whittam, Optically nonlinear materials, PhD Thesis, Cranfield University, 2001.

[223] R.L. Carroll, C.B. Gorman, *Angew. Chem. Int. Ed.*, **41**, 4378, 2002.

[224] N. Robertson, C.A. McGowan, *Chem. Soc. Rev.*, **32**, 96, 2003.

[225] H.C. Yang, K. Aoki, H.G. Hong, D.D. Sackett, M.F. Arendt, S.L. Yau, C.M. Bell, T.E. Mallouk, *J. Am. Chem. Soc.*, **115**, 11855, 1993.

[226] D.G. Castner, K. Hinds, D.W. Grainger, *Langmuir*, **12**, 5083, 1996.

[227] W. Haiss, C. Wang, R. Jitchati, I. Grace, S. Martín, A.S. Batsanov, S.J. Higgins, M.R. Bryce, C.J. Lambert, P.S. Jensen, R.J. Nichols, *J. Phys.: Condensed Matter.*, **20**, 374119, 2008.

[228] I.F. Perepichka, L.G. Kuz'mina, D.F. Perepichka, M.R. Bryce, L.M. Goldenberg, A.F. Popov, J.A.K. Howard, *J. Org. Chem.*, **63**, 6484, 1998.

[229] S. Liao, Y. Shnidman, A. Ulman, *J. Am. Chem. Soc.*, **122**, 3688, 2000.

[230] L. Cai, Y. Yao, J. Yang, D.W. Price, J.M. Tour, *Chem. Mater.*, **14**, 2905, 2002.

[231] J.J. Stapleton, P. Harder, T.A. Daniel, M.D. Reinard, Y. Yao, D.W. Price, J.M. Tour, D.L. Allara, *Langmuir*, **19**, 8245, 2003.

[232] J.G. Kushmerick, D.B. Holt, J.C. Yang, J. Naciri, M.H. Moore, R. Shashidhar, *Phys. Rev. Lett.*, **89**, 086802, 2002.

[233] J.M. Tour, *J. Am. Chem. Soc.* **117**, 9529, 1995.

[234] W. Haiss, S. Martin, E. Leary, H. van Zalinge, S.J. Higgins, L. Bouffier, R.J. Nichols, *J. Phys. Chem. C*, **113**, 5823, 2009

[235] J. Tang, Y. Wang, J.E. Klare, G.S. Tulevski, S. J. Wind, C. Nuckolls, *Angew. Chem.*, **46**, 3892, 2007.

[236] G.J. Ashwell, B. Urasinska-Wojcik, *Pat. Appl.* 0909244.6, **2009**.

[237] M.K. Nazeeruddin, A. Kay, I. Rodicio, B.R. Humphry, E. Mueller, P. Liska, N. Vlachopoulos, M. Gratzel, M. *J. Am. Chem. Soc.*, **115**, 6382, 1993.

[238] T.J. Meyer, G.J. Meyer, B.W. Pfennig, J.R. Schoonover, C.J. Timpson, J.F. Wall, C. Kobusch, X.H. Chen, B.M. Peek, C.G. Wall, W. Ou, B.W. Erickson, C.A. Bignozzi, *Inorg. Chem.*, **33**, 3952, 1994.